

Evaluation of lipid biomarkers as proxies for sea ice and ocean temperatures along the Antarctic continental margin

Nele Lamping¹, Juliane Müller^{1,2,3}, Jens Hefter¹, Gesine Mollenhauer^{1,2,3}, Christian Haas¹, Xiaoxu Shi¹, Maria-Elena Vorrath¹, Gerrit Lohmann^{1,3,4}, Claus-Dieter Hillenbrand⁵

¹Alfred Wegener Institute, Helmholtz Center for Polar and Marine Research, Am Alten Hafen 26, 27568 Bremerhaven, Germany

²Department of Geosciences, University of Bremen, Klagenfurter Straße, 28359 Bremen, Germany

³Marum - Center for Marine Environmental Sciences, Leobener Straße 8, 28359 Bremen, Germany

⁴Department of Environmental Physics, University of Bremen, 28359 Bremen, Germany

⁵British Antarctic Survey, High Cross, Madingley Road, Cambridge CB3 0ET, United Kingdom

Correspondence to: Nele Lamping (nele.lamping@awi.de)

Abstract

The importance of Antarctic sea ice and Southern Ocean warming has come into the focus of polar research in the last couple of decades. Especially in West Antarctica, where warm water masses approach the continent and where sea ice has declined, the distribution and evolution of sea ice play a critical role for the stability of nearby ice shelves. Organic geochemical analyses of marine seafloor surface sediments from the Antarctic continental margin permit an evaluation of the applicability of biomarker-based sea ice and ocean temperature reconstructions in these vulnerable areas. We analysed highly branched isoprenoids (HBIs), such as the sea-ice proxy IPSO₂₅ and phytoplankton-derived HBI-trienes, but also phytosterols and isoprenoidal glycerol dialkyl glycerol tetraethers (GDGTs), which are established tools for the assessment of primary productivity and ocean temperatures, respectively. The combination of IPSO₂₅ with a phytoplankton marker (i.e. the PIPSO₂₅ index) permits semi-quantitative sea ice reconstructions and avoids misleading over- or underestimations of sea-ice cover. Comparisons

Formatvorlagendefinition	... [2]
Gelöscht: Elucidating modern West Antarctic sea	... [3]
Gelöscht: , instrumental	
Formatiert	... [4]
Formatiert	... [5]
Gelöscht: biomarker	
Gelöscht: numerical-model data	
Formatiert	... [6]
Formatiert	... [8]
Formatiert	... [7]
Formatiert	... [9]
Formatiert	... [10]
Formatiert	... [11]
Gelöscht: ⁴ ,	
Formatiert	... [13]
Gelöscht: ⁵	
Formatiert	... [12]
Formatiert	... [14]
Formatiert	... [15]
Formatiert	... [16]
Gelöscht: -	
Formatiert	... [17]
Gelöscht: -Institut	
Formatiert	... [18]
Gelöscht: -Zentrum für	
Formatiert	... [19]
Gelöscht: - und Meeresforschung	
Formatiert	... [20]
Formatiert	... [21]
Gelöscht: ⁴ Laboratoire des Sciences de l'Environnement	
Formatiert	... [23]
Formatiert	... [24]
Formatiert	... [25]
Formatiert	... [26]
Formatiert	... [27]
Formatiert	... [28]
Formatiert	... [29]
Formatiert	... [30]
Gelöscht: sea ice	
Formatiert	... [31]
Gelöscht: its	
Formatiert	... [32]
Gelöscht: West	
Formatiert	... [33]
Gelöscht: shelves	
Formatiert	... [34]
Gelöscht: a	
Formatiert	... [35]
Gelöscht: reconstruction of	
Formatiert	... [36]
Gelöscht: surface conditions	
Formatiert	... [37]
Gelöscht: reconstruction	
Formatiert	... [38]
Gelöscht: sea surface	
Formatiert	... [39]
Gelöscht: results in	
Formatiert	... [40]
Gelöscht: -	
Formatiert	... [41]
Gelöscht: index PIPSO ₂₅ , which provides useful	
Gelöscht: of sea-ice conditions, avoiding	
Formatiert	... [42]
Formatiert	[43]

of the PIP_{SO_2} -based sea-ice distribution patterns and $\text{TEX}^{\text{L}}_{86}$ - and RI-OH^2 -derived ocean temperatures with (1) sea-ice concentrations obtained from satellite observations and (2) instrumental sea surface and subsurface temperatures corroborate the general capability of these proxies to properly display oceanic key variables. This is further supported by model data. We also highlight specific aspects and limitations that need to be considered when interpreting such biomarker data and discuss the potential of IPSO_{25} to reflect the former occurrence of platelet ice and/or the export of ice shelf water.

- Gelöscht: biomarker
- Formatiert: Schriftart: (Standard) Times New Roman
- Gelöscht: GDGT-based
- Formatiert: Schriftart: (Standard) Times New Roman
- Gelöscht: distributions
- Gelöscht: estimated sea-ice patterns and SSTs deduced from modelled
- Formatiert: Schriftart: (Standard) Times New Roman
- Formatiert: Schriftart: (Standard) Times New Roman
- Gelöscht: are in reasonable agreement, but
- Formatiert: Schriftart: (Standard) Times New Roman
- Formatiert: Schriftart: (Standard) Times New Roman
- Formatiert: Schriftart: (Standard) Times New Roman
- Gelöscht: . We further
- Formatiert: Schriftart: (Standard) Times New Roman
- Gelöscht: concentrations in the vicinity of ice shelves, where elevated values could be related to the
- Formatiert: Schriftart: (Standard) Times New Roman
- Formatiert: Schriftart: (Standard) Times New Roman
- Formatiert: Schriftart: (Standard) Times New Roman
- Gelöscht: basal melt
- Formatiert: Schriftart: (Standard) Times New Roman
- Gelöscht: and platelet ice under landfast sea ice
- Formatiert: Schriftart: (Standard) Times New Roman

Formatiert: Nach: 0.63 cm

Formatiert	... [45]
Formatiert	... [46]
Formatiert	... [47]
Formatiert	... [48]
Gelöscht: ,	
Formatiert	... [49]
Gelöscht:)	
Formatiert	... [50]
Gelöscht:	
Formatiert	... [51]
Gelöscht: Southern Ocean sea-ice extent has	... [52]
Formatiert	... [53]
Gelöscht: in East Antarctica is	
Gelöscht: ,	
Formatiert	... [54]
Formatiert	... [55]
Gelöscht: even exceeding the drastic decay rates	... [56]
Formatiert	... [57]
Gelöscht: , however, is	
Formatiert	... [58]
Gelöscht: since the beginning of satellite-based	... [59]
Formatiert	... [60]
Gelöscht:). Here,	
Formatiert	... [61]
Gelöscht: has been	
Formatiert	... [62]
Gelöscht: changes	
Formatiert	... [63]
Gelöscht: duration over the past few decades,	... [64]
Gelöscht: warming (
Formatiert	... [65]
Formatiert	... [66]
Gelöscht: at	
Formatiert	... [67]
Gelöscht: East	
Formatiert	... [68]
Gelöscht: Massom et al. (2018) linked to	
Formatiert	... [69]
Gelöscht: .	
Formatiert	... [70]
Gelöscht: stark	
Formatiert	... [71]
Gelöscht: Glaciers	
Formatiert	... [72]
Gelöscht: basal	
Formatiert	... [73]
Gelöscht: , thinning the adjacent ice shelves from below	
Formatiert	... [74]
Gelöscht:).	
Formatiert	... [75]
Gelöscht: force for the West Antarctic Ice Sheet	
Formatiert	... [76]
Gelöscht: ice shelves in these	
Formatiert	... [77]
Formatiert	... [44]

1. Introduction

One of the key components of the global climate system, influencing major atmospheric and oceanic processes, is floating on the ocean's surface at high latitudes – sea ice (Thomas, 2017). Southern Ocean sea ice is one of the most strongly changing features of the Earth's surface as it experiences considerable seasonal variabilities with decreasing sea-ice extent from a maximum of $20 \times 10^6 \text{ km}^2$ in September to a minimum of $4 \times 10^6 \text{ km}^2$ in March (Arrigo et al., 1997; Zwally, 1983). This seasonal waxing and waning of sea ice substantially modifies deep-water formation, as well as the ocean-atmosphere exchange of heat and gas, strongly affects surface albedo and radiation budgets (Abernathy et al., 2016; Nicholls et al., 2009; Turner et al., 2017), and also regulates ocean buoyancy flux, upwelling and primary production (Schofield et al., 2018).

Based on the 40-year satellite record, Southern Ocean sea-ice extent as a whole followed an increasing trend (Comiso et al., 2017; Parkinson and Cavalieri, 2012), experiencing an abrupt reversal from 2014 to 2018 (Parkinson, 2019; Turner et al., 2020; Wang et al., 2019), which has been attributed to a decades-long oceanic warming and increased advection of atmospheric heat (Eayrs et al., 2021). In addition, the sea-ice extent around major parts of West Antarctica has been decreasing (Parkinson and Cavalieri, 2012), with the Antarctic Peninsula being affected by a significant reduction in sea-ice extent and rapid atmospheric and oceanic warming (Etourneau et al., 2019; Li et al., 2014; Massom et al., 2018; Vaughan et al., 2003). The Larsen Ice Shelves A and B, located east of the Antarctic Peninsula, collapsed in 1995 and 2002, respectively, which was triggered by the loss of a sea-ice buffer, enabling an increased flexure of the ice shelf margins by ocean swells (Massom et al., 2018). The Bellingshausen and Amundsen Seas are also affected by a major sea-ice decline and regional surface ocean warming (Hobbs et al., 2016; Parkinson, 2019). Marine-terminating glaciers draining into the Amundsen Sea are thinning at an alarming rate, which has been linked to sub-ice shelf melting caused by relatively warm Circumpolar Deep Water (CDW) incursions into sub-ice shelf cavities (e.g., Jacobs et al., 2011; Khazendar et al., 2016; Nakayama et al., 2018; Rignot et al., 2019; Smith et al., 2017). The disintegration of ice shelves reduces the buttressing effect that they exert on ice grounded further upstream, which may lead to a partial collapse of the catchments of the affected glaciers, eventually

98 raising global sea level considerably (3.4 to 4.4 m resulting from a WAIS collapse: Fretwell et al., 2013;
 99 Jenkins et al., 2018; Pritchard et al., 2012; Vaughan, 2008),
 100 State-of-the-art climate models are not yet fully able to depict sea-ice seasonality and sea-ice cover,
 101 which the 5th Assessment Report of the Intergovernmental Panel on Climate Change (Stocker et al.,
 102 2013) attributes to a lack of validation efforts using proxy-based sea-ice reconstructions. Knowledge
 103 about (paleo-)sea-ice conditions and ocean temperatures in the climate sensitive areas around the West
 104 Antarctic Ice Sheet is hence considered as crucial for understanding past and future climate evolution.
 105 To date, the most common proxy-based sea-ice reconstructions in the Southern Ocean are conducted
 106 by the use of sympagic diatom assemblages, which are strongly dependent on their preservation within
 107 the sediments (Allen et al., 2011; Armand and Leventer, 2003; Crosta et al., 1998; Esper and Gersonde,
 108 2014; Gersonde and Zielinski, 2000; Leventer, 1998). Dissolution effects within the water column or
 109 after deposition determine the preservation state of the small, lightly silicified microfossils and may
 110 alter the diatom record, leading to inaccurate sea-ice reconstructions (Leventer, 1998; Zielinski et al.,
 111 1998). Recently, the molecular remains of certain diatoms, specific organic geochemical lipids, have
 112 emerged as a potential proxy for reconstructing past Antarctic sea ice cover (Barbara et al., 2013;
 113 Collins et al., 2013; Crosta et al., 2021; Denis et al., 2010; Etourneau et al., 2013; Lamping et al., 2020;
 114 Massé et al., 2011; Vorrath et al., 2019; 2020). Specifically, a di-unsaturated highly branched isoprenoid
 115 (HBI) alkene (HBI diene, C_{25:2}) has been detected in both sea-ice diatoms and sediments in the Southern
 116 Ocean (Johns et al., 1999; Massé et al., 2011; Nichols et al., 1988), and recently the sympagic (*i.e.* living
 117 within sea-ice) tube-dwelling diatom *Berkeleya adeliensis* has been identified as producer, which
 118 preferably proliferates in platelet ice (Belt et al., 2016; Riaux-Gobin and Poulin, 2004). However, *B.*
 119 *adeliensis* seems rather flexible concerning its habitat, since it was also recorded in the bottom ice layer
 120 and seems to be well adapted to changes in texture during ice melt (Riaux-Gobin et al., 2013). Belt et
 121 al. (2016) introduced the term IPSO₂₅ ("Ice Proxy of the Southern Ocean with 25 carbon atoms") by
 122 analogy to the counterpart IP₂₅ in the Arctic. Commonly, for a more detailed assessment of sea-ice
 123 conditions, IP₂₅ in the Arctic Ocean and IPSO₂₅ in the Southern Ocean have been measured alongside
 124 complementary phytoplankton-derived lipids, such as sterols and/or HBI-trienes, which are indicative
 125 of open-water conditions (Belt and Müller, 2013; Lamping et al., 2020; Etourneau et al., 2013; Vorrath

- Gelöscht: impacting
- Gelöscht: rise significantly (
- Formatiert: Schriftart: (Standard) Times New Roman
- Formatiert: Schriftart: (Standard) Times New Roman
- Formatiert: Schriftart: (Standard) Times New Roman, Hervorheben
- Formatiert: Schriftart: (Standard) Times New Roman
- Formatiert: Schriftart: (Standard) Times New Roman, Schriftfarbe: Automatisch
- Gelöscht: explains by
- Formatiert: Schriftart: (Standard) Times New Roman
- Gelöscht:
- Formatiert: Schriftart: (Standard) Times New Roman
- Formatiert: Schriftart: (Standard) Times New Roman
- Formatiert: Schriftart: (Standard) Times New Roman, Schriftfarbe: Automatisch
- Gelöscht: To avoid ambiguous interpretations
- Formatiert: Schriftart: (Standard) Times New Roman, Schriftfarbe: Automatisch
- Gelöscht: recently
- Formatiert: Schriftart: (Standard) Times New Roman, Schriftfarbe: Automatisch
- Gelöscht: robust
- Formatiert: Schriftart: (Standard) Times New Roman, Schriftfarbe: Automatisch
- Gelöscht: (and present)
- Formatiert ... [78]
- Gelöscht:
- Formatiert ... [79]
- Formatiert ... [80]
- Formatiert ... [81]
- Gelöscht:)
- Formatiert ... [82]
- Formatiert ... [83]
- Formatiert ... [84]
- Formatiert ... [85]
- Gelöscht: was recently
- Formatiert ... [86]
- Gelöscht: because of the structurally close relationship
- Formatiert ... [88]
- Gelöscht:
- Formatiert ... [89]
- Gelöscht: Müller
- Formatiert ... [90]
- Gelöscht: 2011
- Formatiert ... [91]
- Formatiert: Nach: 0.63 cm

150 et al., 2019; 2020). The combination of the sea-ice biomarker and a phytoplankton biomarker, the so-
 151 called PIPSO₂₅ index (Vorrath et al., 2019), allows for a more quantitative differentiation of contrasting
 152 sea-ice settings and helps to avoid misinterpretations of the absence of IPSO₂₅, which can result from
 153 either a lack of sea-ice cover or a permanently thick sea-ice cover, that prevents light penetration hence
 154 limiting ice algae growth. Recently, Lamping et al. (2020) used this approach to study changes in sea-
 155 ice conditions during the last deglaciation of the Amundsen Sea shelf, which were likely linked to
 156 advance and retreat phases of the Getz Ice Shelf.
 157 Multiple mechanisms exist that can cause ice shelf instability. As previously mentioned, relatively warm
 158 CDW is considered one of the main drivers for ice shelf thinning in the Amundsen Sea Embayment
 159 (Nakayama et al., 2018; Jenkins and Jacobs, 2008; Rignot et al., 2019). Accordingly, changing ocean
 160 temperatures are another crucial factor for the stability of the marine-based ice streams draining most
 161 of the West Antarctic Ice Sheet (e.g., Colleoni et al., 2018). As for sea-ice reconstructions, organic
 162 geochemical lipids for reconstructing ocean temperatures in high latitudes have come into focus in the
 163 past decades, since the preservation of calcareous microfossils, which are commonly used for such
 164 reconstructions, is very poor in polar marine sediments (e.g., Zamelczyk et al., 2012). Archaeal
 165 isoprenoidal glycerol dialkyl glycerol tetraethers (isoGDGTs), sensitive to temperature change and
 166 relatively resistant to degradation processes, are well-preserved in marine sediments (Huguet et al.,
 167 2008; Schouten et al., 2013). Schouten et al. (2002) found that the number of rings in sedimentary
 168 GDGTs is correlated with surface water temperatures and developed the first archaeal lipid
 169 paleothermometer TEX₈₆, a ratio of certain GDGTs, as a sea surface temperature (SST) proxy. For polar
 170 oceans, Kim et al. (2010) developed a more specific calibration model for temperatures below 15 °C.
 171 TEX₈₆¹, which employs a different GDGT combination. There is an emerging consensus that GDGTs
 172 are rather reflecting subsurface ocean temperatures (SOT) along the Antarctic margin (Kim et al., 2012;
 173 Etoumeau et al., 2019; Liu et al., 2020). This is supported by observations of elevated archaeal
 174 abundances (and GDGTs) in warmer subsurface waters (Liu et al., 2020; Spencer-Jones et al., 2021).
 175 Archaea adapt their membrane in cold waters by adding hydroxyl groups and changing the number of
 176 rings. OH-GDGTs (Fietz et al., 2020). The additional hydroxyl moieties lead to an increase of the
 177 membrane fluidity that aids trans-membrane transport in cold environments, which Huguet et al. (2017)

- Gelöscht:
- Formatiert ... [93]
- Gelöscht: PIP₂₅ index for the Arctic (Müller et al., 2014)
- Gelöscht: for the Antarctic
- Gelöscht: allow
- Formatiert ... [95]
- Formatiert ... [96]
- Formatiert ... [97]
- Gelöscht: . A misinterpretation
- Gelöscht: of
- Formatiert ... [98]
- Gelöscht: an absent sea-ice biomarker,
- Formatiert ... [99]
- Gelöscht: be the
- Formatiert ... [100]
- Formatiert ... [101]
- Gelöscht: no
- Formatiert ... [102]
- Gelöscht: severe
- Formatiert ... [103]
- Gelöscht: , can be circumvented with
- Formatiert ... [104]
- Gelöscht: Mechanisms contributing to
- Formatiert ... [105]
- Gelöscht: are manifold
- Formatiert ... [106]
- Gelöscht: Jacobs
- Formatiert ... [107]
- Gelöscht: 2011
- Gelöscht:).
- Formatiert ... [108]
- Formatiert ... [109]
- Gelöscht: fate
- Formatiert ... [110]
- Gelöscht: stability
- Formatiert ... [111]
- Gelöscht: past and recent
- Formatiert ... [112]
- Gelöscht: calcium carbonate
- Formatiert ... [113]
- Gelöscht: not continuous
- Formatiert ... [114]
- Gelöscht: high latitude
- Formatiert ... [115]
- Gelöscht: Hence, isoGDGTs are considered to be...
- Formatiert ... [92]



232 found in molecular dynamic simulations, explaining the higher relative abundance of OH Archaea lipids
 233 in cold environments. Taking the OH-GDGTs into account, Lü et al. (2015) proposed an SST-proxy for
 234 the polar oceans, the RI-OH'.
 235 Our aim with this study is to provide insight into the application of biomarkers for sea ice as well as
 236 ocean temperature reconstructions, in Southern Ocean sediments. Estimates on recent sea-ice coverage
 237 and ocean temperatures along the eastern and western Antarctic Peninsula (EAP and WAP) as well as
 238 in the Amundsen and Weddell Seas, are based on the analyses of IPSO₂₅, HBI-trienes and phytosterols
 239 as well as GDGTs in seafloor surface sediment samples from these areas. An intercomparison of
 240 biomarker-based sea ice as well as ocean temperature estimates with (1) sea-ice distributions obtained
 241 from satellite observations and (2) ocean temperatures deduced from instrumental data allows for an
 242 evaluation of the proxy approaches. We further consider AWI-ESM2 climate model data to assess the
 243 model's performance in depicting recent oceanic key variables and to examine the potential impact of
 244 paleoclimate conditions on the biomarker composition of the investigated surface sediments. In regard
 245 of the various factors affecting the use of marine biomarkers as paleoenvironmental proxies, we further
 246 comment on the limitations of GDGT temperature estimates and the novel PIPSO₂₅ approach, and we
 247 discuss the potential connection between IPSO₂₅ and platelet ice formation under near-coastal fast ice,
 248 which is related to the near-surface presence of sub-ice shelf melt water.

2. Regional setting

251 The areas of investigation in this study include the southern Drake Passage, the continental shelves of
 252 the WAP and EAP (~60° S) and the more southerly located Amundsen and Weddell Seas (~75° S; Fig.
 253 1). The different study areas are all connected by the Antarctic Circumpolar Current (ACC), the
 254 Antarctic Coastal Current and the Weddell Gyre (Meredith et al., 2011; Rintoul et al., 2001).

Formatiert: Schriftart: (Standard) Times New Roman, Schriftfarbe: Automatisch

Formatiert: Schriftart: (Standard) Times New Roman

Gelöscht: ,

Formatiert: Schriftart: (Standard) Times New Roman

Gelöscht: conditions

Gelöscht: ,

Formatiert: Schriftart: (Standard) Times New Roman, Schriftfarbe: Automatisch

Formatiert: Schriftart: (Standard) Times New Roman

Formatiert: Schriftart: (Standard) Times New Roman

Gelöscht: in

Formatiert: Schriftart: (Standard) Times New Roman

Formatiert: Schriftart: (Standard) Times New Roman

Gelöscht: address

Formatiert: Schriftart: (Standard) Times New Roman

Gelöscht: presence of near-surface ice shelf basal melt water. An intercomparison of sea ice as well as temperature reconstructions (based on GDGT analyses) with (1) sea-ice distributions obtained from satellite observations and (2) estimated sea-ice distribution and SSTs deduced from modelled data provides for an evaluation of the proxy approaches. For a more semi-quantitative sea-ice estimate, the relatively new approach of PIPSO₂₅ has been used to further assess the advantages and limitations of the sea-ice index as a potential tool to validate and improve numerical climate models to better understand current and past trends in sea-ice development in the Southern Ocean.

Formatiert: Schriftart: (Standard) Times New Roman, Schriftfarbe: Automatisch

Gelöscht: Abschnittswechsel (Nächste Seite)

Formatiert: Standard, Block, Einzug: Vor: 0.74 cm, Hängend: 0.74 cm, Zeilenabstand: Doppelt, Keine Aufzählungen oder Nummerierungen

Formatiert: Schriftart: (Standard) Times New Roman

Gelöscht:

Formatiert: Block, Zeilenabstand: Doppelt

Formatiert: Schriftart: (Standard) Times New Roman

Gelöscht: West

Formatiert: Schriftart: (Standard) Times New Roman

Gelöscht: East Antarctic Peninsula (~

Formatiert: Schriftart: (Standard) Times New Roman

Gelöscht:

Formatiert: Schriftart: (Standard) Times New Roman

Gelöscht: only current circumnavigating the globe, the

Gelöscht: ;

Formatiert: Schriftart: (Standard) Times New Roman

Formatiert: Schriftart: (Standard) Times New Roman

Formatiert: Nach: 0.63 cm

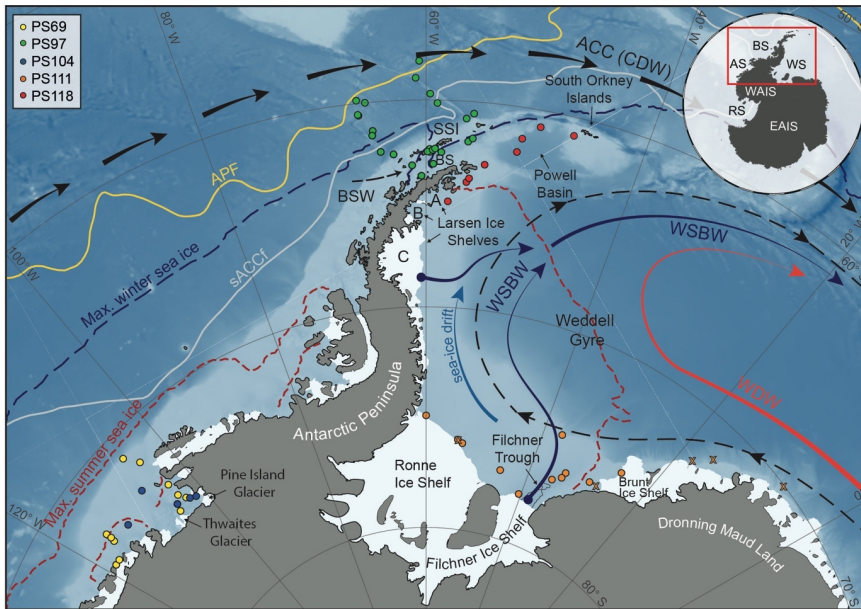


Fig. 1: Map of the study area (location indicated by red box in insert map) including all 41 sample locations (see different colored dots for individual *RV Polarstern* expeditions in the top left corner; for detailed sample information, see Table S1) and main oceanographic features. Maximum summer and winter sea-ice boundaries are marked by dashed red and blue line, respectively (Fetterer et al., 2016). Orange crosses indicate samples where a PIPSO₂s value of 1 has been assigned due to low biomarker concentrations, close to detection limit. ACC: Antarctic Circumpolar Current, APF: Antarctic Polar Front, sACCf: southern Antarctic Circumpolar Current Front, SSI: South Shetland Islands, BS: Bransfield Strait, BSW: Bellingshausen Sea Water, CDW: Circumpolar Deep Water, WDW: Weddell Deep Water, WSBW: Weddell Sea Bottom Water (Mathiot et al., 2011; Orsi et al., 1995). Insert map shows grounded ice only (i.e., no ice shelves), WAIS: West Antarctic Ice Sheet, EAIS: East Antarctic Ice Sheet, RS: Ross Sea, AS: Amundsen Sea, BS: Bellingshausen Sea, WS: Weddell Sea. Background bathymetry derived from IBCSO data (Amtdt et al., 2013).

281 The ACC is mainly composed of CDW and is the largest current system in the world characterised by
 282 a strong eastward flow, which finds its narrowest constriction in the Drake Passage. Along the
 283 Bellingshausen Sea, the Amundsen Sea and WAP, where the ACC flows close to the continental shelf
 284 edge, CDW is upwelling onto the shelf and flows to the coast via bathymetric troughs, contributing to
 285 basal melt and retreat of marine-terminating glaciers and ice shelves (Cook et al., 2016; Jacobs et al.,
 286 2011; Jenkins and Jacobs, 2008; Klinck et al., 2004). In the Weddell Sea, a subpolar cyclonic circulation
 287 is present south of the ACC, the Weddell Gyre, which deflects part of the ACC's CDW towards the
 288 south turning it into Warm Deep Water (WDW; Fig. 1; Hellmer et al., 2016; Vernet et al., 2019). In
 289 close vicinity to the Filchner-Ronne and Larsen Ice Shelves, glacially derived freshwater as well as

[1] verschoben (Einfügung)

Formatiert: Schriftart: (Standard) +Überschriften CS (Times New Roman), 10 Pt., Fett, Nicht Kursiv, Schriftfarbe: Text 1, Englisch (Vereinigtes Königreich)

Formatiert: Schriftart: (Standard) Times New Roman

Formatiert: Block, Zeilenabstand: Doppelt

Formatiert: Schriftart: (Standard) Times New Roman

Gelöscht: It is mainly composed of CDW, which is generally divided into the Upper CDW with low oxygen and high nutrient concentrations, and Lower CDW with high salinities (Rintoul et al., 2001).

Formatiert: Schriftart: (Standard) Times New Roman

Gelöscht: West Antarctic Peninsula (i.e., the Bransfield Strait),

Formatiert: Schriftart: (Standard) Times New Roman

Formatiert: Schriftart: (Standard) Times New Roman

Gelöscht: the adjoining

Formatiert: Schriftart: (Standard) Times New Roman

Formatiert: Schriftart: (Standard) Times New Roman

Gelöscht: where the ACC is located sufficiently far from the Antarctic continent,

Formatiert: Schriftart: (Standard) Times New Roman

Gelöscht: . The Weddell Gyre is the main circulation in the

Formatiert: Nach: 0.63 cm

301 dense brine released during sea-ice formation contribute to Weddell Sea Bottom Water (WSBW) - a
 302 major precursor of Antarctic Bottom Water (Hellmer et al., 2016). Wind and currents force a northward
 303 sea-ice drift in the western Weddell Sea along the eastern coast of the Antarctic Peninsula (Harms et
 304 al., 2001) until leaving it to melt in warmer waters to the North and up to the Powell Basin (Vernet et
 305 al., 2019). At the northern tip of the Antarctic Peninsula, colder and saltier Weddell Sea water masses
 306 branch off westwards into the Bransfield Strait where they encounter the well-stratified, warm, and
 307 fresh Bellingshausen Sea Water (BSW; Fig. 1), which is entering the Bransfield Strait from the West
 308 (Sangrà et al., 2011).

309 Since 1978, satellite observations show strong seasonal as well as decadal changes in sea-ice cover at
 310 the Antarctic Peninsula, which are less pronounced in the more southerly Amundsen and Weddell Seas
 311 (Fig. 2a-e). Mean monthly sea-ice concentrations (SIC) for winter (JJA), spring (SON) and summer
 312 (DJF) reveal a permanently ice-free Drake Passage, while the WAP and EAP shelf areas are influenced
 313 by a changing sea-ice cover in the course of a year (Fig. 2a-c). For the Amundsen and Weddell Seas,
 314 satellite data reveal a closed seasonal sea-ice cover with up to ~90 % concentration during winter and
 315 spring (Fig. 2a+b), and a late break-up of sea-ice cover to a minimum concentration of ~30 % during
 316 summer (Fig. 2c).

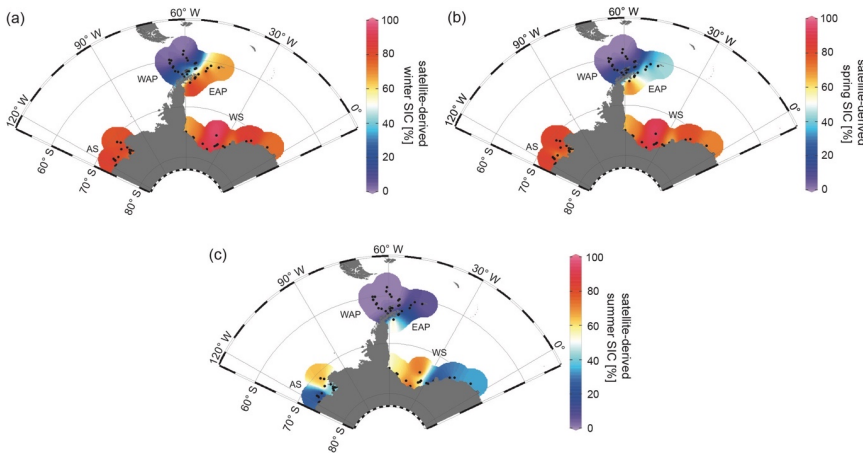


Fig. 2: Distribution of mean monthly satellite-derived sea-ice concentrations for (a) winter (JJA), (b) spring (SON) and (c) summer (DJF) in % (downloaded from the National Snow and Ice Data Center, NSIDC; Cavalieri et al., 1996). AS: Amundsen Sea, WAP: West Antarctic Peninsula, EAP: East Antarctic Peninsula, WS: Weddell Sea.

- Formatiert: Schriftart: (Standard) Times New Roman
- Gelöscht: and the most important source
- Formatiert: Schriftart: (Standard) Times New Roman
- Gelöscht: Deacon, 1979), with sea-ice formation as an important factor in generating these dense water masses (Harms et al., 2001).
- Formatiert: Schriftart: (Standard) Times New Roman
- Gelöscht: East
- Formatiert: Schriftart: (Standard) Times New Roman
- Formatiert: Schriftart: (Standard) Times New Roman
- Gelöscht: Transitional
- Formatiert: Schriftart: (Standard) Times New Roman
- Gelöscht: Water (TWW) branches
- Formatiert: Schriftart: (Standard) Times New Roman
- Formatiert: Schriftart: (Standard) Times New Roman
- Gelöscht: and is characterised by colder temperatures and higher salinities as a result of extended sea-ice formation in the Weddell Gyre (Collares et al., 2018; Thompson et al., 2009). Here, it encounters
- Formatiert: Schriftart: (Standard) Times New Roman, Schriftfarbe: Automatisch
- Formatiert: Schriftart: (Standard) Times New Roman, Schriftfarbe: Rot
- Formatiert: Schriftart: (Standard) Times New Roman, Schriftfarbe: Automatisch
- Formatiert: Schriftart: (Standard) Times New Roman
- Formatiert: Schriftart: (Standard) Times New Roman
- Gelöscht: shifts of
- Formatiert: Schriftart: (Standard) Times New Roman
- Gelöscht: is
- Formatiert: Schriftart: (Standard) Times New Roman
- Gelöscht: West
- Formatiert: Schriftart: (Standard) Times New Roman
- Gelöscht: East Antarctic Peninsula
- Formatiert: Schriftart: (Standard) Times New Roman
- Gelöscht:
- Formatiert: Schriftart: (Standard) Times New Roman
- Gelöscht: <Objekt><Objekt>
- Formatiert: Schriftart: (Standard) Times New Roman
- Gelöscht:
- Formatiert: Schriftart: (Standard) Times New Roman

- [2] verschoben (Einfügung)
- Formatiert: Schriftart: (Standard) +Überschriften CS (Times New Roman), 10 Pt., Fett, Nicht Kursiv, Schriftfarbe: Text 1
- Gelöscht:Abschnittswechsel (Nächste Seite).....
- Formatiert: Nach: 0.63 cm

336 **3. Material and methods**

337 **3.1 Sediment samples**

338 In total, we analysed a set of 41 surface sediment samples from different areas of the Southern Ocean

339 (Fig. 1) retrieved by multicorers and giant box corers during RV Polarstern expeditions over the past

340 15 years. Sixteen surface sediment samples from the Amundsen Sea continental shelf were collected

341 during RV Polarstern expeditions PS69 in 2006 (Gohl, 2007) and PS104 in 2017 (Gohl, 2017). Twenty-

342 five surface sediment samples from the southeastern and southwestern Weddell Sea continental shelf

343 were collected during RV Polarstern expeditions PS111 in 2018 (Schröder, 2018) and PS118 in 2019

344 (Dorschel, 2019). This set of samples was complemented by 26 surface sediment samples from the

345 Bransfield Strait/WAP for which the analytical results had been previously published by Vorrath et al.

346 (2019).

347

348 **3.2 Bulk sediment and organic geochemical analyses**

349 The sediment material was freeze-dried and homogenized with an agate mortar and stored in glass vials

350 at -20 °C before and after these initial preparation steps to avoid degradation of targeted molecular

351 components. Total organic carbon (TOC) contents were measured on 0.1 g of sediment after removing

352 inorganic carbon (total inorganic carbon, carbonates) with 500 µl 12 N hydrochloric acid.

353 Measurements were conducted by means of a carbon-sulphur determinator (CS 2000; Eltra) with

354 standards being measured for calibration before sample analyses and after every tenth sample to ensure

355 accuracy (error ± 0.02 %).

356 Lipid biomarkers were extracted from the sediments (4 g for PS69 and PS104; 6 g for PS111 and PS118)

357 by ultrasonication (3 x 15 min), using dichloromethane:methanol (3 x 6 ml for PS69 and PS104; 3 x 8

358 ml for PS111 and PS118; 2:1 v/v) as solvent. Prior to this step, the internal standards 7-hexylnonadecane

359 (7-HND; 0.038 µg/sample for PS69 and PS104 and 0.057 µg/sample for PS111 and PS118), 5α-

360 androstan-3-ol (1.04 µg/sample) and C₄₆ (0.98 µg/sample) were added to the sample for quantification

361 of HBIs, sterols and GDGTs, respectively. Via open-column chromatography, with SiO₂ as stationary

362 phase, fractionation of the extract was achieved by eluting the apolar fraction (HBIs) and the polar

- Formatiert ... [118]
- Formatiert ... [120]
- Formatiert ... [119]
- Formatiert ... [121]
- Gelöscht: material
- Formatiert ... [122]
- Formatiert ... [123]
- Gelöscht:), all have been
- Formatiert ... [124]
- Gelöscht: in
- Formatiert ... [125]
- Gelöscht: 16
- Formatiert ... [126]
- Gelöscht: 2007
- Formatiert ... [127]
- Gelöscht: 25
- Formatiert ... [128]
- Gelöscht: West Antarctic Peninsula
- Formatiert ... [129]
- Gelöscht: were already
- Formatiert ... [130]
- Gelöscht:
- Formatiert ... [131]
- Gelöscht: ¶
- Formatiert ... [132]
- Formatiert ... [133]
- Formatiert ... [134]
- Gelöscht: The analysis of total
- Formatiert ... [135]
- Gelöscht: was conducted
- Formatiert ... [136]
- Gelöscht: biomarker extraction of
- Formatiert ... [137]
- Gelöscht: sediment
- Formatiert ... [138]
- Gelöscht: was done
- Formatiert ... [139]
- Gelöscht: 20 µl
- Formatiert ... [140]
- Gelöscht: 30 µl
- Formatiert ... [141]
- Gelöscht: 40 µl
- Formatiert ... [142]
- Gelöscht: 100 µl
- Formatiert ... [143]
- Formatiert ... [117]

403 fraction (sterols and GDGTs) with 5 ml n-hexane and 5 ml DCM/MeOH 1:1, respectively. The polar
 404 fraction was subsequently split into two fractions (sterols and GDGTs) for further processing. The sterol
 405 fraction was silylated with 300 µl bis-trimethylsilyl-trifluoroacetamide (BSTFA; 2h at 60 °C).
 406 Compound analyses of HBIs and sterols were carried out on an Agilent Technologies 7890B gas
 407 chromatograph (GC; fitted with a 30 m DB 1MS column; 0.25 mm diameter and 0.25 µm film thickness)
 408 coupled to an Agilent Technologies 5977B mass selective detector (MSD; with 70 eV constant
 409 ionization potential, ion source temperature of 230 °C). The GC oven was set to: 60 °C (3 min), 150 °C
 410 (rate: 15 °C/min), 320 °C (rate: 10 °C/min), 320 °C (15 min isothermal) for the analysis of hydrocarbons
 411 and to: 60 °C (2 min), 150 °C (rate: 15 °C/min), 320 °C (rate: 3 °C/min), 320 °C (20 min isothermal)
 412 for the analysis of sterols. Helium was used as carrier gas. The identification of HBI and sterol
 413 compounds is based upon their GC retention times and mass spectra (Belt, 2018; Belt et al., 2000; Boon
 414 et al., 1979). Lipid quantification was obtained by setting the individual, manually integrated, GC-MS
 415 peak area in relation to the peak area of the respective internal standard and normalization to the amount
 416 of extracted sediment. Quantification of IP_{SO}₂₅ and HBI trienes was achieved using their molecular
 417 ions (IP_{SO}₂₅: m/z 348 and HBI trienes: m/z 346) in relation to the fragment ion m/z 266 of the internal
 418 standard 7-HND (Belt, 2018). Quantification of sterols was achieved by comparison of the molecular
 419 ion of the individual sterol with the molecular ion m/z 348 of the internal standard 5 α -androstan-3-ol.
 420 Instrumental response factors for the target lipids were considered as recommended by Belt et al. (2014)
 421 and Fahl and Stein (2012). All biomarker concentrations were subsequently normalized to the TOC
 422 content of each sample to account for different depositional settings within the different study areas.
 423 For calculating the phytoplankton-IP_{SO}₂₅ (PIP_{SO}₂₅) index, we used the equation introduced by Vorrath
 424 et al. (2019):
 425
$$PIP_{SO_{25}} = IP_{SO_{25}} / (IP_{SO_{25}} + (\text{phytoplankton marker} \times c)) \quad (1)$$

 426 where c (c = mean IP_{SO}₂₅/mean phytoplankton marker) is applied as a concentration balance factor to
 427 account for high concentration offsets between IP_{SO}₂₅ and the phytoplankton biomarker (see Table S1
 428 for c-factors of individual PIP_{SO}₂₅ calculations).
 429 Following the approach by Müller and Stein (2014) and Lamping et al. (2020), samples with
 430 exceptionally low (at detection limit) concentrations of both biomarkers have been assigned a PIP_{SO}₂₅

- Gelöscht: Z-triene
- Formatiert: Schriftart: (Standard) Times New Roman
- Gelöscht: ion
- Formatiert: Schriftart: (Standard) Times New Roman
- Formatiert: Schriftart: (Standard) +Überschriften CS (Times New Roman)
- Gelöscht: Z-triene
- Formatiert: Schriftart: (Standard) +Überschriften CS (Times New Roman)
- Gelöscht: fragment
- Formatiert: Schriftart: (Standard) +Überschriften CS (Times New Roman)
- Gelöscht: fragment
- Formatiert: Schriftart: (Standard) +Überschriften CS (Times New Roman)
- Formatiert: Schriftart: (Standard) +Überschriften CS (Times New Roman)
- Formatiert: Schriftart: (Standard) +Überschriften CS (Times New Roman), Schriftfarbe: Automatisch
- Formatiert: Schriftart: (Standard) +Überschriften CS (Times New Roman)
- Gelöscht:
- Formatiert: Schriftart: (Standard) +Überschriften CS (Times New Roman)
- Formatiert: Schriftart: (Standard) Times New Roman
- Gelöscht: $PIP_{SO_{25}} = IP_{SO_{25}} / (IP_{SO_{25}} + (\text{phytoplankton marker} \times c)) \rightarrow (1)$
- Formatiert: Schriftart: (Standard) Times New Roman
- Formatiert: Block, Zeilenabstand: Doppelt
- Formatiert: Schriftart: (Standard) Times New Roman, Schriftfarbe: Automatisch
- Formatiert: Nach: 0.63 cm

439 value of 1 (see chapter 4.1.2). This comprises the five Weddell Seam samples PS111/13-2, /15-1, /16-
 440 3, /29-3 and /40-2 (marked as orange x in Fig. 1).

441 The GDGT fraction was dried under N₂, redissolved with 120 µl hexane:isopropanol (v/v 99:1) and
 442 then filtered using a polytetrafluoroethylene (PTFE) filter with a 0.45 µm pore sized membrane. GDGT
 443 measurements were carried out using high performance liquid chromatography (HPLC; Agilent 1200
 444 series HPLC system) coupled to an Agilent 6120 mass spectrometer (MS), operating with atmospheric
 445 pressure chemical ionization (APCI). The injection volume was 20 µl. For separating the GDGTs, a
 446 Prevail Cyano 3 µm column (Grace, 150 mm * 2.1 mm) was kept at 30 °C. Each sample was eluted
 447 isocratically for 5 min with solvent A = hexane/2-propanol/chloroform; 98:1:1 at a flow rate of 0.2
 448 ml/min, then the volume of solvent B = hexane/2-propanol/chloroform; 89:10:1 was increased linearly
 449 to 10 % within 20 min and then to 100 % within 10 min. The column was back-flushed (5 min, flow
 450 0.6 ml/min) after 7 min after each sample and re-equilibrated with solvent A (10 min, flow 0.2 ml/min).
 451 The APCI was set to the following: N₂ drying gas flow at 5 l/min and temperature to 350 °C, nebulizer
 452 pressure to 50 psi, vaporizer gas temperature to 350 °C, capillary voltage to 4 kV and corona current to
 453 +5 µA. Detection of GDGTs was achieved by means of selective ion monitoring (SIM) of [M+H]⁺ ions
 454 (dwell time 76 ms). Determination and quantification of the molecular ions of GDGT-0 (*m/z* 1302),
 455 GDGT-1 (*m/z* 1300), GDGT-2 (*m/z* 1298), GDGT-3 (*m/z* 1296) and crenarchaeol (*m/z* 1292) as well as
 456 of brGDGT-III (*m/z* 1050), brGDGT-II (*m/z* 1036) and brGDGT-I (*m/z* 1022) was done in relation to
 457 the molecular ion *m/z* 744 of the internal standard C₄₆-GDGT. The late eluting hydroxylated GDGTs
 458 (OH-GDGT-0, OH-GDGT-1 and OH-GDGT-2 with *m/z* 1318, 1316 and 1314, respectively) were
 459 quantified in the scans (*m/z* 1300, 1298, 1296) of their related GDGTs, as described by Fietz et al.
 460 (2013).

461 TEX₈₆^I values and their conversion into SOTs were determined following Kim et al. (2012):

462
$$TEX_{86}^I = \text{LOG} \frac{[GDGT-2]}{[GDGT-1]+[GDGT-2]+[GDGT-3]} \quad (2)$$

463
$$SOT^{TEX} [^{\circ}C] = 50.8 \times TEX_{86}^I + 36.1 \quad (3)$$

464 Temperature calculations based on OH-GDGTs were carried out according to Lü et al. (2015):

465
$$RI - OH' = \frac{[OH-GDGT-1]+2 \times [OH-GDGT-2]}{[OH-GDGT-0]+[OH-GDGT-1]+[OH-GDGT-2]} \quad (4)$$

Gelöscht: accounts for

Gelöscht: sample stations in the

Gelöscht: Sea

Formatiert: Schriftart: (Standard) Times New Roman, Schriftfarbe: Automatisch

Formatiert: Schriftart: (Standard) Times New Roman, Schriftfarbe: Automatisch

Formatiert: Schriftart: (Standard) Times New Roman, Schriftfarbe: Automatisch

Gelöscht: ;

Formatiert: Schriftart: (Standard) Times New Roman, Schriftfarbe: Automatisch

Formatiert: Schriftart: (Standard) Times New Roman

Formatiert: Schriftart: (Standard) Times New Roman, Englisch (Vereinigtes Königreich)

Formatiert: Schriftart: (Standard) Times New Roman

Formatiert: Schriftart: (Standard) Times New Roman, Schriftfarbe: Automatisch

Formatiert: Schriftart: (Standard) Times New Roman

Gelöscht:

Formatiert: Schriftart: (Standard) Times New Roman, Schriftfarbe: Automatisch

Formatiert: Schriftart: (Standard) +Überschriften CS (Times New Roman)

Gelöscht: temperatures

Formatiert: Schriftart: (Standard) +Überschriften CS (Times New Roman)

Gelöscht: 2010

Formatiert: Schriftart: (Standard) +Überschriften CS (Times New Roman)

Gelöscht: TEX_{86}^I

Gelöscht: $\text{LOG} \frac{[GDGT-2]}{[GDGT-1]+[GDGT-2]+[GDGT-3]}$

Formatiert: Schriftart: (Standard) +Überschriften CS (Times New Roman)

Gelöscht: → → → →

Formatiert: Schriftart: (Standard) +Überschriften CS (Times New Roman)

Gelöscht: $SST^{TEX} [^{\circ}C] = 67.5 \times TEX_{86}^I + 46.9$. → → → → →

Formatiert: Schriftart: (Standard) +Überschriften CS (Times New Roman)

Formatiert: Block, Zeilenabstand: Doppelt

Gelöscht: $RI - OH' = \frac{[OH-GDGT-1]+2 \times [OH-GDGT-2]}{[OH-GDGT-0]+[OH-GDGT-1]+[OH-GDGT-2]}$

$SST^{OH} [^{\circ}C] = (RI - OH' - 0.1) / 0.0382$. → → → → →

(5) ||

Formatiert: Nach: 0.63 cm

482 $SST^{OH} [^{\circ}C] = RI - OH' - 0.1/0.0382 .$ (5)

483 To determine the relative influence of terrestrial organic matter input, the **Branched Isoprenoid**
 484 **Tetraether (BIT)** index was calculated following Hopmans et al. (2004):

485
$$BIT = \frac{[brGDGT-I]+[brGDGT-II]+[brGDGT-III]}{[Chrenarchaeol]+[brGDGT-I]+[brGDGT-II]+[brGDGT-III]}$$
 (6)

487 **3.3 Numerical model**

488 **3.3.1 Model description**

489 AWI-ESM2 is a state-of-the-art coupled climate model developed by Sidorenko et al. (2019) which
 490 comprises an atmospheric component ECHAM6 (Stevens et al., 2013) as well as an ocean-sea ice
 491 component FESOM2 (Danilov et al., 2017). The atmospheric module ECHAM6 is the most recent
 492 version of the ECHAM model developed at the Max Planck Institute for Meteorology (MPI) in
 493 Hamburg. The model is branched from an early release of the European Center (EC) for Medium Range
 494 Weather Forecasts (ECMWF) model (Roeckner et al., 1989). ECHAM6 dynamics is based on
 495 hydrostatic primitive equations with traditional approximation. We used a T63 Gaussian grid which has
 496 a spatial resolution of about 1.9 x 1.9 degree (1.9 ° or 210 km). There are 47 vertical layers in the
 497 atmosphere.

498 Momentum transport arising from boundary effects is configured using the subgrid orography scheme
 499 as described by Lott (1999). Radiative transfer in ECHAM6 is represented by the method described in
 500 Iacono et al. (2008). ECHAM6 also contains a Land-Surface Model (JSBACH) which includes 12
 501 functional plant types of dynamic vegetation and 2 bare-surface types (Loveland et al., 2000; Raddatz
 502 et al., 2007). The ice-ocean module in AWI-ESM2 is based on the finite volume discretization
 503 formulated on unstructured meshes. The multi-resolution for the ocean is up to 15 km over polar and
 504 coastal regions, and 135 km for far-field oceans, with 46 uneven vertical depths. The impact of local
 505 dynamics on the global ocean is related to a number of FESOM-based studies (Danilov et al., 2017).
 506 The multi-resolution approach advocated by FESOM allows one to explore the impact of local
 507 processes on the global ocean with moderate computational effort (Danilov et al., 2017). AWI-ESM2
 508 employs the OASIS3-MCT coupler (Valcke, 2013) with an intermediate regular exchange grid.

Formatiert: Schriftart: (Standard) +Überschriften CS (Times New Roman)

Formatiert: Block, Zeilenabstand: Doppelt

Formatiert: Schriftart: (Standard) +Überschriften CS (Times New Roman)

Gelöscht: -

Formatiert: Schriftart: (Standard) +Überschriften CS (Times New Roman)

Gelöscht:
$$BIT = \frac{[brGDGT-I]+[brGDGT-II]+[brGDGT-III]}{[Chrenarchaeol]+[brGDGT-I]+[brGDGT-II]+[brGDGT-III]}$$
 (6)

Formatiert: Standard, Block, Einzug: Vor: 0.99 cm, Hängend: 1.01 cm, Zeilenabstand: Doppelt, Keine Aufzählungen oder Nummerierungen

Formatiert: Schriftart: (Standard) Times New Roman, Schriftfarbe: Automatisch

Gelöscht:

Formatiert: Schriftart: (Standard) Times New Roman

Formatiert: Schriftart: (Standard) Times New Roman, Englisch (Vereinigtes Königreich)

Formatiert: Block, Einzug: Vor: 1.5 cm, Zeilenabstand: Doppelt

Formatiert: Block, Zeilenabstand: Doppelt

Formatiert: Schriftart: (Standard) Times New Roman, Englisch (Vereinigtes Königreich)

Formatiert: Nach: 0.63 cm

515 Mapping between the intermediate grid and the atmospheric/oceanic grid is handled with bilinear
516 interpolation. The atmosphere component computes 12 air-sea fluxes based on four surface fields
517 provided by the ocean module FESOM2. AWI-ESM2 has been validated under modern climate
518 conditions (Sidorenko et al., 2019) and has been applied for marine radiocarbon concentrations
519 (Lohmann et al., 2020), the latest Holocene (Vorrath et al., 2020), and the Last Interglacial (Otto-
520 Bliesner et al., 2021).

521 3.3.2 Experimental design

522 One transient experiment was conducted using AWI-ESM2, which applied the boundary conditions,
523 including orbital parameters and greenhouse gases. Orbital parameters are calculated according to
524 Berger (1978), and the concentrations of greenhouse gases are taken from ice-core records as well as
525 from recent measurements of firn air and atmospheric samples (Köhler et al., 2017). The model was
526 initialized from a 1,000-year spin-up run under mid-Holocene (6,000 before present, BP) boundary
527 conditions as described by Otto-Bliesner et al. (2017). In our modeling strategy, we follow Lorenz and
528 Lohmann (2004) and use the climate condition from the mid-Holocene spin-up run as the initial state
529 for the subsequent transient simulation covering the period from 6,000 BP to 2014 CE. In the present
530 study we derived seasonal SIC, SSTs and SOTs in the study area from a segment of the transient
531 experiment (1950-2014 CE). Topography including prescribed ice sheet configuration was kept
532 constant in our transient simulation. All model data are provided in Table S2.

533 3.4 Satellite SIC and SSTs

534 Satellite sea-ice data are derived from Nimbus-7 SMMR and DMSP SSM/I-SSMIS passive microwave
535 data and downloaded from the National Snow and Ice Data Center (NSIDC; Cavalieri et al., 1996). The
536 sea-ice data represent mean monthly SIC, which are expressed to range from 0 % to 100 % and are
537 averaged over a period of the beginning of satellite observations in 1978 CE to the individual year of
538 sample retrieval. The monthly mean SIC were then split into different seasons: winter (JJF), spring
539 (SON) and summer (DJF) (Fig. 2a-c) and the data are considered to represent the recent mean state of
540 sea-ice coverage. All satellite data are provided in Table S3.

Formatiert: Schriftart: (Standard) Times New Roman, Schriftfarbe: Automatisch, Englisch (Vereinigtes Königreich)

Formatiert: Schriftart: (Standard) Times New Roman, Englisch (Vereinigtes Königreich)

Formatiert: Block, Einzug: Vor: 1.5 cm, Zeilenabstand: Doppelt

Formatiert: Block, Zeilenabstand: Doppelt

Formatiert: Schriftart: (Standard) Times New Roman, Englisch (Vereinigtes Königreich)

Formatiert: Schriftart: (Standard) Times New Roman, Englisch (Vereinigtes Königreich)

Gelöscht: (

Formatiert: Schriftart: (Standard) Times New Roman, Englisch (Vereinigtes Königreich)

Gelöscht: ,

Formatiert: Schriftart: (Standard) Times New Roman, Schriftfarbe: Automatisch, Englisch (Vereinigtes Königreich)

Formatiert: Schriftart: (Standard) Times New Roman, Englisch (Vereinigtes Königreich)

Gelöscht: preindustrial state as

Formatiert: Schriftart: (Standard) Times New Roman, Englisch (Vereinigtes Königreich)

Gelöscht: and

Formatiert: Schriftart: (Standard) Times New Roman, Englisch (Vereinigtes Königreich)

Formatiert: Schriftart: (Standard) Times New Roman, Englisch (Vereinigtes Königreich)

Gelöscht: .

Formatiert: Schriftart: (Standard) Times New Roman, Englisch (Vereinigtes Königreich)

Formatiert: Schriftart: (Standard) Times New Roman, Englisch (Vereinigtes Königreich)

Formatiert: Schriftart: (Standard) Times New Roman, Englisch (Vereinigtes Königreich)

Formatiert: Block, Einzug: Vor: 1 cm, Zeilenabstand: Doppelt

Gelöscht:

Formatiert: Schriftart: (Standard) Times New Roman, Englisch (Vereinigtes Königreich)

Gelöscht:

Formatiert: Schriftart: (Standard) Times New Roman, Englisch (Vereinigtes Königreich)

Formatiert: Block, Zeilenabstand: Doppelt

Formatiert: Schriftart: (Standard) Times New Roman, Englisch (Vereinigtes Königreich)

Formatiert: Schriftart: (Standard) Times New Roman, Englisch (Vereinigtes Königreich)

Formatiert: Nach: 0.63 cm



550 Modern annual mean SSTs and SOTs are derived from the World Ocean Atlas 13 representing averaged
 551 values for the years 1955-2012 CE (WOA13; Locamini et al., 2013).

553 **4. Results and discussion**

554 In the following, we first present and discuss the biomarker data assembled during this study from North
 555 (Antarctic Peninsula) to South (Amundsen and Weddell Seas) and draw conclusions about the
 556 environmental settings deduced from the data set. As phytoplankton-derived biomarkers, we here focus
 557 on the significance of HBI Z-triene and brassicasterol, while HBI E-triene and dinosterol - showing
 558 very similar patterns - are moved to the supplements (Fig. S1) to avoid repetition. All biomarker data
 559 collected during this study are provided in Table S1 and are available via the PANGAEA data repository
 560 (in prep.). For the discussion of the target environmental variables, i.e. PIPSO₂₅-based sea ice and
 561 GDGT-derived ocean temperature estimates, satellite and instrumental as well as modelled data are
 562 considered. In Sect. 5, we further address potential caveats in biomarker-based environmental
 563 reconstructions that need to be considered when applying these proxies.

565 **4.1 TOC content, HBIs and sterols in Antarctic surface sediments**

566 TOC contents in marine sediments in a first approximation are often viewed as an indicator for primary
 567 productivity in surface waters (Meyers, 1997). However, we are aware that additional factors, such as
 568 different water depths or depositional regimes, may exert control on sedimentary TOC as well. The
 569 TOC contents of the herein investigated surface samples are lowest in Drake Passage with values around
 570 0.12-0.54 %, increasing in a northwest-southeast gradient into Bransfield Strait, ranging between 0.59
 571 and 1.06 % (Fig. 3a; WAP). At the EAP, higher TOC contents (0.57-0.86 %) prevail around the Larsen
 572 Ice Shelf with a decreasing trend towards the Powell Basin (0.22-0.37 %) and an increase to 0.50 %
 573 around the area of the South Orkney Islands, which may point to elevated productivity or enhanced
 574 supply of reworked terrigenous organic matter in these areas (Fig. 3a; EAP).

- Formatiert ... [145]
- [1] nach oben verschoben: Fig.
- Gelöscht: (
- Formatiert ... [146]
- Gelöscht: 5c;
- Gelöscht: →
- Gelöscht: Abschnittswechsel (Nächste Seite)
- Formatiert ... [147]
- Formatiert ... [148]
- Formatiert ... [149]
- Gelöscht: <#>Environmental settings of the Southern
- Gelöscht: <#> and model
- Formatiert ... [154]
- Formatiert ... [151]
- Formatiert ... [152]
- Gelöscht: <#>describe
- Formatiert ... [153]
- Gelöscht: ¶
- Formatiert ... [155]
- Formatiert ... [156]
- Gelöscht:
- Formatiert ... [157]
- Gelöscht:
- Formatiert ... [158]
- Formatiert ... [159]
- Gelöscht:), however
- Formatiert ... [160]
- Gelöscht: the
- Formatiert ... [161]
- Gelöscht: the
- Gelöscht: -
- Formatiert ... [162]
- Formatiert ... [163]
- Gelöscht: ¶
- Formatiert ... [164]
- Gelöscht: East Antarctic Peninsula
- Formatiert ... [165]
- Gelöscht: pointing
- Formatiert ... [166]
- Gelöscht: in these areas (Fig.
- [3] nach unten verschoben: 3a; EAP.
- Formatiert ... [167]
- Gelöscht: The elevated TOC contents in this area may
- Formatiert ... [169]
- [3] verschoben (Einfügung)
- Formatiert ... [170]
- Gelöscht: .
- Formatiert ... [171]
- Formatiert ... [144]

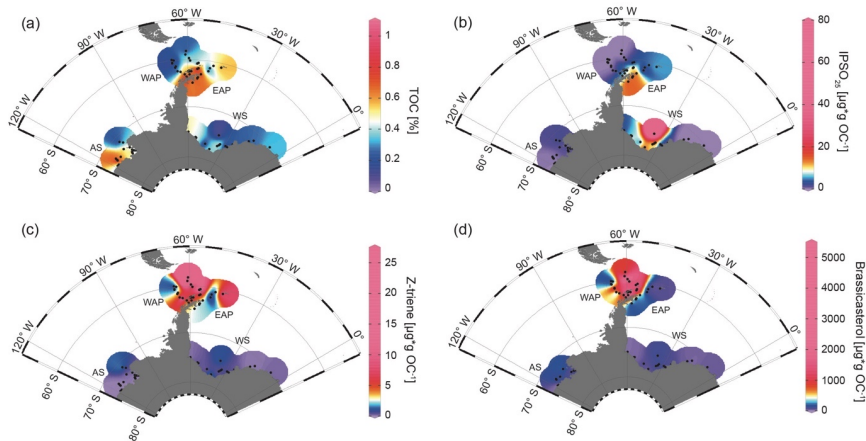


Fig. 3: Distribution of (a) TOC [%], (b) IPSO₂₅, (c) Z-triene and (d) brassicasterol in surface sediment samples. Sample locations are marked as black dots. Concentrations of biomarkers [$\mu\text{g} \cdot \text{g} \text{OC}^{-1}$] were normalized to the TOC content of each sample. AS: Amundsen Sea, WAP: West Antarctic Peninsula, EAP: East Antarctic Peninsula, WS: Weddell Sea.

627 At the WAP, concentrations of the sea-ice biomarker IPSO₂₅ show a northwest-southeast gradient with
 628 IPSO₂₅ being absent in samples from the permanently ice-free Drake Passage and increasing
 629 concentrations towards the continental slope and the seasonally ice-covered continental shelf (0.37-
 630 17.81 $\mu\text{g} \cdot \text{g} \text{OC}^{-1}$; Fig. 3b; Vorrath et al., 2019). Highest IPSO₂₅ concentrations are observed in samples
 631 of the northern Bransfield Strait which is affected by inflow of water masses from the Weddell Sea
 632 through the Antarctic Sound and along the Antarctic Peninsula and frequent transport of sea ice into the
 633 Bransfield Strait (Vorrath et al., 2019). Elevated IPSO₂₅ concentrations are also observed at the EAP,
 634 influenced by a seasonal sea-ice cover, where relatively higher concentrations of the sea-ice biomarker
 635 prevail in those samples located in front of the Larsen Ice Shelf (12.59-17.74 $\mu\text{g} \cdot \text{g} \text{OC}^{-1}$; Fig. 3b). As
 636 these locations are also influenced by the northward drift of sea ice within the Weddell Gyre (Fig. 1),
 637 the elevated IPSO₂₅ concentrations could also result from sea ice advected from the southern Weddell
 638 Sea. We suggest that the decreasing IPSO₂₅ concentrations towards the Powell Basin and the South
 639 Orkney Islands (0.59-5.36 $\mu\text{g} \cdot \text{g} \text{OC}^{-1}$; Fig. 3b) can be connected to warmer ocean temperatures towards
 640 the North and less sea-ice coverage during spring.

Gelöscht: At the West Antarctic Peninsula

Formatiert: Schriftart: (Standard) Times New Roman

Formatiert: Block, Zeilenabstand: Doppelt

Formatiert: Schriftart: (Standard) Times New Roman

Gelöscht: TWW

Formatiert: Schriftart: (Standard) Times New Roman

Formatiert: Schriftart: (Standard) Times New Roman

Gelöscht: which frequently exports

Formatiert: Schriftart: (Standard) Times New Roman

Gelöscht: from the Weddell Sea

Formatiert: Schriftart: (Standard) Times New Roman

Gelöscht: High

Formatiert: Schriftart: (Standard) Times New Roman

Gelöscht: East Antarctic Peninsula

Formatiert: Schriftart: (Standard) Times New Roman

Gelöscht: by

Formatiert: Schriftart: (Standard) Times New Roman

Gelöscht: the

Formatiert: Schriftart: (Standard) Times New Roman

Gelöscht: increased

Formatiert: Schriftart: (Standard) Times New Roman

Gelöscht: melt

Formatiert: Schriftart: (Standard) Times New Roman

Gelöscht: and summer

Formatiert: Schriftart: (Standard) Times New Roman

Formatiert: Schriftart: (Standard) Times New Roman, Schriftfarbe: Automatisch

Formatiert: Nach: 0.63 cm

651 Concentrations of the phytoplankton biomarker HBI Z-triene around the Antarctic Peninsula are highest
652 in the eastern Drake Passage and along the continental slope (where IPSO₂₅ is absent) and decrease in
653 the Bransfield Strait (0.33-26.86 µg*g OC⁻¹; Fig. 3c; Vorrath et al., 2019). Elevated HBI Z-triene
654 concentrations have thus far been detected in surface waters along an ice edge (Smik et al., 2016) and
655 hence suggested to be a proxy for marginal ice zone conditions (Belt et al., 2015; Collins et al., 2013;
656 Schmidt et al., 2018). Vorrath et al. (2019), however, relate the high concentrations of HBI Z-triene at
657 the northernmost stations in the permanently ice-free eastern Drake Passage to their proximity to the
658 Antarctic Polar Front. Here, productivity of the source diatoms of HBI-trienes (e.g., *Rhizosolenia* spp.;
659 Belt et al., 2017) may be enhanced by meander-induced upwelling leading to increased nutrient flux to
660 surface waters (Moore and Abbott, 2002). Since Cardenas et al. (2019) document only minor
661 abundances of *Rhizosolenia* spp. in surface sediments from this area, we assume that HBI-trienes might
662 also be biosynthesized by other diatoms. Moderate concentrations along the continental slope of the
663 WAP and in the Bransfield Strait have been associated with elevated inflow of warm BSW which leads
664 to a retreating sea-ice margin during spring and summer (for more details, see Vorrath et al., 2019,
665 2020). Samples from the EAP continental shelf and the Powell Basin are characterised by relatively
666 low concentrations of HBI Z-triene (Fig. 3c; 0.1-2.37 µg*g OC⁻¹), showing a southwest-northeast
667 gradient, while the northernmost sample closest to the South Orkney Islands is characterized by an
668 elevated HBI Z-triene concentration of ~8.49 µg*g OC⁻¹ (Fig. 3c; EAP). This relatively high
669 concentration may be related to an “Island Mass Effect”, coined by Doty and Oguri (1956), which refers
670 to an increased primary production around oceanic islands in comparison to surrounding waters. Nolting
671 et al. (1991) found extraordinarily high dissolved iron levels (as high as 50-60 nM) on the shelf of the
672 South Orkney Islands, and Nielsdóttir et al. (2012) observed enhanced iron and Chl *a* concentrations in
673 the vicinity of the South Orkney Islands. These authors explain the increased dissolved iron levels with
674 input from seasonally retreating sea ice, which is recorded by satellites (Fig. 2a-c) and probably leads
675 to substantial annual phytoplankton blooms, which may also cause the elevated TOC content in the
676 corresponding seafloor sediment sample (Fig. 3a). Alternatively, remobilization of shelf sediments or
677 vertical mixing of iron-rich deep waters leading to high iron contents in surface waters may stimulate
678 primary productivity (Blain et al., 2007; de Jong et al., 2012). However, it remains unclear why the

- Formatiert: Schriftart: (Standard) Times New Roman
- Gelöscht: with lower concentrations
- Formatiert: Schriftart: (Standard) Times New Roman
- Gelöscht: MIZ
- Formatiert: Schriftart: (Standard) Times New Roman
- Formatiert: Schriftart: (Standard) Times New Roman, Schriftfarbe: Automatisch
- Formatiert: Schriftart: (Standard) Times New Roman
- Formatiert: Schriftart: (Standard) Times New Roman
- Formatiert: Schriftart: (Standard) Times New Roman
- Gelöscht: West Antarctic Peninsula
- Formatiert: Schriftart: (Standard) Times New Roman
- Gelöscht: lead
- Formatiert: Schriftart: (Standard) Times New Roman
- Gelöscht: . (
- Formatiert ... [173]
- Gelöscht:) and Vorrath et al. (
- Formatiert ... [172]
- Formatiert ... [174]
- Formatiert: Schriftart: (Standard) Times New Roman
- Gelöscht: East Antarctic Peninsula
- Formatiert: Schriftart: (Standard) Times New Roman
- Gelöscht: where IPSO₂₅ concentrations are highest;
- Formatiert: Schriftart: (Standard) Times New Roman
- Gelöscht: ; Fig. 3b
- Formatiert: Schriftart: (Standard) Times New Roman
- Gelöscht: higher
- Formatiert: Schriftart: (Standard) Times New Roman
- Gelöscht:
- Formatiert: Schriftart: (Standard) Times New Roman
- Gelöscht: also
- Formatiert: Schriftart: (Standard) Times New Roman
- Formatiert: Schriftart: (Standard) Times New Roman
- Gelöscht: They connect, among others,
- Formatiert: Schriftart: (Standard) Times New Roman
- Formatiert: Schriftart: (Standard) Times New Roman
- Formatiert: Schriftart: (Standard) Times New Roman
- Gelöscht: a
- Formatiert: Schriftart: (Standard) Times New Roman
- Gelöscht: bloom
- Formatiert: Schriftart: (Standard) Times New Roman
- Gelöscht: contents in that
- Formatiert: Schriftart: (Standard) Times New Roman
- Gelöscht: 3a). We
- Formatiert: Nach: 0.63 cm

696 brassicasterol concentration is distinctly low in this sample, and we assume that different environmental
 697 preferences of the source organisms may account for this. In Drake Passage and the EAP, brassicasterol
 698 displays a similar pattern as the HBI Z-triene, with relatively high concentrations (more than 2 orders
 699 of magnitudes), ranging between 1.86 and 5017.44 $\mu\text{g} \cdot \text{g} \text{OC}^{-1}$ (Fig. 3d).
 700 In the Weddell Sea, TOC contents are generally lower ($< 0.4\%$), with slightly elevated values in the
 701 West (up to 0.50 %) and right in front of the Filchner Ice Shelf (up to 0.52 %; Fig. 3a). The Amundsen
 702 Sea is characterized by slightly higher TOC contents, with concentrations of up to 0.91 % in the West
 703 and lower values in the East (0.33 %; Fig. 3a; AS).
 704 In the samples from the Amundsen and Weddell Seas, dominated by a strong winter sea-ice cover
 705 lasting until spring (Fig. 2a-c), all three biomarkers are present in low concentrations only. An exception
 706 are the samples located in front of the Filchner Ice Shelf with significantly higher concentrations of
 707 IP_{SO}₂₅ (7.09-73.87 $\mu\text{g} \cdot \text{g} \text{OC}^{-1}$; Fig. 3b; WS). Concentrations of IP_{SO}₂₅ on the Amundsen Sea shelf are
 708 relatively low (0.04-3.3 $\mu\text{g} \cdot \text{g} \text{OC}^{-1}$), with slightly higher values observed towards the north-east (Fig.
 709 3b; AS). HBI Z-triene is also very low concentrated, showing slightly higher concentrations in Filchner
 710 Trough (0.04-1 $\mu\text{g} \cdot \text{g} \text{OC}^{-1}$) and towards the more distal locations in the northeastern Amundsen Sea
 711 (0.01-1.88 $\mu\text{g} \cdot \text{g} \text{OC}^{-1}$; Fig. 3c). Brassicasterol generally shows similar patterns as the HBI Z-triene,
 712 with concentrations ranging between 1.86 and 220.54 $\mu\text{g} \cdot \text{g} \text{OC}^{-1}$ (Fig. 3d; for HBI E-triene and
 713 dinosterol distribution, see Fig. S1).

714 4.2 Combining individual biomarker records: the PIPSO₂₅ index

716 The PIPSO₂₅ index combines the relative concentrations of IP_{SO}₂₅ and a selected phytoplankton
 717 biomarker, such as HBI-trienes and sterols, as indicator for an open-ocean environment (Vorrath et al.,
 718 2019). The combination of both end members (sea ice vs. open-ocean) prevents misleading
 719 interpretations regarding the absence of IP_{SO}₂₅ in the sediments, which can be the result of two entirely
 720 different scenarios. At heavy/perennial sea-ice conditions, the thickness of sea ice hinders light
 721 penetration, thereby limiting the productivity of algae living in basal sea ice (Hancke et al., 2018). This
 722 scenario may cause the absence of both phytoplankton and sea-ice biomarkers in the sediment. The
 723 other scenario depicts a permanently open ocean, where the sea-ice biomarker is absent as well, but

- Gelöscht: these conditions are favourable
- Formatiert ... [176]
- Formatiert ... [177]
- Gelöscht: the growth of the source diatoms of HBI Z-triene
- Formatiert ... [179]
- Gelöscht: the
- Formatiert ... [180]
- Gelöscht: East Antarctic Peninsula
- Formatiert ... [181]
- Gelöscht: higher
- Formatiert ... [182]
- [2] nach oben verschoben: Fig.
- Gelöscht:)
- Formatiert ... [183]
- Gelöscht: In the sample closest to the South Orkney
- Formatiert ... [185]
- Gelöscht: 3d; EAP), which could refer to different
- Formatiert ... [187]
- Formatiert ... [188]
- Gelöscht: %) (
- Formatiert ... [189]
- Gelöscht:
- Formatiert ... [190]
- Formatiert ... [191]
- Gelöscht: concentrated.
- Formatiert ... [192]
- Gelöscht: can be observed in
- Formatiert ... [193]
- Gelöscht: from right
- Formatiert ... [194]
- Gelöscht:)
- Formatiert ... [195]
- Gelöscht: within the
- Formatiert ... [196]
- Gelöscht: northeast of the
- Formatiert ... [197]
- Gelöscht: ¶
- Formatiert ... [198]
- Formatiert ... [199]
- Gelöscht: Targeting at a more quantitative assessment
- Formatiert ... [201]
- Gelöscht: the sea-ice biomarker
- Formatiert ... [202]
- Gelöscht: with
- Formatiert ... [203]
- Gelöscht: (P),
- Formatiert ... [204]
- Gelöscht: bottom
- Formatiert ... [205]
- Gelöscht: -
- Formatiert ... [206]
- Gelöscht: algae
- Formatiert ... [207]
- Gelöscht: result in
- Formatiert ... [208]
- Gelöscht: is dominated by
- Formatiert ... [209]
- Formatiert ... [175]

here, the phytoplankton biomarkers are present in variable concentrations (Müller et al., 2011). The presence of both biomarkers in the sediment is indicative of seasonal sea-ice coverage and/or the occurrence of stable sea-ice margin conditions, promoting biosynthesis of both biomarkers (Müller et al., 2011). We here distinguish between P_Z IPSO₂₅ and P_B IPSO₂₅ using HBI Z-triene and brassicasterol as phytoplankton biomarker, respectively (Fig. 4a+b; for PIPSO₂₅ values based on HBI E-triene and dinosterol see Table S1 and Fig. S2).

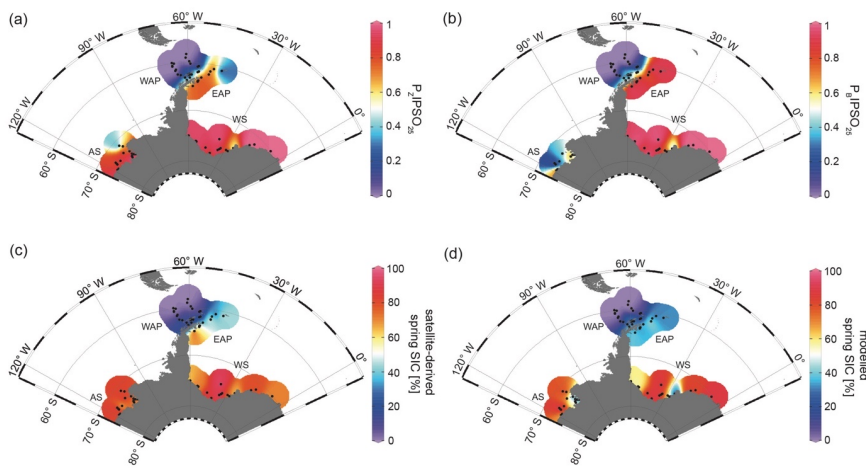


Fig. 4: Distribution of the sea-ice index PIPSO₂₅ in surface sediment samples, with (a) P_Z IPSO₂₅ based on Z-triene and (b) P_B IPSO₂₅ based on brassicasterol. (c) satellite-derived spring SIC [%] and (d) modelled spring SIC [%]. AS: Amundsen Sea, WAP: West Antarctic Peninsula, EAP: East Antarctic Peninsula, WS: Weddell Sea.

Both PIPSO₂₅ indices are 0 in the predominantly ice-free Drake Passage and display a northwest-southeast gradient to intermediate values towards the continental slope and the South Shetland Islands, reflecting increased influence of marginal sea-ice cover towards the coast (0.02-0.70; Vorrath et al., 2019). At the seasonally sea-ice covered EAP, P_Z IPSO₂₅ values reach 0.84, while lower values of around 0.25 are observed close to the South Orkney Islands, which relates to the elevated HBI Z-triene concentrations at the stations there (Fig. 3c; EAP). The P_B IPSO₂₅ index exhibits even higher values of up to 0.98 at the EAP/northwestern Weddell Sea. These elevated PIPSO₂₅ indices align well with the significant northward ice-drift within the Weddell Gyre in that region, which leads to prolonged sea-ice cover along the EAP.

Formatiert: Schriftart: (Standard) Times New Roman

Gelöscht: 4

Formatiert: Schriftart: (Standard) Times New Roman

Gelöscht: <Objekt><Objekt>

Formatiert: Schriftart: (Standard) Times New Roman

[4] verschoben (Einfügung)

Formatiert: Schriftart: (Standard) +Überschriften CS (Times New Roman), 10 Pt., Fett, Nicht Kursiv, Schriftfarbe: Text 1

Formatiert: Schriftart: Arial, Englisch (USA)

Formatiert: Zeilennummern unterdrücken

Formatiert: Schriftart: (Standard) Times New Roman

Formatiert: Block, Zeilenabstand: Doppelt

Gelöscht: influenced East Antarctic Peninsula

Formatiert: Schriftart: (Standard) Times New Roman

Gelöscht: that station

Formatiert: Schriftart: (Standard) Times New Roman

Gelöscht: , however, reveals

Formatiert: Schriftart: (Standard) Times New Roman

Formatiert: Schriftart: (Standard) Times New Roman

Gelöscht: East Antarctic Peninsula

Formatiert: Schriftart: (Standard) Times New Roman

Gelöscht: of up to 0.98 with no elevated values towards the South Orkney Islands.

Formatiert: Schriftart: (Standard) Times New Roman

Formatiert: Schriftart: (Standard) Times New Roman, Schriftfarbe: Automatisch

Gelöscht: in that region by

Formatiert: Schriftart: (Standard) Times New Roman, Schriftfarbe: Automatisch

Formatiert: Schriftart: (Standard) Times New Roman, Schriftfarbe: Automatisch

Gelöscht: high proximal

Formatiert: Schriftart: (Standard) Times New Roman, Schriftfarbe: Automatisch

Gelöscht: coverage at

Gelöscht: East Antarctic Peninsula.

Formatiert: Schriftart: (Standard) Times New Roman, Schriftfarbe: Automatisch

Formatiert: Schriftart: (Standard) Times New Roman

Formatiert: Nach: 0.63 cm

829 In samples from the southern Weddell Sea, both PIPSO₂₅ indices show a similar pattern with high values
830 up to 0.9, and slightly lower values in front of the Brunt Ice Shelf (0.6; Fig. 4a+b). Very low
831 concentrations (close to detection limit) of both biomarkers in samples located on the continental shelf
832 off Dronning Maud Land (Fig. 1) result in low PIPSO₂₅ values, strongly underestimating the sea-ice
833 cover in that area. Regarding the satellite-derived sea-ice data, this area of the continental shelf is
834 influenced by a severe seasonal sea-ice cover (Fig. 2). As previously mentioned, we followed the
835 approach by Müller and Stein (2014) and Lamping et al. (2020) and assigned a maximum PIPSO₂₅ value
836 of 1 to these samples to circumvent misleading interpretations and aid visualisation.

837 The intermediate PIPSO₂₅ value (~0.51) derived for one sample collected in front of the Brunt Ice Shelf
838 points to a less severe sea-ice cover in that area. A possible explanation for the relatively lower PIPSO₂₅
839 value may be the presence of a coastal polynya that has been reported by Anderson (1993) and which
840 is further supported by Paul et al. (2015), who note that the sea-ice area around the Brunt Ice Shelf is
841 the most active in the southern Weddell Sea, with an annual average polynya area of 3516 ± 1420 km².

842 Interestingly, the reduced SIC here is also captured by our model (see Sect. 4.3).
843 PIPSO₂₅ values in the Amundsen Sea point to different scenarios. The P_ZIPSO₂₅ index ranges around
844 0.9 with only the easterly, more distal locations showing lower values between 0.3 and 0.6 (Fig. 4a).
845 The P_BIPSO₂₅ index generally presents lower values ranging from 0.6 in the coastal area to 0.2 in the
846 more distal samples (Fig. 4b). This difference between P_ZIPSO₂₅ and P_BIPSO₂₅ may be explained by
847 the different source organisms biosynthesizing the individual phytoplankton biomarkers. While the
848 main origin of HBI-trienes seems to be restricted to diatoms (Belt et al., 2017), brassicasterol is known
849 to be produced by several algal groups adapted to a wider range of sea surface conditions (Volkman,
850 2006; see Sect. 5.2).

4.3 Biomarker-based sea ice estimates vs. satellite and model data

853 The main ice algae bloom in the Southern Ocean occurs during spring, when solar insolation and air
854 temperatures/SSTs increase and sea ice starts melting, which results in the release of nutrients and
855 stratification of the water column stimulating the productivity of photosynthesizing organisms (Arrigo,
856 2017; Belt, 2018). The sea-ice biomarker IP_{SO}₂₅ is hence commonly interpreted as a spring sea-ice

- Gelöscht: 4
- Formatiert ... [210]
- Gelöscht: .
- Formatiert ... [211]
- Gelöscht: Interestingly, we obtained an
- Gelöscht:
- Formatiert ... [212]
- Gelöscht: , which may be indicative of
- Formatiert: Schriftart: (Standard) Times New Roman
- Formatiert: Schriftart: (Standard) Times New Roman
- Gelöscht: areas
- Formatiert: Schriftart: (Standard) Times New Roman
- Gelöscht: The
- Gelöscht: are
- Formatiert: Schriftart: (Standard) Times New Roman
- Gelöscht: , which is further described in
- Formatiert: Schriftart: (Standard) Times New Roman
- Gelöscht: 1.4.
- Formatiert: Schriftart: (Standard) Times New Roman
- Formatiert ... [213]
- Formatiert: Schriftart: (Standard) Times New Roman
- Gelöscht: While the
- Formatiert: Schriftart: (Standard) Times New Roman
- Gelöscht: a slight decrease to a value of 0.3 in
- Formatiert: Schriftart: (Standard) Times New Roman
- Gelöscht: location
- Formatiert: Schriftart: (Standard) Times New Roman
- Gelöscht:), the
- Formatiert: Schriftart: (Standard) Times New Roman
- Gelöscht: is
- Formatiert ... [214]
- Gelöscht: ,
- Formatiert: Schriftart: (Standard) Times New Roman
- Gelöscht: around
- Formatiert: Schriftart: (Standard) Times New Roman
- Gelöscht: and with a much steeper decline towards
- Formatiert: Schriftart: (Standard) Times New Roman
- Gelöscht: locations to 0.2
- Formatiert ... [215]
- Gelöscht: , such as dinoflagellates, diatoms, ... [216]
- Formatiert ... [217]
- Gelöscht:).
- Formatiert: Schriftart: (Standard) Times New Roman
- Formatiert ... [218]
- Formatiert: Nach: 0.63 cm

902 indicator, which is why, in the following, we compare the biomarker-based sea-ice reconstructions to
903 satellite-derived and modelled spring SIC. IPSO₂₅ concentrations in the surface sediments around the
904 Antarctic Peninsula exhibit similar trends as the satellite-derived and modelled SIC (Figs. 3+4), while
905 they differ significantly in the Amundsen and Weddell Seas, where high SIC are depicted by satellites
906 and the model ~~but IPSO₂₅ is very low concentrated~~. The low IPSO₂₅ concentrations in these areas
907 highlight the uncertainty when considering IPSO₂₅ as a sea-ice proxy alone, since such low
908 concentrations are not only observed under open water conditions, but also under a severe sea-ice cover.
909 In this case, the low concentrations of IPSO₂₅ are the result of the latter, where limited light availability
910 hinders ice algae growth, leading to an underestimation of sea-ice cover. Accordingly, we note a weak
911 correlation between IPSO₂₅ data and satellite SIC ($R^2 = 0.19$; Fig. 5a). As stated above, the combination
912 of IPSO₂₅ and a phytoplankton marker may prevent this ambiguity. The higher sea-ice concentrations
913 in the Amundsen and Weddell Seas are better reflected by maximum P₇IPSO₂₅ values than by IPSO₂₅
914 alone. However, we note that the P₇IPSO₂₅ index seems to not further resolve SICs higher than 50 %
915 (see Fig. S3), which may indicate a threshold (here ~50 % SIC) where the growth of the HBI triene and
916 IPSO₂₅ producing algae is limited.

[5] verschoben (Einfügung)

Formatiert: Schriftart: (Standard) Times New Roman

Formatiert: Nach: 0.63 cm

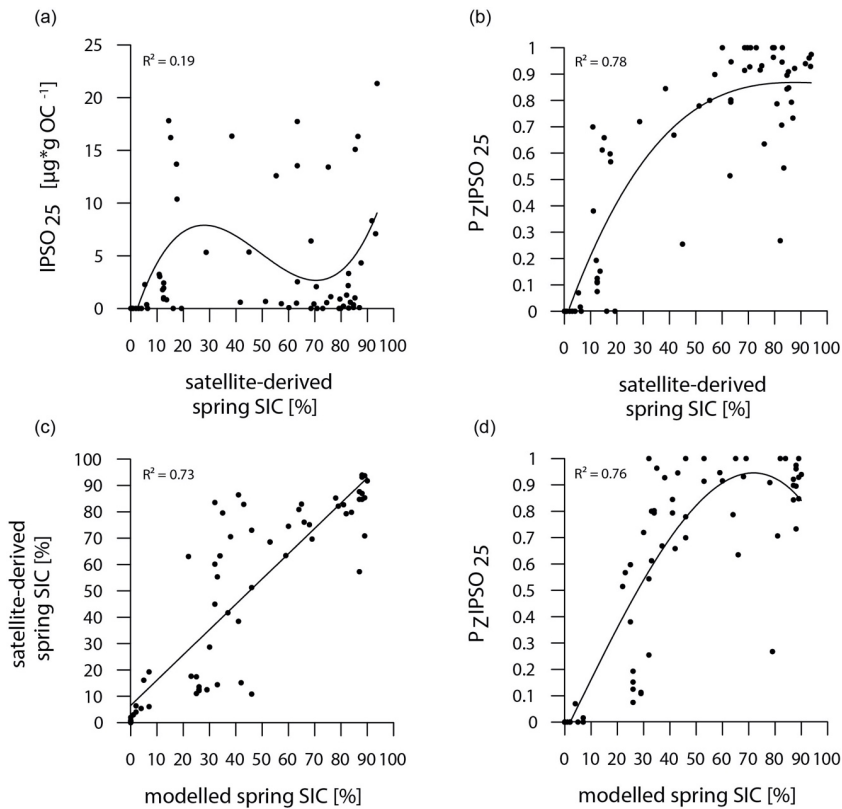


Fig. 5: Correlations of (a) IPSO₂₅ concentrations vs. satellite-derived spring SIC, (b) P_zIPSO₂₅ values vs. satellite-derived spring SIC, (c) satellite-derived spring SIC vs. modelled spring SIC and (d) P_zIPSO₂₅ values vs. modelled spring SIC. Coefficients of determination (R^2) are given for the respective regression lines.

[6] verschoben (Einfügung)
 Formatiert: Schriftart: (Standard) +Überschriften CS (Times New Roman), 10 Pt., Fett, Nicht Kursiv, Schriftfarbe: Text 1

917 In general, however, the P_zIPSO₂₅ values correlate much better with satellite and modelled SIC ($R^2 =$
 918 0.78 and $R^2 = 0.76$, respectively; Fig. 5b+d) than IPSO₂₅ concentrations. Correlations of satellite and
 919 model data with PIPSO₂₅ calculated using the HBI E-triene, brassicasterol and dinosterol, respectively,
 920 are also positive but less significant (Fig. S4) and we hence focus the discussion on P_zIPSO₂₅. The AWI-
 921 ESM2-derived spring SICs correctly display the permanently ice-free Drake Passage and the northwest-
 922 southeast gradient in sea-ice cover from the WAP continental slope towards the Bransfield Strait (Fig.
 923 4d). The model, however, significantly underestimates the elevated sea-ice concentrations (up to 70 %)
 924 in front of the former Larsen Ice Shelf A and east of James Ross Island at the EAP depicted by satellite

Formatiert: Nach: 0.63 cm

925 data. In the Amundsen and Weddell Seas, the model shows a heavy sea-ice cover (~90 %), only slightly
 926 underestimating the sea-ice cover at the near-coastal sites in front of Pine Island Glacier and the Ronne
 927 Ice Shelf. Interestingly, modelled SIC in the area in front of the Brunt Ice Shelf is as low as ~45 % (Fig.
 928 4d+e), corresponding well with the reduced P_7IPSO_{25} value of ~0.51, and may reflect the polynya
 929 conditions in that region documented by Anderson (1993) and Paul et al. (2015). Overall, we note that
 930 modelled modern SICs correlate well with satellite data ($R^2 = 0.73$; Fig. 5c) and P_7IPSO_{25} values ($R^2 =$
 931 0.76 ; Fig. 5d), while we observe weaker correlations between modelled paleo-SICs and P_7IPSO_{25} values
 932 (Fig. S5; see Sect. 5.1).

934 4.4 TEX^{l}_{86} and RI-OH' derived ocean temperatures

935 For a critical appraisal of the applicability and reliability of GDGT indices as temperature proxies in
 936 polar latitudes, we here focus on the TEX^{l}_{86} proxy by Kim et al. (2012), potentially reflecting SOTs,
 937 and the RI-OH' proxy, assumed to reflect SSTs, by Lü et al. (2015). The reconstructions are considered
 938 to represent annual mean ocean temperatures, (for correlations of TEX^{l}_{86} -derived SOTs with WOA
 939 spring and winter SOTs, see Fig. S6). In all samples, the BIT-index (Eq. 6) is <0.3 , indicating no
 940 significant contribution of terrestrial input influencing the distribution and hence applicability of
 941 GDGTs to estimate ocean temperatures. RI-OH'-derived temperatures and TEX^{l}_{86} -derived SOTs both
 942 show a similar pattern, but different temperatures, ranging between -2.62 to $+4.67$ °C and -2.38 to
 943 $+8.75$ °C, respectively (Fig. 6a+b). At the WAP, RI-OH'- as well as TEX^{l}_{86} -derived temperatures
 944 follow a northwest-southeast gradient with higher temperatures in the permanently ice-free Drake
 945 Passage and on the Antarctic continental slope, influenced by the ACC and relatively warm CDW (Orsi
 946 et al., 1995; Rintoul et al., 2001). Temperatures decrease towards the Bransfield Strait and the EAP,
 947 which are influenced by a seasonal sea-ice cover and relatively colder and highly saline water from the
 948 Weddell Sea, branching off the Weddell Gyre (Collares et al., 2018; Thompson et al., 2009). At the
 949 EAP, a southwest-northeast gradient can be observed with relatively lower temperatures along the

[7] verschoben (Einfügung)	
Formatiert	... [220]
Formatiert	... [221]
Gelöscht: temperatures	... [225]
Formatiert	... [222]
Gelöscht: -	
Gelöscht: -	
Gelöscht: (Schouten et al., 2002). These specific	[227]
Formatiert	... [223]
Formatiert	... [224]
Formatiert	... [226]
Formatiert	... [228]
Gelöscht:	
Formatiert	... [230]
Formatiert	... [229]
Gelöscht: our investigated regions	
Formatiert	... [231]
Gelöscht: make use of two temperature proxy	... [232]
Formatiert	... [233]
Gelöscht: high latitude polar oceans: The	
Formatiert	... [234]
Gelöscht: (2010)	
Formatiert	... [235]
Gelöscht:), calculated and calibrated using Eq. 3 and 5	[236]
Formatiert	... [237]
Gelöscht: .	
Formatiert	... [238]
Gelöscht:	
Formatiert	... [239]
Gelöscht: and RI-OH'	
Formatiert	... [240]
Gelöscht: ,	
Formatiert	... [241]
Gelöscht: 4.23 to +10.57 °C and -2.	
Formatiert	... [242]
Gelöscht: 5a	
Formatiert	... [243]
Gelöscht: West Antarctic Peninsula,	
Formatiert	... [244]
Gelöscht: relatively	
Formatiert	... [245]
Gelöscht: East Antarctic Peninsula	
Formatiert	... [246]
Gelöscht: the	
Formatiert	... [247]
Gelöscht: TWW	
Formatiert	... [248]
Gelöscht: East Antarctic Peninsula	
Formatiert	... [249]
Gelöscht: around	
Formatiert	... [250]
Formatiert	... [219]

1026 Larsen Ice Shelf and higher temperatures towards the Powell Basin and the South Orkney Islands (Fig. 6a+b).

1027

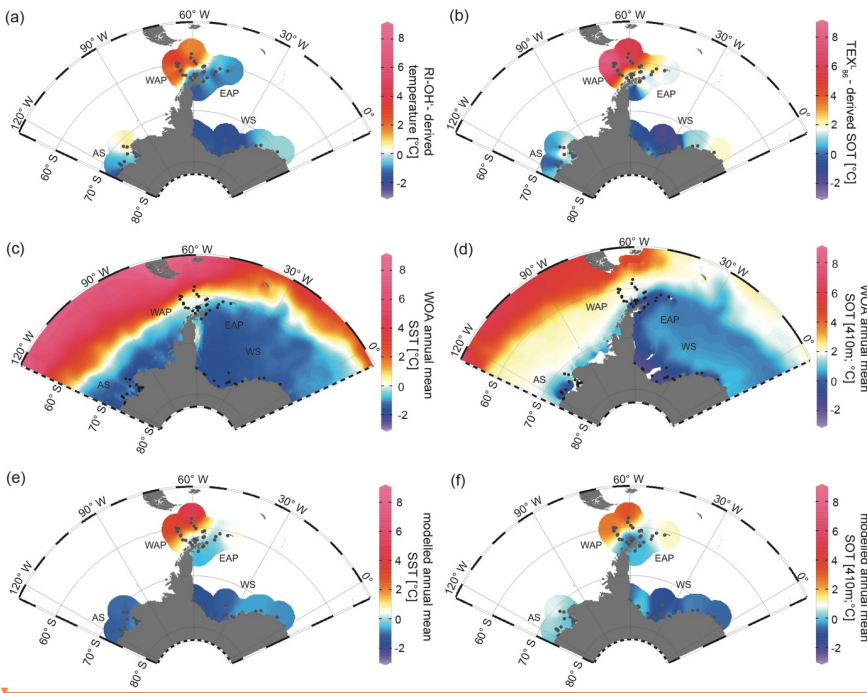


Fig. 6: Annual mean temperature distributions with (a) RI-OH'-derived temperature, (b) TEX^L₈₆-derived SOT, (c) WOA13 SST (Locarnini et al., 2013), (d) WOA13 SOT (410 m; Locarnini et al., 2013), (e) modelled SST and (f) modelled SOT (410 m) in °C. AS: Amundsen Sea, WAP: West Antarctic Peninsula, EAP: East Antarctic Peninsula, WS: Weddell Sea.

1028 Further to the South, in the Amundsen and Weddell Seas, temperatures are generally lower than at the

1029 Antarctic Peninsula. Samples from the Weddell Sea display a temperature decrease from east to west,

1030 which may reflect the eddy-driven route in the north-eastern corner of the Weddell Gyre carrying

1031 relatively warm, salty CDW, which then advects westward along the southern edge of the Weddell Gyre

1032 as WDW (Vernet et al., 2019). Coldest TEX^L₈₆ as well as RI-OH' temperatures (<0 °C) at sites along

1033 the Filchner-Ronne Ice Shelf front may be further linked to the presence of cold precursor water masses

1034 for WSBW.

Gelöscht: , towards the North. These general temperature patterns align well with the decreasing sea-ice cover in that area towards the North.

Formatiert: Schriftart: (Standard) Times New Roman

Gelöscht: Absolute temperature estimates derived from the two paleothermometers show significantly different ranges. While the TEX₈₆ signal is reflecting temperatures in the Amundsen and Weddell Seas quite well, it seems to be significantly warm-biased further to the North, in the Drake Passage, with up to ~ 11 °C. This warm-biased TEX₈₆ signal is a known caveat in that area

[8] nach unten verschoben: and is, among others, assumed to be connected to GDGTs produced by deep-dwelling Euryarchaeota (Park et al., 2019), which have been reported in CDW (Alonso-Sáez et al.,

Gelöscht: 2011) and in deep waters of the Antarctic Polar Front (López-García et al., 2001). Interestingly, our reconstructions suggest that the TEX₈₆-derived temperatures (Fig. 5a) are only warm-biased in the relatively warmer Drake Passage but depict temperatures in the colder regions (Amundsen and Weddell Seas) reasonably well or only slightly warm-biased, if compared to the WOA13 temperatures (Fig. 5c).

Formatiert: Schriftart: (Standard) Times New Roman

Formatiert: Schriftart: Arial, Englisch (USA)

Formatiert: Zeilennummern unterdrücken

Formatiert: Schriftart: (Standard) Times New Roman

Formatiert: Block, Zeilenabstand: Doppelt

Gelöscht: record

Formatiert: Schriftart: (Standard) Times New Roman

Formatiert: Schriftart: (Standard) Times New Roman, Schriftfarbe: Automatisch

Gelöscht: an

Formatiert: Schriftart: (Standard) Times New Roman, Schriftfarbe: Automatisch

Gelöscht: (Vernet et al., 2019). While the origin of GDGTs is not yet fully understood and still debated (Ho et al., 2014), the biosynthesis of intact polar lipid GDGTs in CDW, as just recently suggested by Spencer-Jones et al. (2020), might, however, support the hypothesis of advected CDW in that area. In the Amundsen Sea, relatively higher temperatures (~ 0.5 °C) at the sample locations in the north-eastern part of the embayment are reflected in the RI-OH'-derived temperatures but are not reflected in the TEX₈₆-based reconstruction

Formatiert: Schriftart: (Standard) Times New Roman

Formatiert: Schriftart: (Standard) Times New Roman, Englisch (Vereinigtes Königreich)

Formatiert: Nach: 0.63 cm

1051 With regard to ongoing discussions, whether GDGT-based temperature reconstructions represent SSTs
1052 or SOTs (Kalanetra et al., 2009; Kim et al., 2012; Park et al., 2019), we here compare our RI-OH' and
1053 TEX₈₆^L-derived temperatures with instrumental and modelled surface as well as subsurface temperature
1054 data (Fig. 6c-f). Based on correlations of GDGT-derived temperatures with WOA13 temperatures
1055 reflecting different water depths, we observe the highest significance at a water depth of 410 m (for
1056 respective correlations, see Fig. S7). When discussing instrumental and modelled SOTs, we hence refer
1057 to 410 m water depth.

[9] verschoben (Einfügung)

Formatiert: Schriftart: (Standard) Times New Roman

Formatiert: Nach: 0.63 cm

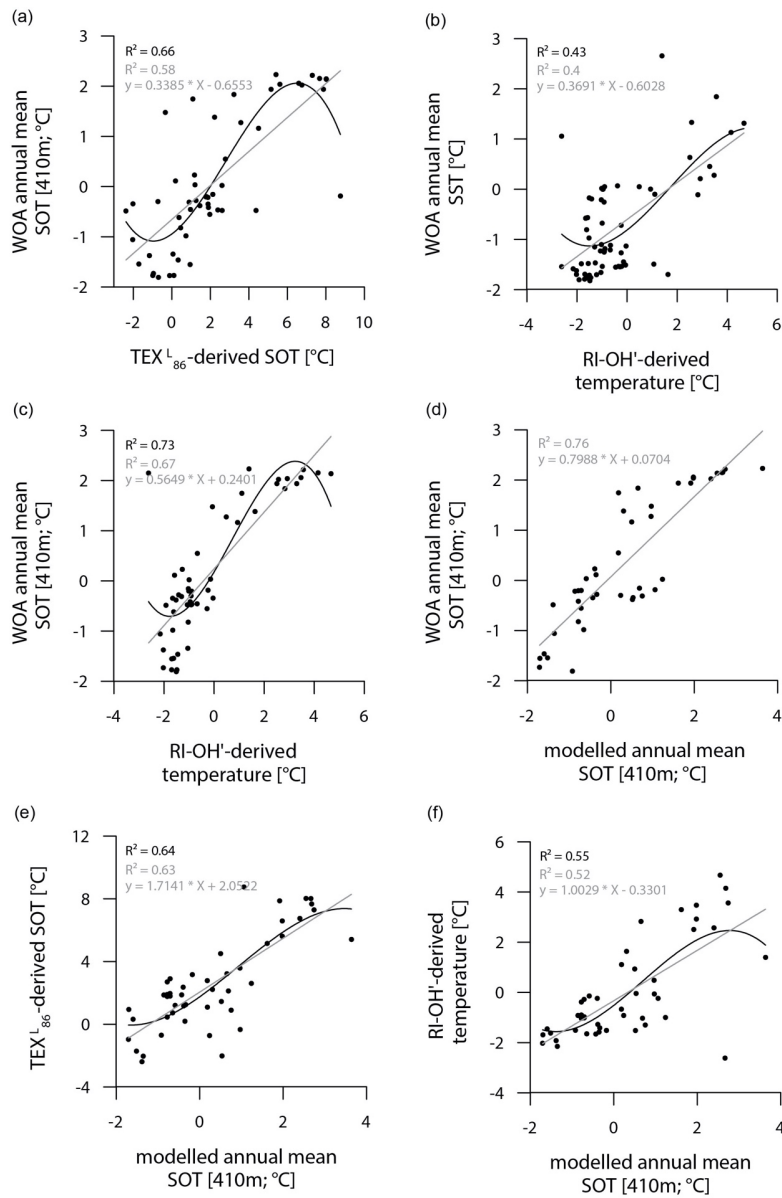


Fig. 7: Correlations of (a) WOA annual mean SOT (410 m) vs. $TEX^{L_{86}}$ -derived SOT, (b) WOA annual mean SST vs. RI-OH'-derived temperature, (c) WOA annual mean SOT (410 m) vs. RI-OH'-derived temperature, (d) WOA annual mean SOT (410 m) vs. modelled annual mean SOT (410 m), (e) $TEX^{L_{86}}$ -derived SOT vs. modelled annual mean SOT (410 m), (f) RI-OH'-derived temperature vs. modelled annual mean SOT (410 m) in °C. Coefficients of determination (R^2) are given for the respective regression lines.

Formatiert: Nach: 0.63 cm

1058 While the correlation between $\text{TEX}^{L_{86}}$ -derived SOTs and instrumental SOTs is reasonably (Fig. 7a; $R^2 = 0.66$), also supporting the assumption of a subsurface origin, we note a significant overestimation of SOTs by up to 6 °C in the Drake Passage (Fig. S8). This warm-biased $\text{TEX}^{L_{86}}$ signal is a known caveat, and is, among others, assumed to be connected to GDGTs produced by deep-dwelling Euryarchaeota (Park et al., 2019), which have been reported in CDW (Alonso-Sáez et al., 2011) and in deep waters at the Antarctic Polar Front (López-García et al., 2001). Maximum $\text{TEX}^{L_{86}}$ -based SOTs of 5 °C - 8 °C in the central Drake Passage (Fig. 6b), however, distinctly exceed the common temperature range of CDW (0-2 °C). Interestingly, $\text{TEX}^{L_{86}}$ -derived SOTs in the colder regions of the Amundsen and Weddell Seas relate reasonably well to instrumental temperatures and are only slightly warm-biased (Fig. S8). Correlations between RI-OH'-derived temperatures with instrumental SSTs are comparatively weak ($R^2 = 0.43$; Fig. 7b). Recently, Liu et al. (2020) concluded in their study on surface sediments from Prydz Bay (East Antarctica), that also the RI-OH' index holds promise as a tool to reconstruct SOTs rather than SSTs. When correlating our RI-OH'-derived temperatures with instrumental SOTs, we find a high correlation ($R^2 = 0.73$; Fig. 7c), supporting this hypothesis. We further note that the temperature range of RI-OH' is much more realistic than $\text{TEX}^{L_{86}}$, supporting the study by Park et al. (2019) and demonstrating that the addition of OH-isoGDGTs in the temperature index is a promising step towards high latitude temperature reconstructions and may improve our understanding of the temperature responses of archaeal membranes in Southern Ocean waters (Fietz et al., 2020; Park et al., 2019). Clearly, more data – ideally obtained from sediment traps, surface samples as well as longer sediment cores – and calibration studies will help to further elucidate the applicability of this approach.

Similar to the model-derived sea-ice data, we here also evaluate the model's performance in depicting ocean temperatures (Fig. 6e+f). Modelled annual mean SSTs and SOTs are highest with up to 5 °C and 3 °C, respectively, in the permanently ice-free Drake Passage, influenced by the relatively warm ACC. Decreasing SSTs are simulated towards the Antarctic Peninsula continental slope and the Bransfield Strait (~0.5 to 1 °C), coinciding with the increase in the duration of seasonal sea-ice cover in that area. At the EAP/northwestern Weddell Sea, modelled SSTs as well as SOTs show a southwest-northeast

Formatiert: Block, Zeilenabstand: Doppelt

[8] verschoben (Einfügung)

Formatiert: Schriftart: (Standard) Times New Roman

[10] verschoben (Einfügung)

Formatiert: Englisch (Vereinigtes Königreich)

[11] verschoben (Einfügung)

Formatiert: Schriftart: (Standard) Times New Roman

Gelöscht: <#>Modelled SIC and SSTs ¶
<#> The global climate model setup AWI-ESM2 was used to simulate SSTs and SIC in the study area for modern conditions (1951-2014; Fig. 5d and 6, respectively). Modelled SIC indicate an absence of sea ice in the permanently ice-free Drake Passage (Fig. 6a-c) and a northwest-southeast gradient from the continental slope to the Bransfield Strait during winter and spring (Fig. 6a+b) with the latter as being ice-free during summer (

[4] nach oben verschoben: <#>Fig.

Formatiert: Schriftart: (Standard) Times New Roman

Gelöscht: <#>(Fig. 5d)

Formatiert: Schriftart: (Standard) +Überschriften CS (Times New Roman), 10 Pt., Fett, Schriftfarbe: Text 1

Gelöscht: <#>6c). During all three seasons (from winter through spring and summer), a southwest-northeast gradient at the East Antarctic Peninsula can

[7] nach oben verschoben: <#> and may reflect the

Gelöscht: <#>During summer, the model suggests a

Formatiert: Schriftart: (Standard) Times New Roman

Formatiert ... [252]

Formatiert: Schriftart: (Standard) Times New Roman

Formatiert: Schriftart: (Standard) Times New Roman

Formatiert ... [254]

Gelöscht: <#>temperatures

Formatiert ... [255]

Formatiert ... [256]

Gelöscht: <#>

Formatiert ... [257]

Gelöscht: <#>

Formatiert ... [258]

Gelöscht: <#>intensifying influence

Formatiert ... [259]

Formatiert ... [260]

Formatiert: Schriftart: (Standard) Times New Roman

Gelöscht: <#>East Antarctic Peninsula

Formatiert: Schriftart: (Standard) Times New Roman

Gelöscht: <#>the

Formatiert: Schriftart: (Standard) Times New Roman

Formatiert: Schriftart: (Standard) Times New Roman

Formatiert: Nach: 0.63 cm

1129 directed increase towards Powell Basin. In the Amundsen and Weddell Seas, annual mean SSTs are
1130 negative, with temperatures ranging from -1 to -0.5 °C, while SOTs are positive in the Amundsen Sea
1131 and negative in the Weddell Sea. Overall, we note that modelled SOTs reflect instrumental SOTs
1132 reasonably well ($R^2 = 0.76$; Fig. 7d). Interestingly, while RI-OH'-derived SOTs relate better to
1133 instrumental SOTs (than TEX^{L}_{86} -based SOTs), we note a better correlation between TEX^{L}_{86} -derived
1134 SOTs and modelled SOTs ($R^2 = 0.64$; Fig. 7e) and a weaker correlation with Ri-OH'-derived
1135 temperatures ($R^2 = 0.55$; Fig. 7f).

1137 5. Caveats and recommendations for future research

1138 Marine core top studies to elucidate the applicability of climate proxies are often concerned with
1139 limitations and uncertainties regarding the age control of the investigated surface sediments as well as
1140 the production, preservation and degradation of target compounds. In the following, we shortly address
1141 some of these factors and provide brief recommendations for future investigations.

1143 5.1 Age control

1144 Information on the actual age of the surface sediments are a major requirement determining their
1145 suitability to reflect modern sea surface conditions. When comparing sea-ice conditions or ocean
1146 temperatures estimated from sedimentary biomarker data (easily spanning decades to millennia,
1147 depending on sedimentation rates) with satellite-derived sea-ice data or instrumental records (covering
1148 only the past ~40 and 65 years, respectively), the different time periods reflected in the data sets need
1149 to be considered when interpreting the results. To address the issue of lacking age constraints for the
1150 herein studied surface sediments, we also performed paleoclimate simulations providing sea-ice
1151 concentration data for three time slices (2 ka, 4 ka and 6 ka BP; see Fig. S5) to evaluate if the surface
1152 sediments may have recorded significantly older environmental conditions. Correlations of $PIPSO_{25}$
1153 values against these paleo time slice sea-ice concentrations depicted notably weaker relations (Fig. S5)
1154 compared to the recent (1951-2014 CE) model output, which points to a relatively young age of the
1155 majority of the herein studied sediments. This is further supported by AMS ^{14}C -dating of calcareous

Gelöscht: <#>gradient

Gelöscht: <#>the Powell Basin with temperatures increasing from -0.5 °C in the South to 0.5 °C in the North, aligning well with the other modelled records.

Formatiert: Schriftart: (Standard) Times New Roman

Formatiert: Schriftart: (Standard) Times New Roman

Formatiert: Schriftart: (Standard) Times New Roman

Gelöscht: <#>-0.5 to

Formatiert: Schriftart: (Standard) Times New Roman

Gelöscht: <#>°C.¶

<#>Comparing biomarker data with satellite and numerical model data ¶

<#>Here, we discuss the advantages and caveats of the sea-ice biomarker $IPSO_{25}$ and the semi-quantitative sea-ice index $PIPSO_{25}$ by comparing the proxy data to satellite and numerical model data. The main ice algae bloom in the Southern Ocean occurs during spring, when temperatures increase, sea ice starts melting, which results

Formatiert: Schriftart: (Standard) Times New Roman

Gelöscht: <#>release of nutrients and stratification of the water column and the increasing solar insolation stimulates the productivity of photosynthesizing organisms (Arrigo, 2017; Belt, 2018). The sea-ice biomarker $IPSO_{25}$ is hence commonly interpreted as a spring sea-ice indicator, which is why,

Formatiert: Schriftart: (Standard) Times New Roman

Gelöscht: <#>following, we compare the biomarker-based sea-ice reconstructions to satellite-derived spring SIC and modelled spring SIC.

Formatiert: Schriftart: (Standard) Times New Roman

Formatiert: Schriftart: (Standard) Times New Roman, 12 Pt.

Gelöscht: Comparison of proxy-based, modelled

Formatiert: Schriftart: (Standard) Times New Roman, Fett

Gelöscht: observed

Formatiert: Standard, Block, Zeilenabstand: Doppelt, Keine Aufzählungen oder Nummerierungen

Formatiert: Schriftart: (Standard) Times New Roman

Gelöscht: -ice

Formatiert: Schriftart: (Standard) Times New Roman

Formatiert: Nach: 0.63 cm

1183 microfossils and ²¹⁰Pb-dating of seafloor surface sediments from the Amundsen Sea shelf documenting
1184 recent ages for most sites (Hillenbrand et al., 2010, 2013, 2017; Smith et al., 2011, 2014, 2017; Witus
1185 et al., 2014) as well as modern ²¹⁰Pb-dates obtained for three multicores collected in the Bransfield
1186 Strait (PS97/56, PS97/68, PS97/72; Vorrath et al., 2020), which are considered in this ~~study~~ AMS
1187 ¹⁴C dates obtained for nearby surface samples in the vicinity of the South Shetland Islands and the
1188 Antarctic Sound revealed ages of 100 years and 142 years BP, respectively (Vorrath et al., 2019). As
1189 both uncorrected ages lie within the range of the modern marine reservoir effect (e.g. Gordon and
1190 Harkness, 1992), we may consider these two dates still modern. However, in an area that is significantly
1191 affected by rapid climate warming over the past decades and a regionally variable sea-ice coverage
1192 uncertainties associated with ¹⁴C dating of calcareous material may easily lead to an over- or
1193 underestimation of biomarker-based sea-ice cover and ocean temperature estimates, respectively, which
1194 needs to be considered for comparisons with instrumental data. While the utilization of (paleo) model
1195 data may alleviate the lack of age control for each seafloor sediment sample to some extent, we
1196 accordingly recommend that for a robust calibration of e.g. PIPSO₂₅ values against satellite-derived sea-
1197 ice concentrations (and this is not the aim of this study) only surface sediment samples with a modern
1198 age confirmed by ²¹⁰Pb-dating are incorporated.

1200 5.2 Production and preservation of biomarkers

1201 Biomarkers are considered to reveal the former occurrence of their precursor organisms, which requires
1202 a certain source specificity. While there is general consensus on e.g. Thaumarchaeota being the major
1203 source for iso-GDGTs (Fietz et al., 2020 and references therein) or diatoms synthesizing HBIs
1204 (Volkman 2006), this is not the case for brassicasterol, which is not only found in diatoms but also in
1205 e.g. dinoflagellates and haptophytes (Volkman 2006). Accordingly, the use of brassicasterol to
1206 determine the PIPSO₂₅ index may introduce uncertainties regarding the environmental information
1207 pertinent to this phytoplankton biomarker. A further aspect concerns the different chemical structures
1208 of HBIs and sterols, which raises the risk of a selective degradation (see Belt, 2018 and Rontani et al.,
1209 2018; 2019 for detailed discussion) with potentially considerable effects on the PIPSO₂₅ index.
1210 Regarding the different sectors of the study area, also spatially different microbial communities as well

Formatiert: Schriftart: (Standard) Times New Roman, Englisch (USA)

Gelöscht: Our satellite-derived SIC represent monthly mean (spring) SIC averaged from 1978 to the individual year of sample retrieval. The herein modelled spring SIC cover a period from 1951 to 2014. When comparing sea-ice conditions estimated from sedimentary biomarker data (easily spanning decades to centuries, depending on sedimentation rates) with sea-ice conditions recorded by satellite observations (spanning ~ 40 years), and with modelled sea-ice conditions (spanning 63 years) the different time periods covered by the different methods need to be considered and kept in mind when interpreting the results. Vorrath et al. (2019) conducted radiocarbon dating on selected surface sediment samples from the Bransfield Strait, concluding that their biomarker data reflect the past two centuries. We hence note that biomarker data from the Antarctic Peninsula, which is affected by a very recent ice loss, may hence overestimate the sea-ice cover and underestimate ocean temperatures. Nonetheless we here correlate the biomarker data with satellite and model data to further investigate the quantitative significance of the sea ice proxy (

[6] nach oben verschoben: Fig.

Gelöscht: As a result, IPSO₂₅ and satellite/model data show low correlations ($R^2 = 0.19/R^2 = 0.16$; Fig. 7a+c), requiring caution when interpreting IPSO₂₅ as a sea-ice proxy alone. As stated in earlier sections, the combination of IPSO₂₅ and a phytoplankton marker may prevent this ambiguity. The perennial sea-ice cover in the Amundsen and Weddell Seas is better represented by the P₂IPSO₂₅ values than by the sea-ice proxy alone. However, we note that at the southern sampling sites, the PIPSO₂₅ index may not be able to further resolve/detail sea-ice concentrations higher than 50 % reasonably well (see Fig. S3). This may be an indicator for a threshold (here ~ 50 % SIC) where the growth of the HBI triene and IPSO₂₅ producing algae is limited.¶ In general, however, the P₂IPSO₂₅ values correlate much better with satellite/modelled SIC ($R^2 = 0.78/R^2 = 0.76$; Fig. 7b+d) than IPSO₂₅ concentrations. For correlations of satellite/model data with PIPSO₂₅ calculated using the HBI E-triene, brassicasterol and dinosterol, respectively, we refer the reader to Fig. S4. There are, however, also limitations in the semi-quantitative sea-ice index PIPSO₂₅, that need to be [262]

Formatiert: Schriftart: (Standard) +Überschriften CS (Times New Roman), 10 Pt., Fett, Schriftfarbe: Text 1

Gelöscht: 7). Following Esper and Gersonde (2014), who, assuming a non-linear response of sea-ice diatom productivity to sea-ice dynamics, propose the usage of a polynomial regression instead of a linear correlation, we here use a polynomial regression (third degree).¶ ... [261]

Formatiert: Schriftart: (Standard) Times New Roman

[5] nach oben verschoben: low IPSO₂₅ concentrations in these areas highlight the uncertainty when considering IPSO₂₅ as a sea-ice proxy alone, since such low concentrations are not only observed under open water conditions, but also under a severe sea-ice cover. In this case, the low concentrations of IPSO₂₅ are the result of the latter, where

Formatiert: Nach: 0.63 cm

1312 as varying depositional regimes, such as sedimentation rate, redox conditions and water depth, may lead
 1313 to different degradation patterns which means that variations in the biomarker concentrations between
 1314 different sectors may not strictly reflect changes in the production of these compounds (driven by sea
 1315 surface conditions) but may also relate to different degradation states. In particular, lower sedimentation
 1316 rates and thus extended oxygen exposure times promote chemical alteration and degradation processes
 1317 (Hedges et al., 1990; Schouten et al., 2013). Regarding the transport of organic matter from the sea
 1318 surface through the water column, it has been previously noted that the formation of mineral aggregates
 1319 and fecal pellets, however, often accelerates the vertical export towards the seafloor during the melting
 1320 season leading to a more rapid burial and hence better preservation (Bauerfeind et al., 2005; Etourneau
 1321 et al., 2019; Müller et al., 2011).

1322 Another rather technical drawback concerning the use of the PIPSO₂₅ index may appear when the
 1323 concentrations of the sea-ice proxy IP SO₂₅ and the phytoplankton marker are similarly low (due to
 1324 unfavourable conditions for both ice algae as well as phytoplankton) or similarly high (due to a
 1325 significant seasonal shift in sea-ice cover and/or stable ice edge conditions). This may lead to similar
 1326 PIPSO₂₅ values, although the sea-ice conditions are fundamentally different from each other. This
 1327 scenario occurred at five sampling sites in the Weddell Sea (PS111/13-2, /15-1, /16-3, /29-3, and /40-
 1328 2; Fig. 3b+c), where IP SO₂₅ and the HBI Z-triene concentrations are close to the detection limit and
 1329 P₂IPSO₂₅ values are very low, suggesting a reduced sea-ice cover. Satellite and model data, however,
 1330 show that these sample locations are influenced by heavy, nearly year-round sea-ice cover. We conclude
 1331 that biomarker concentrations of both biomarkers at or close to the detection limit, indicative of a severe
 1332 ice cover, need to be treated with caution. As mentioned above, we assigned a maximum P₂IPSO₂₅
 1333 value of 1 to these samples and we note that such practice always needs to be made clear when applying
 1334 the PIPSO₂₅ approach. The coupling of IP SO₂₅ with a phytoplankton marker, nonetheless, provides
 1335 more reliable sea-ice reconstructions. Regarding the above-mentioned ambiguities, we recommend not
 1336 only to calculate the PIPSO₂₅ index, but also to carefully consider individual biomarker concentrations
 1337 and, if possible, to utilize other sea-ice measures, such as well-preserved diatom assemblage data
 1338 (Lamping et al., 2020; Vorrath et al., 2019; 2020). While the PIPSO₂₅ index is not yet a fully quantitative
 1339 proxy to provide paleo sea-ice concentrations, the GDGT-paleothermometers have gone through several

Formatiert: Block, Zeilenabstand: Doppelt

Formatiert: Schriftart: (Standard) Times New Roman

Gelöscht: both

Formatiert: Schriftart: (Standard) Times New Roman

Formatiert: Schriftart: (Standard) Times New Roman

Gelöscht:), which

Formatiert: Schriftart: (Standard) Times New Roman

Gelöscht: completely

Formatiert: Schriftart: (Standard) Times New Roman

Gelöscht: was detected in

Formatiert: Schriftart: (Standard) Times New Roman

Gelöscht: samples from

Gelöscht: ;

Formatiert: Schriftart: (Standard) Times New Roman

Formatiert: Schriftart: (Standard) Times New Roman, Schriftfarbe: Automatisch

Formatiert: Schriftart: (Standard) Times New Roman, Schriftfarbe: Automatisch

Formatiert: Schriftart: (Standard) Times New Roman

Gelöscht: , while

Formatiert: Schriftart: (Standard) Times New Roman

Gelöscht: perennial

Formatiert: Schriftart: (Standard) Times New Roman

Gelöscht: conditions

Formatiert: Schriftart: (Standard) Times New Roman, Schriftfarbe: Automatisch

Formatiert: Nach: 0.63 cm

1349 calibration iterations (Fietz et al., 2020). As noted above, the observation of distinctly warm-biased
 1350 TEX₈₆-derived SOTs calls for further efforts in terms of regional calibration studies and/or
 1351 investigations of archaean adaptation strategies regarding different water depths, nutrient and
 1352 temperature conditions.

1353

1354 5.3 The role of platelet ice for the production of IPSO₂₅

1355 The sympagic, tube-dwelling, diatom *B. adeliensis* is a common constituent of Antarctic sea ice,
 1356 preferably flourishing in the relatively open channels of sub-ice platelet layers in near-shore locations
 1357 covered by fast ice (Medlin, 1990; Riaux-Gobin and Poulin, 2004). Based on investigations of sea-ice
 1358 samples from the Southern Ocean, Belt et al. (2016) detected this diatom species to be a source of
 1359 IPSO₂₅, which, according to its habitat, led to the assumption of the sea-ice proxy being a potential
 1360 indicator for the presence of platelet ice. As stated above, *B. adeliensis* is not confined to platelet ice,
 1361 but is also observed in basal sea ice and described as well adapted to changes in the texture of sea ice
 1362 during ice melt (Riaux-Gobin et al., 2013). Platelet ice formation, however, plays an important role in
 1363 sea-ice generation along some coastal regions of Antarctica (Hoppmann et al., 2015; 2020; Lange et al.,
 1364 1989; Langhorne et al., 2015). In these regions, CDW and High Saline Shelf Water (HSSW) flowing
 1365 into sub-ice shelf cavities of ice shelves cause basal melting and the discharge of cold and less saline
 1366 water (Fig. 8; Hoppmann et al., 2020; Scambos et al., 2017). The surrounding water is cooled and
 1367 freshened and is then transported towards the surface. Under the large Filchner-Ronne and Ross ice
 1368 shelves the pressure relief can cause this water, called Ice Shelf Water (ISW), to be supercooled (Foldvik
 1369 and Kvinge, 1974). The temperature of the supercooled ISW is potentially below the in-situ freezing
 1370 point, which may eventually cause the formation of ice platelets that accumulate under landfast ice
 1371 attached to adjacent ice shelves (Fig. 8; Holland et al., 2007; Hoppmann et al., 2015; 2020).

- Formatiert: Schriftart: (Standard) Times New Roman
- Gelöscht: The coupling of IPSO₂₅ with a phytoplankton marker, nonetheless, provides the more robust and reliable sea-ice reconstructions. Regarding the above-mentioned ambiguities, we recommend to not only calculate the PIPSO₂₅ index, but also consider individual biomarker concentrations and, if possible, take other sea-ice measures, such as satellite data and/or well-preserved diatom assemblage data (Lamping et al., 2020; Vorrath et al., 2019; 2020) into account. ¶
- ¶ ... [263]
- [9] nach oben verschoben: (Kalanetra et al., 2009; Kim et
- [12] verschoben (Einfügung)
- Formatiert: Schriftart: (Standard) Times New Roman
- Formatiert: Block, Zeilenabstand: Doppelt
- Gelöscht: 2019) we here refer to ocean ... [264]
- Formatiert: Schriftart: (Standard) Times New Roman
- Formatiert ... [265]
- [13] verschoben (Einfügung)
- Formatiert: Schriftart: (Standard) Times New Roman
- [10] nach oben verschoben: addition of OH-isoGDGTs in
- Formatiert: Englisch (Vereinigtes Königreich)
- [11] nach oben verschoben: Clearly, more data – ideally
- Gelöscht: ¶ ... [266]
- Formatiert ... [267]
- Gelöscht: for IPSO₂₅ production ¶ ... [268]
- Formatiert: Schriftart: (Standard) Times New Roman
- Formatiert: Schriftart: (Standard) Times New Roman
- Formatiert: Schriftart: (Standard) Times New Roman
- Gelöscht: flows
- Formatiert: Schriftart: (Standard) Times New Roman
- Gelöscht: Antarctica's continental
- Formatiert: Schriftart: (Standard) Times New Roman
- Gelöscht: , initiating
- Formatiert: Schriftart: (Standard) Times New Roman
- Gelöscht: melt
- Formatiert: Schriftart: (Standard) Times New Roman
- Gelöscht: the adjacent ice shelves
- Gelöscht: 9).
- Formatiert: Schriftart: (Standard) Times New Roman
- Formatiert: Schriftart: (Standard) Times New Roman
- Gelöscht: , where
- Formatiert: Schriftart: (Standard) Times New Roman
- Gelöscht: 9
- Formatiert: Schriftart: (Standard) Times New Roman
- Formatiert ... [269]
- Formatiert: Nach: 0.63 cm

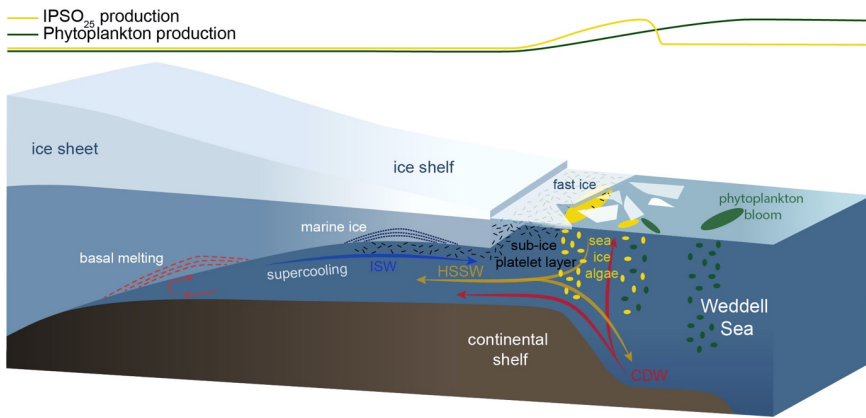


Fig. 8: Schematic illustration of the formation of platelet ice and the main production areas of sea ice algae producing IPSO₂₅ (yellow ovals) and phytoplankton (green ovals), also displayed by yellow and green curves at the top. CDW: Circumpolar Deep Water, HSSW: High Saline Shelf Water, ISW: Ice Shelf Water. Schematic modified after Scambos et al. (2017).

1460 In an attempt to elucidate the relationship of IPSO₂₅ and platelet ice more clearly, we here regard our
 1461 data in connection to observed platelet ice occurrences.
 1462 While the maximum IPSO₂₅ concentrations in front of the Filchner Ice Shelf could be directly related
 1463 to the above-mentioned platelet ice formation in this area, the elevated IPSO₂₅ concentrations in front
 1464 of the Larsen Ice Shelves at the FAP could be linked to several processes. According to Langhorne et
 1465 al. (2015), sea-ice cores retrieved from that area did not incorporate platelet ice. The high IPSO₂₅
 1466 concentrations could hence be explicable by either input from drift ice transported with the Weddell
 1467 Gyre or by basal freeze-on. We do, however, note that our samples may reflect much longer time frames
 1468 than the sea-ice samples investigated by Langhorne et al. (2015) and the lack of platelet ice in their
 1469 investigated sea-ice cores does not rule out the former presence of platelet ice, which may be captured
 1470 in our investigated sediment samples.
 1471 There are several previous studies on IPSO₂₅ which report a close connection of the proxy to proximal,
 1472 coastal locations and polynyas in the seasonal ice zone (i.e., Collins et al., 2013; Smik et al., 2016).
 1473 They do not, however, discuss the relation to adjacent ice shelves as possible “platelet ice factories”.
 1474 We note that the core locations investigated by Smik et al. (2016) are in the vicinity of the Moscow
 1475 University Ice Shelf, where Langhorne et al. (2015) did not observe platelet ice within sea-ice cores.

[12] nach oben verschoben: The sympagic, tube-dwelling, diatom *B. adeliensis* is a common constituent of Antarctic sea ice, preferably flourishing in the relatively open channels of sub-ice platelet layers in near-shore locations covered by fast ice (Medlin, 1990; Riaux-Gobin and Poulin, 2004). Based on investigations of sea-ice samples from the Southern Ocean, Belt et al.

Formatiert: Schriftart: (Standard) Times New Roman

Formatiert: Block, Zeilenabstand: Doppelt

Formatiert: Schriftart: (Standard) Times New Roman, Schriftfarbe: Automatisch

[13] nach oben verschoben: IPSO₂₅, which, according to its habitat, led to the assumption of the sea-ice proxy being a potential indicator for the presence of platelet ice. As stated above, *B.*

Gelöscht: (2016) detected this diatom species to be a source of the HBI diene

Formatiert: Schriftart: (Standard) Times New Roman

Gelöscht: *adeliensis* is not confined to platelet ice, but is also observed in bottom ice and described as well! [270]

Formatiert: Schriftart: (Standard) Times New Roman

Gelöscht:

Formatiert: Schriftart: (Standard) Times New Roman

Gelöscht: Elevated

Formatiert: Schriftart: (Standard) Times New Roman

Gelöscht: East Antarctic Peninsula

Formatiert: Schriftart: (Standard) Times New Roman

Gelöscht: So far, it is hard to differentiate between [271]

Formatiert: Schriftart: (Standard) Times New Roman

Formatiert: Schriftart: (Standard) Times New Roman

Gelöscht: by

Formatiert: Schriftart: (Standard) Times New Roman

Gelöscht: bottom ice production.

Formatiert: Schriftart: (Standard) Times New Roman

Formatiert: Schriftart: (Standard) Times New Roman

Gelöscht:). The

Formatiert: Schriftart: (Standard) Times New Roman

Gelöscht: observed

Formatiert: Schriftart: (Standard) Times New Roman

Gelöscht: , covering a much longer time interval.

Formatiert: Schriftart: (Standard) Times New Roman

Formatiert ... [273]

Formatiert ... [272]

Formatiert: Schriftart: (Standard) Times New Roman

Formatiert ... [274]

Formatiert: Schriftart: (Standard) Times New Roman

Formatiert ... [275]

Formatiert: Nach: 0.63 cm

1507 Hoppmann et al. (2020), however, report a sea-ice core from that area, which incorporates platelet ice.

1508 The different observations by Langhorne et al. (2015) and Hoppmann et al. (2020) highlight the

1509 temporal variability in the occurrence of platelet ice in the cold water regime around the East Antarctic

1510 margin.

1511 Regarding the minimum abundance of IPSO₂₅ in the Amundsen Sea (Fig. 3b; AS), which we tentatively

1512 relate to the extended and thick sea-ice coverage, the absence of platelet ice in that region may be an

1513 alternative explanation. The Amundsen/Bellingshausen Sea and WAP shelves are classified as warm

1514 shelves (Thompson et al., 2018) characterized by the upwelling of warm CDW (Schmidtko et al., 2014),

1515 hindering the formation of ISW and making the presence of platelet ice in recent conditions highly

1516 unlikely (Hoppmann et al., 2020). This theory is also supported by Langhorne et al. (2015), stating that

1517 platelet ice formation is not observed, where thinning from basal melting of ice shelves is believed to

1518 be greatest, which applies to the warm West Antarctic continental shelf in the eastern Pacific sector of

1519 the Southern Ocean (Thompson et al., 2018). Accordingly, if the formation and accumulation of platelet

1520 ice – up to a certain degree – is indicative of basal ice shelf melting on fresh shelves (Hoppmann et al.,

1521 2015; Thompson et al., 2018), high IPSO₂₅ concentrations determined in marine sediments may hence

1522 serve as indicator of JSW formation and associated ice shelf dynamics. This may, however, only be true

1523 up to a certain threshold where platelet ice formation is diminished/hampered due to warm oceanic

1524 conditions causing too intense sub-ice shelf melting (Langhorne et al., 2015).

1525 While using IPSO₂₅ as a sea-ice proxy in Antarctica, it is hence important to also consider regional

1526 platelet ice formation processes as these may affect the IPSO₂₅ budget. Determining thresholds

1527 associated with platelet ice formation is challenging. Therefore, further investigations, such as in-situ

1528 measurements of IPSO₂₅ concentrations in platelet ice or culture experiments in home laboratories, are

1529 needed to better depict the connection between IPSO₂₅ and platelet ice formation (and ice shelf basal

1530 melting).

7. Conclusions

1533 Biomarker analyses focusing on IPSO₂₅, HBI-trienes, phytosterols and GDGTs in surface sediment

1534 samples from the Antarctic continental margin were investigated to depict recent sea-ice conditions and

Gelöscht: on

Formatiert: Schriftart: (Standard) Times New Roman, Schriftfarbe: Automatisch

Gelöscht: incorporating

Formatiert ... [276]

Gelöscht: show how variable

Gelöscht: can be

Formatiert: Schriftart: (Standard) Times New Roman, Schriftfarbe: Automatisch

Formatiert ... [277]

Gelöscht: The absence

Formatiert: Block, Zeilenabstand: Doppelt

Formatiert: Schriftart: (Standard) Times New Roman

Gelöscht:) might in turn be explicable by

Formatiert: Schriftart: (Standard) Times New Roman

Gelöscht: .

Formatiert ... [278]

Gelöscht: shelf is

Formatiert: Schriftart: (Standard) Times New Roman

Gelöscht: a

Formatiert: Schriftart: (Standard) Times New Roman

Gelöscht: shelf

Formatiert: Schriftart: (Standard) Times New Roman

Gelöscht: and

Formatiert ... [279]

Gelöscht: Amundsen Sea

Formatiert: Schriftart: (Standard) Times New Roman

Gelöscht: past basal melting processes

Formatiert: Schriftart: (Standard) Times New Roman

Gelöscht: leading to a

Formatiert: Schriftart: (Standard) Times New Roman

Gelöscht: basal

Formatiert: Schriftart: (Standard) Times New Roman

Formatiert: Schriftart: (Standard) Times New Roman, Englisch (Vereinigtes Königreich)

Gelöscht: , therefore

Formatiert ... [280]

Gelöscht:Abschnittswechsel (Nächste Seite)..... Conclusion

Formatiert: Block, Zeilenabstand: Doppelt

Gelöscht: ... in surface sediment samples from the Antarctic continental shelves off West Antarctica...argin were investigated to depict recent sea surface and temperature [281]

Formatiert: Nach: 0.63 cm

1577 ocean temperatures in this climate sensitive region. Proxy-based reconstructions of these key variables
 1578 were compared to (1) satellite sea-ice data, (2) instrumental ocean temperature data as well as (3)
 1579 modelled sea-ice patterns and ocean temperatures. The semi-quantitative sea-ice index PIPSO₂₅,
 1580 combining the sea-ice proxy IPSO₂₅ with an open-water phytoplankton marker, yielded reasonably good
 1581 correlations with satellite observations and numerical model results, while correlations with the sea-ice
 1582 proxy IPSO₂₅ alone are rather low. Minimum concentrations of both biomarkers, used for the PIPSO₂₅
 1583 calculations, however, may lead to ambiguous interpretations and significant underestimations of sea-
 1584 ice conditions. Different sea-ice measures when interpreting biomarker data should hence be
 1585 considered.
 1586 Ocean temperature reconstructions based on the TEX^L₈₆ and RI-OH'-paleothermometers show similar
 1587 patterns, but different absolute temperatures. While TEX^L₈₆-derived temperatures are significantly
 1588 biased towards warm temperatures in Drake Passage, the RI-OH'-derived temperature range seems
 1589 more realistic when compared to temperature data based on the WOA13 and modelled annual mean
 1590 SOTs.
 1591 Further investigations of HBI- as well as GDGT-synthesis, transport, sedimentation and preservation
 1592 within the sediments would help to guide the proxies' application. Further taxonomy work, the
 1593 composition of the IPSO₂₅ producer's habitat (basal sea ice, platelet ice, brine channels) and its
 1594 connection to platelet ice formation via in situ or laboratory measurements are required to better
 1595 constrain the IPSO₂₅ potential as a robust sea-ice biomarker. The presumed relationship between IPSO₂₅
 1596 and platelet ice formation in connection to basal melting of ice shelves is supported by our data, showing
 1597 high IPSO₂₅ concentrations in areas where platelet ice formation has previously been reported and low
 1598 IPSO₂₅ concentrations where no platelet ice formation is observed. Accordingly, oceanic conditions and
 1599 the intensity of sub-ice shelf melting need to be considered when using IPSO₂₅ (1) as an indirect
 1600 indicator for sub-ice shelf melting processes and associated ice shelf dynamics, and (2) for the
 1601 application of the PIPSO₂₅ index to estimate sea-ice coverage.

1603 **Data availability**

Gelöscht: the sea surface conditions

Gelöscht: observations and

Formatiert: Schriftart: (Standard) Times New Roman

Formatiert: Schriftart: (Standard) Times New Roman

Gelöscht: estimated

Gelöscht: SSTs deduced from model data

Formatiert: Schriftart: (Standard) Times New Roman

Formatiert: Schriftart: (Standard) Times New Roman

Gelöscht: The combination of different

Formatiert: Schriftart: (Standard) Times New Roman

Gelöscht: strived for

Formatiert: Schriftart: (Standard) Times New Roman

Formatiert: Block, Zeilenabstand: Doppelt

Gelöscht: occurring. Oceanic

Gelöscht: basal

Gelöscht: , however,

Gelöscht: basal

Gelöscht: .

Gelöscht: Temperature reconstructions based on TEX^L₈₆ and RI-OH' paleothermometers show similar patterns, but different absolute temperatures. While TEX^L₈₆-derived temperatures are significantly warm-biased, the RI-OH'-derived temperatures are proven more realistic, when compared to temperature data based on the WOA13 and modelled annual mean SSTs. Further investigations of HBI synthesis, transport, sedimentation and preservation within the sediments as well as the composition of its sources habitat (bottom ice, platelet ice, brine channels) and its connection to platelet ice formation via in situ or laboratory measurements are required to better constrain the proxy's potential as a robust sea-ice biomarker.¶ ... [282]

Formatiert: Schriftart: (Standard) Times New Roman

Formatiert: Block, Zeilenabstand: Doppelt

Formatiert: Nach: 0.63 cm

1630 Datasets related to this article can be found online on *PANGAEA Data Publisher for Earth &*
1631 *Environmental Science* (doi: in prep).

1632 ▲ **Formatiert:** Schriftart: (Standard) Times New Roman

1633 **Author contribution**

1634 N.L. and J.M. designed the concept of the study. N.L. carried out biomarker experiments. X.S and G.L.
1635 developed the model code and X.S. performed the simulations. C.H. provided the satellite data. [M.-](#)
1636 [E.V. provided hitherto unpublished GDGT data for PS97 samples. G.M. and J.H. carried out GDGT](#)
1637 [analyses. C.-D.H. collected surface sediment samples and advised on their ages](#). N.L. prepared the
1638 manuscript and visualizations with contributions from all co-authors. ▲

Formatiert: Schriftart: (Standard) Times New Roman

Formatiert: Schriftart: Helvetica, 14 Pt., Schriftfarbe: Schwarz

Formatiert: Schriftart: (Standard) Times New Roman

1640 **Competing interests**

1641 The authors declare that they have no conflict of interest.

1642 ▲ **Formatiert:** Schriftart: (Standard) Times New Roman

1643 **Acknowledgements**

1644 Denise Diekstall, Mandy Kuck and Jonas Haase are kindly acknowledged for laboratory support. We
1645 thank the captains, crews and science parties of *RV Polarstern* cruises PS69, PS97, PS104, PS111 and
1646 PS118. Especially, ▲ [Frank Niessen, Sabine Hanisch and Michael Schreck](#) are thanked for their support
1647 during PS118. Simon Belt is acknowledged for providing the 7-HND internal standard for HBI
1648 quantification. [AWI, MARUM - University of Bremen, the British Antarctic Survey and NERC UK-](#)
1649 [IODP](#) are acknowledged for funding expedition PS104. N.L., M.-E.V. and J.M. were funded through
1650 the Helmholtz Research Grant VH-NG-1101. [Two anonymous reviewers are thanked for their](#)
1651 [constructive and helpful comments, which lead to a distinct improvement of this manuscript.](#)

Formatiert: Schriftart: (Standard) Times New Roman

Formatiert: Schriftart: (Standard) Times New Roman

Gelöscht: -----Abschnittswechsel (Nächste Seite)-----

1652 **Kommentiert [NLI]:** I will double-check the reference-list before submission.

1653 **Formatiert:** Schriftart: (Standard) Times New Roman

1654 **Formatiert:** Block, Zeilenabstand: Doppelt

1655 **Formatiert:** Schriftart: (Standard) Times New Roman, 9 Pt., Nicht Fett

1656 **Formatiert:** Schriftart: (Standard) Times New Roman

Formatiert: Standard, Block, Einzug: Vor: 0.49 cm, Hängend: 0.49 cm, Zeilenabstand: Doppelt

Formatiert: Nach: 0.63 cm

1558 Allen, C. S., Pike, J., and Pudsey, C. J.: Last glacial–interglacial sea-ice cover in the SW Atlantic
1559 and its potential role in global deglaciation, *Quaternary Science Reviews*, 30, 2446-2458, 2011.

1560 Alonso-Sáez, L., Andersson, A., Heinrich, F., and Bertilsson, S.: High archaeal diversity in Antarctic
1561 circumpolar deep waters, *Environmental microbiology reports*, 3, 689-697, 2011.

1562 Anderson, P. S.: Evidence for an Antarctic winter coastal polynya, *Antarctic science*, 5, 221-226,
1563 1993.

1564 Armand, L. K., and Leventer, A.: Palaeo sea ice distribution–reconstruction and palaeoclimatic
1565 significance, *Sea ice—an introduction to its physics, biology, chemistry, and geology*, 333-372,
1566 2003.

1567 Arrigo, K. R., Worthen, D. L., Lizotte, M. P., Dixon, P., and Dieckmann, G.: Primary production in
1568 Antarctic sea ice, *Science*, 276, 394-397, 1997.

1569 Arrigo, K. R.: Sea ice as a habitat for primary producers, *Sea ice*, 352-369, 2017.

1570 Barbara, L., Crosta, X., Massé, G., and Ther, O.: Deglacial environments in eastern Prydz Bay, East
1571 Antarctica, *Quaternary Science Reviews*, 29, 2731-2740, 2010.

1572 Barbara, L., Crosta, X., Schmidt, S., and Massé, G.: Diatoms and biomarkers evidence for major
1573 changes in sea ice conditions prior the instrumental period in Antarctic Peninsula, *Quaternary
1574 Science Reviews*, 79, 99-110, 2013.

1575 [Bauerfeind, E., Leipe, T. and Ramseier, R.O.: Sedimentation at the permanently ice-covered
1576 Greenland continental shelf \(74°57.7'N/12°58.7'W\): significance of biogenic and lithogenic
1577 particles in particulate matter flux. *Journal of Marine Systems* 56, 151-166, 2005.](#)

1578 [Belt, S. T., Allard, W. G., Massé, G., Robert, J.-M., and Rowland, S. J.: Highly branched isoprenoids
1579 \(HBIs\): identification of the most common and abundant sedimentary isomers, *Geochimica et
1580 Cosmochimica Acta*, 64, 3839-3851, 2000.](#)

1581 Belt, S. T., and Müller, J.: The Arctic sea ice biomarker IP₂₅: a review of current understanding,
1582 recommendations for future research and applications in palaeo sea ice reconstructions,
1583 *Quaternary Science Reviews*, 79, 9-25, 2013.

1584 Belt, S. T., Brown, T. A., Ampel, L., Cabedo-Sanz, P., Fahl, K., Kocis, J. J., Masse, G., Navarro-
1585 Rodriguez, A., Ruan, J., and Xu, Y.: An inter-laboratory investigation of the Arctic sea ice

Formatiert: Schriftart: (Standard) Times New Roman

Formatiert: Standard, Block, Einzug: Vor: 0.49 cm,
Hängend: 0.49 cm, Zeilenabstand: Doppelt

Formatiert: Nach: 0.63 cm

1686 biomarker proxy IP₂₅ in marine sediments: key outcomes and recommendations, *Climate of the*
1687 *Past.*, 10, 155-166, 2014.

1688 Belt, S. T., Cabedo-Sanz, P., Smik, L., Navarro-Rodriguez, A., Berben, S. M. P., Knies, J., and
1689 Husum, K.: Identification of paleo Arctic winter sea ice limits and the marginal ice zone:
1690 Optimised biomarker-based reconstructions of late Quaternary Arctic sea ice, *Earth and Planetary*
1691 *Science Letters*, 431, 127-139, 2015.

1692 Belt, S. T., Smik, L., Brown, T. A., Kim, J. H., Rowland, S. J., Allen, C. S., Gal, J. K., Shin, K. H.,
1693 Lee, J. I., and Taylor, K. W. R.: Source identification and distribution reveals the potential of the
1694 geochemical Antarctic sea ice proxy IPSO₂₅, *Nature Communications*, 7, 12655,
1695 <https://doi.org/10.1038/ncomms12655>, 2016.

1696 Belt, S. T., Brown, T. A., Smik, L., Tatarek, A., Wiktor, J., Stowasser, G., Assmy, P., Allen, C. S.,
1697 and Husum, K.: Identification of C₂₅ highly branched isoprenoid (HBI) alkenes in diatoms of the
1698 genus *Rhizosolenia* in polar and sub-polar marine phytoplankton, *Organic Geochemistry*, 110,
1699 65-72, 2017.

1700 Belt, S. T.: Source-specific biomarkers as proxies for Arctic and Antarctic sea ice, *Organic*
1701 *Geochemistry*, 125, 277-298, 2018.

1702 Berger, A.: Long-term variations of daily insolation and Quaternary climatic changes, *Journal of the*
1703 *atmospheric sciences*, 35, 2362-2367, 1978.

1704 [Blain, S., Quéguiner, B., Armand, L., Belviso, S., Bombled, B., Bopp, L., Bowie, A., Brunet, C.,](#)
1705 [Brussaard, C., Carlotti, F., Christaki, U., Corbière, A., Durand, I., Ebersbach, F., Fuda, J.-L.,](#)
1706 [Garcia, N., Gerringa, L., Griffiths, B., Guigue, C., Guillerm, C., Jacquet, S., Jeandel, C., Laan,](#)
1707 [P., Lefèvre, D., Lo Monaco, C., Malits, A., Mosseri, J., Obernosterer, I., Park, Y.-H., Picheral,](#)
1708 [M., Pondaven, P., Remenyi, T., Sandroni, V., Sarthou, G., Savoye, N., Scouarnec, L., Souhaut,](#)
1709 [M., Thuiller, D., Timmermans, K., Trull, T., Uitz, J., van Beek, P., Veldhuis, M., Vincent, D.,](#)
1710 [Viollier, E., Vong, L. and Wagener, T.: Effect of natural iron fertilization on carbon sequestration](#)
1711 [in the Southern Ocean. *Nature* 446, 1070-1074, 2007.](#)

1712 Boon, J. J., Rijpstra, W. I. C., de Lange, F., De Leeuw, J., Yoshioka, M., and Shimizu, Y.: Black
1713 Sea sterol—a molecular fossil for dinoflagellate blooms, *Nature*, 277, 125-127, 1979.

Formatiert: Schriftart: (Standard) Times New Roman,
Schriftfarbe: Automatisch

Formatiert: Schriftart: (Standard) Times New Roman

Formatiert: Schriftart: (Standard) Times New Roman

Formatiert: Standard, Block, Einzug: Vor: 0.49 cm,
Hängend: 0.49 cm, Zeilenabstand: Doppelt

Formatiert: Nach: 0.63 cm

1714 Cavalieri, D., Parkinson, C., Gloersen, P., and Zwally, H.: Sea ice concentrations from Nimbus-7
 1715 SMMR and DMSP SSM/I passive microwave data, National Snow and Ice Data Center, Boulder,
 1716 Colorado, USA, 1996.

1717 Collares, L. L., Mata, M. M., Kerr, R., Arigony-Neto, J., and Barbat, M. M.: Iceberg drift and ocean
 1718 circulation in the northwestern Weddell Sea, Antarctica, Deep Sea Research Part II: Topical
 1719 Studies in Oceanography, 149, 10-24, 2018.

1720 Colleoni, F., De Santis, L., Siddoway, C. S., Bergamasco, A., Golledge, N. R., Lohmann, G.,
 1721 Passchier, S., and Siegert, M. J.: Spatio-temporal variability of processes across Antarctic ice-
 1722 bed-ocean interfaces, Nature Communications, 9, 2289, [https://doi.org/10.1038/s41467-018-](https://doi.org/10.1038/s41467-018-04583-0)
 1723 [04583-0](https://doi.org/10.1038/s41467-018-04583-0), 2018.

1724 Collins, L. G., Allen, C. S., Pike, J., Hodgson, D. A., Weckström, K., and Massé, G.: Evaluating
 1725 highly branched isoprenoid (HBI) biomarkers as a novel Antarctic sea-ice proxy in deep ocean
 1726 glacial age sediments, Quaternary Science Reviews, 79, 87-98, 2013.

1727 Comiso, J. C., Gersten, R. A., Stock, L. V., Turner, J., Perez, G. J., and Cho, K.: Positive Trend in
 1728 the Antarctic Sea Ice Cover and Associated Changes in Surface Temperature, Journal of Climate,
 1729 30, 2251-2267, 2017.

1730 [Cook, A.J., Holland, P., Meredith, M., Murray, T., Luckman, A., Vaughan, D.G.: Ocean forcing of](#)
 1731 [glacier retreat in the WAP. Science, 353, 283-286, 2016.](#)

1732 [Crosta, X., Pichon, J. J., and Burckle, L.: Application of modern analog technique to marine](#)
 1733 [Antarctic diatoms: Reconstruction of maximum sea-ice extent at the Last Glacial Maximum,](#)
 1734 [Paleoceanography and Paleoclimatology, 13, 284-297, 1998.](#)

1735 [Crosta, X., Etourneau, J., Orme, L.C., Dalaiden, Q., Campagne, P., Swingedouw, D., Gooose, H.,](#)
 1736 [Massé, G., Miettinen, A., McKay, R.M., Dunbar, R.B., Escutia, C. and Ikehara, M.: Multi-](#)
 1737 [decadal trends in Antarctic sea-ice extent driven by ENSO-SAM over the last 2,000 years. Nature](#)
 1738 [Geoscience 14, 156-160, 2021.](#)

1739 [Danilov, S., Sidorenko, D., Wang, Q., and Jung, T.: The Finite-volumE Sea ice-Ocean Model](#)
 1740 [\(FESOM2\), Geosci. Model Dev., 10, 765-789, 2017.](#) [de Jong, J., Schoemann, V., Lannuzel, D.,](#)
 1741 [Croot, P., de Baar, H. and Tison, J.-L.: Natural iron fertilization of the Atlantic sector of the](#)

Formatiert: Schriftart: (Standard) Times New Roman

Formatiert: Standard, Block, Einzug: Vor: 0.49 cm, Hängend: 0.49 cm, Zeilenabstand: Doppelt

Formatiert: Schriftart: (Standard) Times New Roman

Formatiert: Standard, Block, Einzug: Vor: 0.49 cm, Hängend: 0.49 cm, Zeilenabstand: Doppelt

Formatiert: Nach: 0.63 cm

1742 [Southern Ocean by continental shelf sources of the Antarctic Peninsula. Journal of Geophysical](#)
1743 [Research: Biogeosciences 117, 2012.](#)

1744 [Denis, D., Crosta, X., Barbara, L., Massé, G., Renssen, H., Ther, O., and Giraudeau, J.: Sea ice and](#)
1745 [wind variability during the Holocene in East Antarctica: insight on middle–high latitude coupling,](#)
1746 [Quaternary Science Reviews, 29, 3709-3719, 2010.](#)

1747 Dorschel, B.: The Expedition PS118 of the Research Vessel POLARSTERN to the Weddell Sea in
1748 2019, Berichte zur Polar-und Meeresforschung = Reports on polar and marine research, 735,
1749 2019.

1750 Doty, M. S., and Oguri, M.: The island mass effect, ICES Journal of Marine Science, 22, 33-37,
1751 1956.

1752 [Eayrs, C., Li, X., Raphael, M.N. and Holland, D.M.: Rapid decline in Antarctic sea ice in recent](#)
1753 [years hints at future change. Nature Geoscience 14, 460-464, 2021.](#)

1754 [Esper, O., and Gersonde, R.: New tools for the reconstruction of Pleistocene Antarctic sea ice,](#)
1755 [Palaeogeography, Palaeoclimatology, Palaeoecology, 399, 260-283, 2014.](#)

1756 Etourneau, J., Collins, L. G., Willmott, V., Kim, J.-H., Barbara, L., Leventer, A., Schouten, S.,
1757 Damsté, J. S., Bianchini, A., and Klein, V.: Holocene climate variations in the [WAP](#): evidence
1758 for sea ice extent predominantly controlled by changes in insolation and ENSO variability,
1759 Climate of the Past, 9, 1431-1446, 2013.

1760 [Etourneau, J., Sgubin, G., Crosta, X., Swingedouw, D., Willmott, V., Barbara, L., Houssais, M.-N.,](#)
1761 [Schouten, S., Damsté, J.S.S., Goosse, H.: Ocean temperature impact on ice shelf extent in the](#)
1762 [eastern Antarctic Peninsula. Nature Communications 10, 1-8, 2019.](#)

1763 [Fahl, K., and Stein, R.: Modern seasonal variability and deglacial/Holocene change of central Arctic](#)
1764 [Ocean sea-ice cover: new insights from biomarker proxy records, Earth and Planetary Science](#)
1765 [Letters, 351, 123-133, 2012.](#)

1766 Fetterer, F., Knowles, K., Meier, W., Savoie, M., Windnagel, A.K., 2016. Updated Daily. Sea Ice
1767 Index, Version 2. [Median Sea Ice Extent 1981-2010]. NSIDC: National Snow and Ice Data
1768 Center, Boulder, Colorado USA. <https://doi.org/10.7265/N5736NV7> [24 July 2017].

Formatiert: Schriftart: (Standard) Times New Roman

Gelöscht: Deacon, G. R. E.: The Weddell Gyre, Deep Sea Research Part A. Oceanographic Research Papers, 26, 981-995, 1979.

Formatiert: Schriftart: (Standard) Times New Roman

Formatiert: Schriftart: (Standard) Times New Roman

Formatiert: Standard, Block, Einzug: Vor: 0.49 cm, Hängend: 0.49 cm, Zeilenabstand: Doppelt

Gelöscht: western Antarctic Peninsula

Formatiert: Schriftart: (Standard) Times New Roman

Formatiert: Schriftart: (Standard) Times New Roman

Formatiert: Standard, Block, Einzug: Vor: 0.49 cm, Hängend: 0.49 cm, Zeilenabstand: Doppelt

Formatiert: Standard, Block, Einzug: Vor: 0.6 cm, Zeilenabstand: Doppelt

Formatiert: Nach: 0.63 cm

1773 Fietz, S., Huguet, C., Rueda, G., Hambach, B., and Rosell-Melé, A.: Hydroxylated isoprenoidal
 1774 GDGTs in the Nordic Seas, *Marine Chemistry*, 152, 1-10, 2013.

1775 Fietz, S., Ho, S., and Huguet, C.: Archaeal Membrane Lipid-Based Paleothermometry for
 1776 Applications in Polar Oceans, *Oceanography*, 33, 104-114, 2020.

1777 Foldvik, A., and Kvinge, T.: Conditional instability of sea water at the freezing point, *Deep Sea*
 1778 *Research and Oceanographic Abstracts*, 21, 169-174, 1974.

1779 [Fretwell, P., Pritchard, H.D., Vaughan, D.G., 57 others. Bedmap2: improved ice bed, surface and](#)
 1780 [thickness datasets for Antarctica. *Cryosphere* 7, 375-393. \[http://dx.doi.org/10.5194/tc-7-375-\]\(http://dx.doi.org/10.5194/tc-7-375-2013\)](#)
 1781 [2013.2013.](#)

1782 [Gersonde, R., and Zielinski, U.: The reconstruction of late Quaternary Antarctic sea-ice](#)
 1783 [distribution—the use of diatoms as a proxy for sea-ice, *Palaeogeography, Palaeoclimatology,*](#)
 1784 [Palaeoecology](#), 162, 263-286, 2000.

1785 Gohl, K.: The expedition ANTARKTIS-XXIII/4 of the research vessel Polarstern in 2006, *Berichte*
 1786 *zur Polar-und Meeresforschung (Reports on Polar and Marine Research)*, 557, 2007.

1787 Gohl, K.: The Expedition PS104 of the Research Vessel POLARSTERN to the Amundsen Sea in
 1788 2017, *Berichte zur Polar-und Meeresforschung = Reports on polar and marine research*, 712,
 1789 2017.

1790 [Gordon, J.E., Harkness, D.D.: Magnitude and geographic variation of the radiocarbon content in](#)
 1791 [Antarctic marine life: implications for reservoir corrections in radiocarbon dating. *Quaternary*](#)
 1792 [Science Reviews](#) 11, 697-708, 1992.

1793 [Hancke, K., Lund-Hansen, L. C., Lamare, M. L., Højlund Pedersen, S., King, M. D., Andersen, P.,](#)
 1794 [and Sorrell, B. K.: Extreme low light requirement for algae growth underneath sea ice: A case](#)
 1795 [study from Station Nord, NE Greenland, *Journal of Geophysical Research: Oceans*](#), 123, 985-
 1796 1000, 2018.

1797 Harms, S., Fahrbach, E., and Strass, V. H.: Sea ice transports in the Weddell Sea, *Journal of*
 1798 *Geophysical Research: Oceans*, 106, 9057-9073, 2001.

Formatiert: Standard, Block, Einzug: Vor: 0.49 cm, Hängend: 0.49 cm, Zeilenabstand: Doppelt

Formatiert: Schriftart: (Standard) Times New Roman

Formatiert: Standard, Block, Einzug: Vor: 0.49 cm, Hängend: 0.49 cm, Zeilenabstand: Doppelt

Formatiert: Schriftart: (Standard) Times New Roman

Formatiert: Standard, Block, Einzug: Vor: 0.49 cm, Hängend: 0.49 cm, Zeilenabstand: Doppelt

Formatiert: Nach: 0.63 cm

1799 [Hedges, J.I., Hu, F.S., Devol, A.H., Hartnett, H.E., Tsamakis, E. and Keil, R.G.: Sedimentary organic](#)
1800 [matter preservation; a test for selective degradation under oxic conditions. Am J Sci 299, 529-](#)
1801 [555, 1999.](#)

1802 [Hellmer, H.H., Rhein, M., Heinemann, G., Abalichin, J., Abouchami, W., Baars, O., Cubasch, U.,](#)
1803 [Dethloff, K., Ebner, L., Fahrbach, E., Frank, M., Gollan, G., Greatbatch, R.J., Grieger, J.,](#)
1804 [Gryanik, V.M., Gryscha, M., Hauck, J., Hoppema, M., Huhn, O., Kanzow, T., Koch, B.P.,](#)
1805 [König-Langlo, G., Langematz, U., Leckebusch, G.C., Lüpkes, C., Paul, S., Rinke, A., Rost, B.,](#)
1806 [van der Loeff, M.R., Schröder, M., Seckmeyer, G., Stichel, T., Strass, V., Timmermann, R.,](#)
1807 [Trimborn, S., Ulbrich, U., Venchiarutti, C., Wacker, U., Willmes, S. and Wolf-Gladrow, D.:](#)
1808 [Meteorology and oceanography of the Atlantic sector of the Southern Ocean - a review of German](#)
1809 [achievements from the last decade. Ocean Dynamics 66, 1379-1413, 2016.](#)

1810 [Hillenbrand, C.-D., Smith, J.A., Kuhn, G., Esper, O., Gersonde, R., Larter, R.D., Maher, B.,](#)
1811 [Moreton, S.G., Shimmield, T.M., Korte, M.: Age assignment of a diatomaceous ooze deposited](#)
1812 [in the western Amundsen Sea Embayment after the Last Glacial Maximum. Journal of](#)
1813 [Quaternary Science 25, 280-295, 2010.](#)

1814 [Hillenbrand, C.-D., Kuhn, G., Smith, J.A., Gohl, K., Graham, A.G.C., Larter, R.D., Klages, J.P.,](#)
1815 [Downey, R., Moreton, S.G., Forwick, M., Vaughan, D.G.: Grounding-line retreat of the West](#)
1816 [Antarctic Ice Sheet from inner Pine Island Bay. Geology 41, 35-38, 2013.](#)

1817 [Hillenbrand, C.-D., Smith, J.A., Hodell, D.A., Greaves, M., Poole, C.R., Kender, S., Williams, M.,](#)
1818 [Andersen, T.J., Jernas, P.E., Elderfield, H., Klages, J.P., Roberts, S.J., Gohl, K., Larter, R.D.,](#)
1819 [Kuhn, G.: West Antarctic Ice Sheet retreat driven by Holocene warm water intrusions. Nature](#)
1820 [547, 43-48, 2017.](#)

1821 [Ho, S. L., Mollenhauer, G., Fietz, S., Martínez-García, A., Lamy, F., Rueda, G., Schipper, K.,](#)
1822 [Méheust, M., Rosell-Melé, A., Stein, R., and Tiedemann, R.: Appraisal of TEX₈₆ and](#)
1823 [thermometries in subpolar and polar regions, Geochimica et Cosmochimica Acta, 131, 213-226,](#)
1824 [2014.](#)

Formatiert: Schriftart: (Standard) Times New Roman

Formatiert: Standard, Block, Einzug: Vor: 0.49 cm, Hängend: 0.49 cm, Zeilenabstand: Doppelt

Formatiert: Nach: 0.63 cm

- 1825 Hobbs, W. R., Massom, R., Stammerjohn, S., Reid, P., Williams, G., and Meier, W.: A review of
1826 recent changes in Southern Ocean sea ice, their drivers and forcings, *Global and Planetary*
1827 *Change*, 143, 228-250, 2016.
- 1828 Holland, P. R., Feltham, D. L., and Jenkins, A.: Ice shelf water plume flow beneath Filchner-Ronne
1829 Ice Shelf, Antarctica, *Journal of Geophysical Research: Oceans*, 112,
1830 <https://doi.org/10.1029/2006JC003915>, 2007.
- 1831 Hopmans, E. C., Weijers, J. W., Schefuß, E., Herfort, L., Damsté, J. S. S., and Schouten, S.: A novel
1832 proxy for terrestrial organic matter in sediments based on branched and isoprenoid tetraether
1833 lipids, *Earth and Planetary Science Letters*, 224, 107-116, 2004.
- 1834 Hoppmann, M., Nicolaus, M., Paul, S., Hunkeler, P. A., Heinemann, G., Willmes, S., Timmermann,
1835 R., Boebel, O., Schmidt, T., and Kühnel, M.: Ice platelets below Weddell Sea landfast sea ice,
1836 *Annals of Glaciology*, 56, 175-190, 2015.
- 1837 Hoppmann, M., Richter, M. E., Smith, I. J., Jendersie, S., Langhorne, P. J., Thomas, D. N., and
1838 Dieckmann, G. S.: Platelet ice, the Southern Ocean's hidden ice: a review, *Annals of Glaciology*,
1839 1-28, 2020.
- 1840 Huguet, C., de Lange, G. J., Gustafsson, Ö., Middelburg, J. J., Damsté, J. S. S., and Schouten, S.:
1841 Selective preservation of soil organic matter in oxidized marine sediments (Madeira Abyssal
1842 Plain), *Geochimica et Cosmochimica Acta*, 72, 6061-6068, 2008.
- 1843 Iacono, M. J., Delamere, J. S., Mlawer, E. J., Shephard, M. W., Clough, S. A., and Collins, W. D.:
1844 Radiative forcing by long-lived greenhouse gases: Calculations with the AER radiative transfer
1845 models, *Journal of Geophysical Research: Atmospheres*, 113,
1846 <https://doi.org/10.1029/2008JD009944>, 2008.
- 1847 Jacobs, S. S., Jenkins, A., Giulivi, C. F., and Dutrieux, P.: Stronger ocean circulation and increased
1848 melting under Pine Island Glacier ice shelf, *Nature Geoscience*, 4, 519-523, 2011.
- 1849 Jenkins, A., and Jacobs, S.: Circulation and melting beneath George VI ice shelf, Antarctica, *Journal*
1850 *of Geophysical Research: Oceans*, 113, <https://doi.org/10.1029/2007JC004449>, 2008.

Gelöscht:

Formatiert: Schriftart: (Standard) Times New Roman

Formatiert: Nach: 0.63 cm

1352 Johns, L., Wraige, E., Belt, S., Lewis, C., Massé, G., Robert, J.-M., and Rowland, S.: Identification
1353 of a C₂₅ highly branched isoprenoid (HBI) diene in Antarctic sediments, Antarctic sea-ice diatoms
1354 and cultured diatoms, *Organic Geochemistry*, 30, 1471-1475, 1999.

1355 Kalanetra, K. M., Bano, N., and Hollibaugh, J. T.: Ammonia-oxidizing Archaea in the Arctic Ocean
1356 and Antarctic coastal waters, *Environmental Microbiology*, 11, 2434-2445, 2009.

1357 [Khazendar, A., Rignot, E., Schroeder, D.M., Seroussi, H., Schodlok, M.P., Scheuchl, B., Mouginot,](#)
1358 [J., Sutterley, T.C., Velicogna, I.: Rapid submarine ice melting in the grounding zones of ice](#)
1359 [shelves in West Antarctica. *Nature communications* 7, 1-8, 2016.](#)

1360 [Kim, J.-H., Van der Meer, J., Schouten, S., Helmke, P., Willmott, V., Sangiorgi, F., Koç, N.,](#)
1361 [Hopmans, E. C., and Damsté, J. S. S.: New indices and calibrations derived from the distribution](#)
1362 [of crenarchaeal isoprenoid tetraether lipids: Implications for past sea surface temperature](#)
1363 [reconstructions, *Geochimica et Cosmochimica Acta*, 74, 4639-4654, 2010.](#)

1364 Kim, J.-H., Crosta, X., Willmott, V., Renssen, H., Bonnin, J., Helmke, P., Schouten, S., and
1365 Sinninghe Damsté, J. S.: Holocene subsurface temperature variability in the eastern Antarctic
1366 continental margin, *Geophysical Research Letters*, 39, <https://doi.org/10.1029/2012GL051157>,
1367 2012.

1368 Klinck, J. M., Hofmann, E. E., Beardsley, R. C., Salihoglu, B., and Howard, S.: Water-mass
1369 properties and circulation on the [WAP](#) Continental Shelf in Austral Fall and Winter 2001, *Deep*
1370 *Sea Research Part II: Topical Studies in Oceanography*, 51, 1925-1946, 2004.

1371 Köhler, P., Nehrbaas-Ahles, C., Schmitt, J., Stocker, T. F., and Fischer, H.: A 156 kyr smoothed
1372 history of the atmospheric greenhouse gases CO₂, CH₄, and N₂O and their radiative forcing, *Earth*
1373 *Syst. Sci. Data*, 9, 363-387, 2017.

1374 Lamping, N., Müller, J., Esper, O., Hillenbrand, C.-D., Smith, J. A., and Kuhn, G.: Highly branched
1375 isoprenoids reveal onset of deglaciation followed by dynamic sea-ice conditions in the western
1376 Amundsen Sea, Antarctica, *Quaternary Science Reviews*, 228,
1377 <https://doi.org/10.1016/j.quascirev.2019.106103>, 2020.

1378 Lange, M., Ackley, S., Wadhams, P., Dieckmann, G., and Eicken, H.: Development of sea ice in the
1379 Weddell Sea, *Annals of Glaciology*, 12, 92-96, 1989.

Formatiert: Schriftart: (Standard) Times New Roman

Formatiert: Standard, Block, Einzug: Vor: 0.49 cm,
Hängend: 0.49 cm, Zeilenabstand: Doppelt

Gelöscht: west Antarctic Peninsula

Formatiert: Schriftart: (Standard) Times New Roman

Formatiert: Nach: 0.63 cm

1881 Langhorne, P., Hughes, K., Gough, A., Smith, I., Williams, M., Robinson, N., Stevens, C., Rack,
 1882 W., Price, D., and Leonard, G.: Observed platelet ice distributions in Antarctic sea ice: An index
 1883 for ocean-ice shelf heat flux, *Geophysical Research Letters*, 42, 5442-5451, 2015.

1884 Leventer, A.: The fate of Antarctic “sea ice diatoms” and their use as paleoenvironmental indicators,
 1885 Antarctic sea ice. Biological processes, interactions and variability, 121-137, 1998.

1886 [Li, X., Holland, D.M., Gerber, E.P. and Yoo, C.: Impacts of the north and tropical Atlantic Ocean on
 1887 the Antarctic Peninsula and sea ice. *Nature* 505, 538-542, 2014.](#)

1888 [Liu, J., Curry, J. A., and Martinson, D. G.: Interpretation of recent Antarctic sea ice variability,
 1889 *Geophysical Research Letters*, 31, <https://doi.org/10.1029/2003GL018732>, 2004.](#)

1890 [Liu, R., Han, Z., Zhao, J., Zhang, H., Li, D., Ren, J., Pan, J., Zhang, H.: Distribution and source of
 1891 glycerol dialkyl glycerol tetraethers \(GDGTs\) and the applicability of GDGT-based temperature
 1892 proxies in surface sediments of Prydz Bay, East Antarctica. *Polar Research*, 2020.](#)

1893 [Locarnini, R. A., Mishonov, A. V., Antonov, J. I., Boyer, T. P., Garcia, H. E., Baranova, O. K.,
 1894 Zweng, M. M., Paver, C. R., Reagan, J. R., and Johnson, D. R.: World ocean atlas 2013. Volume
 1895 1, Temperature, NOAA Atlas NESDIS 73, 40 pp., doi: 10.7289/V55X26VD, 2013.](#)

1896 Lohmann, G., Butzin, M., Eissner, N., Shi, X., and Stepanek, C.: Abrupt climate and weather
 1897 changes across time scales, *Paleoceanography and Paleoclimatology*, 35,
 1898 <https://doi.org/10.1029/2019PA003782>, 2020.

1899 López-García, P., Rodríguez-Valera, F., Pedrós-Alió, C., and Moreira, D.: Unexpected diversity of
 1900 small eukaryotes in deep-sea Antarctic plankton, *Nature*, 409, 603-607, 2001.

1901 Lorenz, S. J., and Lohmann, G.: Acceleration technique for Milankovitch type forcing in a coupled
 1902 atmosphere-ocean circulation model: method and application for the Holocene, *Climate
 1903 Dynamics*, 23, 727-743, 2004.

1904 Lott, F.: Alleviation of stationary biases in a GCM through a mountain drag parameterization scheme
 1905 and a simple representation of mountain lift forces, *Monthly weather review*, 127, 788-801, 1999.

1906 Loveland, T. R., Reed, B. C., Brown, J. F., Ohlen, D. O., Zhu, Z., Yang, L., and Merchant, J. W.:
 1907 Development of a global land cover characteristics database and IGBP DISCover from 1 km
 1908 AVHRR data, *Int. J. Remote Sens.*, 21, 1303-1330, 2000.

Formatiert: Schriftart: (Standard) Times New Roman

Formatiert: Standard, Block, Einzug: Vor: 0.49 cm,
 Hängend: 0.49 cm, Zeilenabstand: Doppelt

Formatiert: Schriftart: (Standard) Times New Roman

Formatiert: Standard, Block, Einzug: Vor: 0.49 cm,
 Hängend: 0.49 cm, Zeilenabstand: Doppelt

Formatiert: Nach: 0.63 cm

- 1909 Lü, X., Liu, X.-L., Elling, F. J., Yang, H., Xie, S., Song, J., Li, X., Yuan, H., Li, N., and Hinrichs,
1910 K.-U.: Hydroxylated isoprenoid GDGTs in Chinese coastal seas and their potential as a
1911 paleotemperature proxy for mid-to-low latitude marginal seas, *Organic Geochemistry*, 89-90, 31-
1912 43, 2015.
- 1913 Massé, G., Belt, S. T., Crosta, X., Schmidt, S., Snape, I., Thomas, D. N., and Rowland, S. J.: Highly
1914 branched isoprenoids as proxies for variable sea ice conditions in the Southern Ocean, *Antarctic
1915 Science*, 23, 487-498, 2011.
- 1916 Massom, R. A., Scambos, T. A., Bennetts, L. G., Reid, P., Squire, V. A., and Stammerjohn, S. E.:
1917 Antarctic ice shelf disintegration triggered by sea ice loss and ocean swell, *Nature*, 558, 383-389,
1918 2018.
- 1919 Medlin, L.: *Berkeleya* spp. from Antarctic waters, including *Berkeleya adeliensis*, sp. nov., a new
1920 tube dwelling diatom from the undersurface of sea-ice, *Beihefte zur Nova Hedwigia*, 100, 77-89,
1921 1990.
- 1922 Meredith, M. P., Woodworth, P. L., Chereskin, T. K., Marshall, D. P., Allison, L. C., Bigg, G. R.,
1923 Donohue, K., Heywood, K. J., Hughes, C. W., and Hibbert, A.: Sustained monitoring of the
1924 Southern Ocean at Drake Passage: Past achievements and future priorities, *Reviews of
1925 Geophysics*, 49, <https://doi.org/10.1029/2010RG000348>, 2011.
- 1926 Meyers, P. A.: Organic geochemical proxies of paleoceanographic, paleolimnologic, and
1927 paleoclimatic processes, *Organic geochemistry*, 27, 213-250, 1997.
- 1928 Moore, J. K., and Abbott, M. R.: Surface chlorophyll concentrations in relation to the Antarctic Polar
1929 Front: seasonal and spatial patterns from satellite observations, *Journal of Marine Systems*, 37,
1930 69-86, 2002.
- 1931 Müller, J., Wagner, A., Fahl, K., Stein, R., Prange, M., and Lohmann, G.: Towards quantitative sea
1932 ice reconstructions in the northern North Atlantic: A combined biomarker and numerical
1933 modelling approach, *Earth and Planetary Science Letters*, 306, 137-148, 2011.
- 1934 Müller, J., and Stein, R.: High-resolution record of late glacial and deglacial sea ice changes in Fram
1935 Strait corroborates ice-ocean interactions during abrupt climate shifts, *Earth and Planetary
1936 Science Letters*, 403, 446-455, 2014.

1937 [Nakayama, Y., Schröder, M., Hellmer, H.H.: From circumpolar deep water to the glacial meltwater](#)
1938 [plume on the eastern Amundsen Shelf. Deep Sea Research Part I: Oceanographic Research](#)
1939 [Papers 77, 50-62, 2013.](#)

1940 [Nakayama, Y., Menemenlis, D., Zhang, H., Schodlok, M. and Rignot, E.: Origin of Circumpolar](#)
1941 [Deep Water intruding onto the Amundsen and Bellingshausen Sea continental shelves. Nature](#)
1942 [Communications 9, 3403, 2018.](#)

1943 [Nicholls, K. W., Østerhus, S., Makinson, K., Gammelsrød, T., and Fahrbach, E.: Ice-ocean processes](#)
1944 [over the continental shelf of the southern Weddell Sea, Antarctica: A review, Reviews of](#)
1945 [Geophysics, 47, https://doi.org/10.1029/2007RG000250, 2009.](#)

1946 Nichols, P. D., Palmisano, A. C., Volkman, J. K., Smith, G. A., and White, D. C.: Occurrence of an
1947 isoprenoid C₂₅ diunsaturated alkene and high neutral lipid content in Antarctic sea-ice diatom
1948 communities 1, *Journal of Phycology*, 24, 90-96, 1988.

1949 Nielsdóttir, M. C., Bibby, T. S., Moore, C. M., Hinz, D. J., Sanders, R., Whitehouse, M., Korb, R.,
1950 and Achterberg, E. P.: Seasonal and spatial dynamics of iron availability in the Scotia Sea, *Marine*
1951 *Chemistry*, 130, 62-72, 2012.

1952 Nolting, R., De Baar, H., Van Bennekom, A., and Masson, A.: Cadmium, copper and iron in the
1953 Scotia Sea, Weddell Sea and Weddell/Scotia confluence (Antarctica), *Marine Chemistry*, 35,
1954 219-243, 1991.

1955 Orsi, A. H., Whitworth III, T., and Nowlin Jr, W. D.: On the meridional extent and fronts of the
1956 Antarctic Circumpolar Current, *Deep Sea Research Part I: Oceanographic Research Papers*, 42,
1957 641-673, 1995.

1958 Otto-Bliesner, B., Brady, E., Zhao, A., Brierley, C., Axford, Y., Capron, E., Govin, A., Hoffman, J.,
1959 Isaacs, E., and Kageyama, M.: Large-scale features of Last Interglacial climate: Results from
1960 evaluating the lig127k simulations for CMIP6-PMIP4, *Climate of the Past*, 17, 63-94, 2021.

1961 Otto-Bliesner, B. L., Braconnot, P., Harrison, S. P., Lunt, D. J., Abe-Ouchi, A., Albani, S., Bartlein,
1962 P. J., Capron, E., Carlson, A. E., and Dutton, A.: The PMIP4 contribution to CMIP6–Part 2: Two
1963 interglacials, scientific objective and experimental design for Holocene and Last Interglacial
1964 simulations, *Geoscientific Model Development*, 10, 3979-4003, 2017.

Formatiert: Schriftart: (Standard) Times New Roman

Formatiert: Standard, Block, Einzug: Vor: 0.49 cm,
Hängend: 0.49 cm, Zeilenabstand: Doppelt

Formatiert: Nach: 0.63 cm

- 1965 Park, E., Hefter, J., Fischer, G., Iversen, M. H., Ramondenc, S., Nöthig, E.-M., and Mollenhauer,
1966 G.: Seasonality of archaeal lipid flux and GDGT-based thermometry in sinking particles of high-
1967 latitude oceans: Fram Strait (79° N) and Antarctic Polar Front (50° S), *Biogeosciences*, 16, 2247-
1968 2268, 2019.
- 1969 Parkinson, C. L., and Cavalieri, D. J.: Antarctic sea ice variability and trends, 1979-2010, *The*
1970 *Cryosphere*, 6, 871-880, 2012.
- 1971 Parkinson, C. L.: A 40-y record reveals gradual Antarctic sea ice increases followed by decreases at
1972 rates far exceeding the rates seen in the Arctic, *Proceedings of the National Academy of Sciences*,
1973 116, 14414-14423, 2019.
- 1974 Paul, S., Willmes, S., and Heinemann, G.: Long-term coastal-polynya dynamics in the southern
1975 Weddell Sea from MODIS thermal-infrared imagery, *The Cryosphere*, 9, 2027-2041, 2015.
- 1976 Pritchard, H., Ligtenberg, S., Fricker, H., Vaughan, D., Van den Broeke, M., and Padman, L.:
1977 Antarctic ice-sheet loss driven by basal melting of ice shelves, *Nature*, 484, 502-505, 2012.
- 1978 Raddatz, T., Reick, C., Knorr, W., Kattge, J., Roeckner, E., Schnur, R., Schnitzler, K.-G., Wetzela,
1979 P., and JungCLAUS, J.: Will the tropical land biosphere dominate the climate-carbon cycle
1980 feedback during the twenty-first century?, *Climate dynamics*, 29, 565-574, 2007.
- 1981 Riaux-Gobin, C., and Poulin, M.: Possible symbiosis of *Berkeleya adeliensis* Medlin, *Synedropsis*
1982 *fragilis* (Manguin) Hasle et al. and *Nitzschia lecontei* Van Heurck (Bacillariophyta) associated
1983 with land-fast ice in Adélie Land, Antarctica, *Diatom Research*, 19, 265-274, 2004.
- 1984 Riaux-Gobin, C., Dieckmann, G. S., Poulin, M., Neveux, J., Labruno, C., and Vétion, G.:
1985 Environmental conditions, particle flux and sympagic microalgal succession in spring before the
1986 sea-ice break-up in Adélie Land, East Antarctica, *Polar Research*, 32,
1987 <https://doi.org/10.3402/polar.v32i0.19675>, 2013.
- 1988 [Rignot, E., Mouginot, J., Scheuchl, B., Van Den Broeke, M., Van Wessem, M.J., Morlighem, M.:](#)
1989 [Four decades of Antarctic Ice Sheet mass balance from 1979–2017. *Proceedings of the National*](#)
1990 [Academy of Sciences 116, 1095-1103, 2019.](#)
- 1991 [Rintoul, S., Hughes, C., and Olbers, D.:](#) The Antarctic circumpolar current system, *International*
1992 *Geophysics*, 77, 271-302, 2001.

Formatiert: Schriftart: (Standard) Times New Roman

Formatiert: Standard, Block, Einzug: Vor: 0.49 cm,
Hängend: 0.49 cm, Zeilenabstand: Doppelt

Formatiert: Nach: 0.63 cm

1993 Roeckner, E., Dümenil, L., Kirk, E., Lunkeit, F., Ponater, M., Rockel, B., Sausen, R., and Schlese,
1994 U.: The Hamburg version of the ECMWF model (ECHAM), Research activities in atmospheric
1995 and oceanic modelling. CAS/JSC Working Group on Numerical Experimentation, 13, 7.1-7.4,
1996 1989.

1997 [Rontani, J.-F., Smik, L. and Belt, S.T.: Autoxidation of the sea ice biomarker proxy IPSO₂₅ in the](#)
1998 [near-surface oxic layers of Arctic and Antarctic sediments, *Organic Geochemistry* 129, 63-76,](#)
1999 [2019.](#)

2000 [Rontani, J.-F., Belt, S.T. and Amiriaux, R.: Biotic and abiotic degradation of the sea ice diatom](#)
2001 [biomarker IP₂₅ and selected algal sterols in near-surface Arctic sediments, *Organic Geochemistry*](#)
2002 [118, 73-88, 2018.](#)

2003 [Sangrà, P., Gordo, C., Hernández-Arencibia, M., Marrero-Díaz, A., Rodríguez-Santana, A., Stegner,](#)
2004 [A., Martínez-Marrero, A., Pelegrí, J. L., and Pichon, T.: The Bransfield current system, *Deep Sea*](#)
2005 [Research Part I: Oceanographic Research Papers](#), 58, 390-402, 2011.

2006 Scambos, T. A., Bell, R. E., Alley, R. B., Anandakrishnan, S., Bromwich, D., Brunt, K.,
2007 Christianson, K., Creyts, T., Das, S., and DeConto, R.: How much, how fast?: A science review
2008 and outlook for research on the instability of Antarctica's Thwaites Glacier in the 21st century,
2009 *Global and Planetary Change*, 153, 16-34, 2017.

2010 Schmidt, K., Brown, T. A., Belt, S. T., Ireland, L. C., Taylor, K. W., Thorpe, S. E., Ward, P., and
2011 Atkinson, A.: Do pelagic grazers benefit from sea ice? Insights from the Antarctic sea ice proxy
2012 IPSO₂₅, 15, 1987-2006, 2018.

2013 Schmidtko, S., Heywood, K. J., Thompson, A. F., and Aoki, S.: Multidecadal warming of Antarctic
2014 waters, *Science*, 346, 1227-1231, 2014.

2015 Schofield, O., Brown, M., Kohut, J., Nardelli, S., Saba, G., Waite, N., and Ducklow, H.: Changes in
2016 the upper ocean mixed layer and phytoplankton productivity along the West Antarctic Peninsula,
2017 *Philosophical Transactions of the Royal Society A: Mathematical, Physical and Engineering*
2018 *Sciences*, 376, <https://doi.org/10.1098/rsta.2017.0173>, 2018.

Formatiert: Schriftart: (Standard) Times New Roman

Formatiert: Standard, Block, Einzug: Vor: 0.49 cm,
Hängend: 0.49 cm, Zeilenabstand: Doppelt

Formatiert: Nach: 0.63 cm

2019 Schouten, S., Hopmans, E. C., Schefuß, E., and Sinninghe Damsté, J. S.: Distributional variations in
2020 marine crenarchaeotal membrane lipids: a new tool for reconstructing ancient sea water
2021 temperatures?, *Earth and Planetary Science Letters*, 204, 265-274, 2002.

2022 Schouten, S., Hopmans, E. C., and Sinninghe Damsté, J. S.: The organic geochemistry of glycerol
2023 dialkyl glycerol tetraether lipids: A review, *Organic Geochemistry*, 54, 19-61, 2013.

2024 Schröder, M.: The Expedition PS111 of the Research POLARSTERN to the southern Weddell Sea
2025 in 2018, *Berichte zur Polar-und Meeresforschung = Reports on polar and marine research*, 718,
2026 2018.

2027 Sidorenko, D., Goessling, H., Koldunov, N., Scholz, P., Danilov, S., Barbi, D., Cabos, W., Gurses,
2028 O., Harig, S., and Hinrichs, C.: Evaluation of FESOM2. 0 coupled to ECHAM6. 3: Preindustrial
2029 and HighResMIP simulations, *Journal of Advances in Modeling Earth Systems*, 11, 3794-3815,
2030 2019.

2031 Smik, L., Belt, S. T., Lieser, J. L., Armand, L. K., and Leventer, A.: Distributions of highly branched
2032 isoprenoid alkenes and other algal lipids in surface waters from East Antarctica: further insights
2033 for biomarker-based paleo sea-ice reconstruction, *Organic Geochemistry*, 95, 71-80, 2016.

2034 [Smith, J.A., Hillenbrand, C.-D., Kuhn, G., Klages, J.P., Graham, A.G.C., Larter, R.D., Ehrmann,
2035 W., Moreton, S.G., Wiers, S., Frederichs, T.: New constraints on the timing of West Antarctic
2036 Ice Sheet retreat in the eastern Amundsen Sea since the Last Glacial Maximum. *Glob. Planet.
2037 Change* 112, 224-237, 2014.](#)

2038 [Smith, J.A., Hillenbrand, C.-D., Kuhn, G., Larter, R.D., Graham, A.G.C., Ehrmann, W., Moreton,
2039 S.G., Forwick, M.: Deglacial history of the West Antarctic Ice Sheet in the western Amundsen
2040 Sea Embayment, *Quaternary Science Reviews* 30, 488-505, 2011.](#)

2041 [Smith, J.A., Andersen, T., Shortt, M., Gaffney, A., Truffer, M., Stanton, T.P., Bindschadler, R.,
2042 Dutrieux, P., Jenkins, A., Hillenbrand, C.-D.: Sub-ice-shelf sediments record history of twentieth-
2043 century retreat of Pine Island Glacier, *Nature* 541, 77-80, 2017.](#)

2044 [Spencer-Jones, C. L., McClymont, E. L., Bale, N. J., Hopmans, E. C., Schouten, S., Müller, J.,
2045 Abrahamsen, E. P., Allen, C., Bickert, T., Hillenbrand, C. D., Mawbey, E., Peck, V., Svalova,
2046 A., and Smith, J. A.: Archaeal Intact Polar Lipids in Polar Waters: A Comparison Between the](#)

Formatiert: Schriftart: (Standard) Times New Roman

Formatiert: Standard, Block, Einzug: Vor: 0.49 cm,
Hängend: 0.49 cm, Zeilenabstand: Doppelt

Formatiert: Nach: 0.63 cm

2047 Amundsen and Scotia Seas, Biogeosciences Discuss. [preprint], [https://doi.org/10.5194/bg-2020-](https://doi.org/10.5194/bg-2020-333)
2048 [333](https://doi.org/10.5194/bg-2020-333), in review, 2020.

2049 [Stevens, B., Giorgetta, M., Esch, M., Mauritsen, T., Crueger, T., Rast, S., Salzmann, M., Schmidt,](#)
2050 [H., Bader, J., and Block, K.:](#) Atmospheric component of the MPI-M Earth system model:
2051 ECHAM6, *Journal of Advances in Modeling Earth Systems*, 5, 146-172, 2013.

2052 [Stocker, T. F., Qin, D., Plattner, G.-K., Tignor, M., Allen, S. K., Boschung, J., Nauels, A., Xia, Y.,](#)
2053 [Bex, V., and Midgley, P. M.:](#) The physical science basis. Contribution of working group I to the
2054 fifth assessment report of the intergovernmental panel on climate change, *Computational*
2055 *Geometry*, 18, 95-123, 2013.

2056 [Tesi, T., Belt, S., Gariboldi, K., Muschitiello, F., Smik, L., Finocchiaro, F., Giglio, F., Colizza, E.,](#)
2057 [Gazzurra, G., and Giordano, P.:](#) Resolving sea ice dynamics in the north-western Ross Sea during
2058 the last 2.6 ka: From seasonal to millennial timescales, *Quaternary Science Reviews*, 237,
2059 <http://dx.doi.org/10.1016/j.quascirev.2020.106299>, 2020.

2060 [Thomas, D. N.:](#) *Sea ice*, John Wiley & Sons, 2017.

2061 [Thompson, A. F., Heywood, K. J., Thorpe, S. E., Renner, A. H., and Trasviña, A.:](#) Surface circulation
2062 at the tip of the Antarctic Peninsula from drifters, *Journal of Physical Oceanography*, 39, 3-26,
2063 2009.

2064 [Thompson, A. F., Stewart, A. L., Spence, P., and Heywood, K. J.:](#) The Antarctic Slope Current in a
2065 changing climate, *Reviews of Geophysics*, 56, 741-770, 2018.

2066 [Turner, J., Orr, A., Gudmundsson, G. H., Jenkins, A., Bingham, R. G., Hillenbrand, C.-D., and](#)
2067 [Bracegirdle, T. J.:](#) Atmosphere-ocean-ice interactions in the Amundsen Sea Embayment, West
2068 Antarctica, *Reviews of Geophysics*, 55, 235-276, 2017.

2069 [Turner, J., Guarino, M.V., Arnatt, J., Jena, B., Marshall, G.J., Phillips, T., Bajish, C.C., Clem, K.,](#)
2070 [Wang, Z., Andersson, T., Murphy, E.J., Cavanagh, R.:](#) *Recent Decrease of Summer Sea Ice in*
2071 *the Weddell Sea, Antarctica, Geophysical Research Letters* 47, e2020GL087127, 2020.

2072 [Valcke, S.:](#) The OASIS3 coupler: A European climate modelling community software, *Geoscientific*
2073 *Model Development*, 6, 373-388, 2013.

Formatiert: Schriftart: (Standard) Times New Roman, Englisch (Vereinigtes Königreich)

Formatiert: Schriftart: (Standard) Times New Roman

Formatiert: Schriftart: (Standard) Times New Roman, Englisch (Vereinigtes Königreich)

Formatiert: Schriftart: (Standard) Times New Roman

Formatiert: Schriftart: (Standard) Times New Roman

Formatiert: Standard, Block, Einzug: Vor: 0.49 cm, Hängend: 0.49 cm, Zeilenabstand: Doppelt

Formatiert: Nach: 0.63 cm

2074 Vaughan, D. G., Marshall, G. J., Connolley, W. M., Parkinson, C., Mulvaney, R., Hodgson, D. A.,
 2075 King, J. C., Pudsey, C. J., and Turner, J.: Recent rapid regional climate warming on the Antarctic
 2076 Peninsula, *Climatic change*, 60, 243-274, 2003.

2077 Vaughan, D. G.: West Antarctic Ice Sheet collapse—the fall and rise of a paradigm, *Climatic Change*,
 2078 91, 65-79, 2008.

2079 Vernet, M., Geibert, W., Hoppema, M., Brown, P. J., Haas, C., Hellmer, H., Jokat, W., Jullion, L.,
 2080 Mazloff, M., and Bakker, D.: The Weddell Gyre, Southern Ocean: present knowledge and future
 2081 challenges, *Reviews of Geophysics*, 57, 623-708, 2019.

2082 Volkman, J. K.: Lipid markers for marine organic matter, in: *Marine organic matter: Biomarkers,*
 2083 *isotopes and DNA*, Springer, 27-70, 2006.

2084 Vorrath, M.-E., Müller, J., Esper, O., Mollenhauer, G., Haas, C., Schefuß, E., and Fahl, K.: Highly
 2085 branched isoprenoids for Southern Ocean sea ice reconstructions: a pilot study from the WAP,
 2086 *Biogeosciences*, 16, 2961-2981, 2019.

2087 Vorrath, M.-E., Müller, J., Rebolledo, L., Cárdenas, P., Shi, X., Esper, O., Opel, T., Geibert, W.,
 2088 Muñoz, P., and Haas, C.: Sea ice dynamics in the Bransfield Strait, Antarctic Peninsula, during
 2089 the past 240 years: a multi-proxy intercomparison study, *Climate of the Past*, 16, 2459-2483,
 2090 2020.

2091 Wang, Z., Turner, J., Wu, Y., Liu, C.: Rapid Decline of Total Antarctic Sea Ice Extent during 2014–
 2092 16 Controlled by Wind-Driven Sea Ice Drift. *Journal of Climate* 32, 5381-5395. 2019.

2093 Witus, A.E., Branecky, C.M., Anderson, J.B., Szczuciński, W., Schroeder, D.M., Blankenship, D.D.,
 2094 Jakobsson, M.: Meltwater intensive glacial retreat in polar environments and investigation of
 2095 associated sediments: example from Pine Island Bay, West Antarctica, *Quaternary Science*
 2096 *Reviews*, 85, 99–118, 2014.

2097 Xiao, X., Fahl, K., Müller, J., and Stein, R.: Sea-ice distribution in the modern Arctic Ocean:
 2098 Biomarker records from trans-Arctic Ocean surface sediments, *Geochimica et Cosmochimica*
 2099 *Acta*, 155, 16-29, 2015.

Gelöscht: Western Antarctic Peninsula
Formatiert: Schriftart: (Standard) Times New Roman

Formatiert: Schriftart: (Standard) Times New Roman
Formatiert: Standard, Block, Einzug: Vor: 0.49 cm, Hängend: 0.49 cm, Zeilenabstand: Doppelt

Formatiert: Nach: 0.63 cm

2101 Zamelczyk, K., Rasmussen, T. L., Husum, K., Hafliadason, H., de Vernal, A., Ravna, E. K., Hald,
2102 M., and Hillaire-Marcel, C.: Paleoceanographic changes and calcium carbonate dissolution in the
2103 central Fram Strait during the last 20 ka, *Quaternary Research*, 78, 405-416, 2012.
2104 Zielinski, U., Gersonde, R., Sieger, R., and Fütterer, D.: Quaternary surface water temperature
2105 estimations: Calibration of a diatom transfer function for the Southern Ocean, *Paleoceanography*
2106 and *Paleoclimatology*, 13, 365-383, 1998.
2107 Zwally, H. J.: Antarctic sea ice, 1973-1976: Satellite passive-microwave observations, Scientific and
2108 Technical Information Branch, National Aeronautics and Space, 1983.

2109
2110

Formatiert: Standard, Block, Einzug: Vor: 0 cm, Erste Zeile: 0 cm, Zeilenabstand: Doppelt

Formatiert: Nach: 0.63 cm

Seite 1: [1] Formatiert	Nele	16.08.21 18:50:00
-------------------------	------	-------------------

Nach: 0.63 cm

Seite 1: [2] Formatvorlagendefinition	Nele	16.08.21 18:50:00
---------------------------------------	------	-------------------

p1

Seite 1: [2] Formatvorlagendefinition	Nele	16.08.21 18:50:00
---------------------------------------	------	-------------------

p1

Seite 1: [2] Formatvorlagendefinition	Nele	16.08.21 18:50:00
---------------------------------------	------	-------------------

p1

Seite 1: [2] Formatvorlagendefinition	Nele	16.08.21 18:50:00
---------------------------------------	------	-------------------

p1

Seite 1: [2] Formatvorlagendefinition	Nele	16.08.21 18:50:00
---------------------------------------	------	-------------------

p1

Seite 1: [2] Formatvorlagendefinition	Nele	16.08.21 18:50:00
---------------------------------------	------	-------------------

p1

Seite 1: [2] Formatvorlagendefinition	Nele	16.08.21 18:50:00
---------------------------------------	------	-------------------

p1

Seite 1: [2] Formatvorlagendefinition	Nele	16.08.21 18:50:00
---------------------------------------	------	-------------------

p1

Seite 1: [2] Formatvorlagendefinition	Nele	16.08.21 18:50:00
---------------------------------------	------	-------------------

p1

Seite 1: [2] Formatvorlagendefinition	Nele	16.08.21 18:50:00
---------------------------------------	------	-------------------

p1

Seite 1: [2] Formatvorlagendefinition	Nele	16.08.21 18:50:00
---------------------------------------	------	-------------------

p1

Seite 1: [2] Formatvorlagendefinition	Nele	16.08.21 18:50:00
---------------------------------------	------	-------------------

p1

Seite 1: [3] Gelöscht	Nele	16.08.21 18:50:00
-----------------------	------	-------------------

▼

Seite 1: [4] Formatiert	Nele	16.08.21 18:50:00
-------------------------	------	-------------------

Block, Zeilenabstand: Doppelt

Seite 1: [5] Formatiert	Nele	16.08.21 18:50:00
-------------------------	------	-------------------

Links: 2.54 cm, Rechts: 2.54 cm, Oben: 2.54 cm, Unten: 2.54 cm, Breite: 21 cm, Höhe: 29.69 cm, Kopfzeilenabstand vom Rand: 1.27 cm, Fußzeilenabstand vom Rand: 1.27 cm, Nummerierung: Fortlaufend

Seite 1: [6] Formatiert	Nele	16.08.21 18:50:00
-------------------------	------	-------------------

Schriftart: (Standard) Times New Roman

Seite 1: [7] Formatiert	Nele	16.08.21 18:50:00
-------------------------	------	-------------------

Schriftart: (Standard) Times New Roman

Seite 1: [8] Formatiert	Nele	16.08.21 18:50:00
Schriftart: (Standard) Times New Roman		
Seite 1: [9] Formatiert	Nele	16.08.21 18:50:00
Schriftart: (Standard) Times New Roman		
Seite 1: [10] Formatiert	Nele	16.08.21 18:50:00
Schriftart: (Standard) Times New Roman		
Seite 1: [11] Formatiert	Nele	16.08.21 18:50:00
Block, Keine, Zeilenabstand: Doppelt		
Seite 1: [12] Formatiert	Nele	16.08.21 18:50:00
Schriftart: (Standard) Times New Roman, Nicht Hochgestellt/ Tiefgestellt		
Seite 1: [13] Formatiert	Nele	16.08.21 18:50:00
Schriftart: (Standard) Times New Roman		
Seite 1: [14] Formatiert	Nele	16.08.21 18:50:00
Schriftart: (Standard) Times New Roman, Hochgestellt		
Seite 1: [15] Formatiert	Nele	16.08.21 18:50:00
Schriftart: (Standard) Times New Roman, 11 Pt.		
Seite 1: [16] Formatiert	Nele	16.08.21 18:50:00
Block, Zeilenabstand: Doppelt		
Seite 1: [17] Formatiert	Nele	16.08.21 18:50:00
Schriftart: (Standard) Times New Roman, 11 Pt.		
Seite 1: [18] Formatiert	Nele	16.08.21 18:50:00
Schriftart: (Standard) Times New Roman, 11 Pt.		
Seite 1: [19] Formatiert	Nele	16.08.21 18:50:00
Schriftart: (Standard) Times New Roman, 11 Pt.		
Seite 1: [20] Formatiert	Nele	16.08.21 18:50:00
Schriftart: (Standard) Times New Roman, 11 Pt.		
Seite 1: [21] Formatiert	Nele	16.08.21 18:50:00
Schriftart: (Standard) Times New Roman, 11 Pt., Englisch (Vereinigtes Königreich)		
Seite 1: [22] Gelöscht	Nele	16.08.21 18:50:00
▼		
Seite 1: [23] Formatiert	Nele	16.08.21 18:50:00
Schriftart: (Standard) Times New Roman, 11 Pt.		
Seite 1: [24] Formatiert	Nele	16.08.21 18:50:00
Block, Zeilenabstand: Doppelt		
Seite 1: [25] Formatiert	Nele	16.08.21 18:50:00
Schriftart: (Standard) Times New Roman		
Seite 1: [26] Formatiert	Nele	16.08.21 18:50:00
Block, Zeilenabstand: Doppelt, Rahmen: Unten: (Kein Rahmen)		
Seite 1: [27] Formatiert	Nele	16.08.21 18:50:00

Schriftart: (Standard) Times New Roman, Kursiv

Seite 1: [28] Formatiert	Nele	16.08.21 18:50:00
--------------------------	------	-------------------

Block, Zeilenabstand: Doppelt

Seite 1: [29] Formatiert	Nele	16.08.21 18:50:00
--------------------------	------	-------------------

Schriftart: (Standard) Times New Roman

Seite 1: [30] Formatiert	Nele	16.08.21 18:50:00
--------------------------	------	-------------------

Schriftart: (Standard) Times New Roman

Seite 1: [31] Formatiert	Nele	16.08.21 18:50:00
--------------------------	------	-------------------

Schriftart: (Standard) Times New Roman

Seite 1: [31] Formatiert	Nele	16.08.21 18:50:00
--------------------------	------	-------------------

Schriftart: (Standard) Times New Roman

Seite 1: [32] Formatiert	Nele	16.08.21 18:50:00
--------------------------	------	-------------------

Schriftart: (Standard) Times New Roman

Seite 1: [32] Formatiert	Nele	16.08.21 18:50:00
--------------------------	------	-------------------

Schriftart: (Standard) Times New Roman

Seite 1: [32] Formatiert	Nele	16.08.21 18:50:00
--------------------------	------	-------------------

Schriftart: (Standard) Times New Roman

Seite 1: [33] Formatiert	Nele	16.08.21 18:50:00
--------------------------	------	-------------------

Schriftart: (Standard) Times New Roman

Seite 1: [34] Formatiert	Nele	16.08.21 18:50:00
--------------------------	------	-------------------

Schriftart: (Standard) Times New Roman

Seite 1: [35] Formatiert	Nele	16.08.21 18:50:00
--------------------------	------	-------------------

Schriftart: (Standard) Times New Roman

Seite 1: [36] Formatiert	Nele	16.08.21 18:50:00
--------------------------	------	-------------------

Schriftart: (Standard) Times New Roman

Seite 1: [37] Formatiert	Nele	16.08.21 18:50:00
--------------------------	------	-------------------

Schriftart: (Standard) Times New Roman

Seite 1: [38] Formatiert	Nele	16.08.21 18:50:00
--------------------------	------	-------------------

Schriftart: (Standard) Times New Roman

Seite 1: [39] Formatiert	Nele	16.08.21 18:50:00
--------------------------	------	-------------------

Schriftart: (Standard) Times New Roman

Seite 1: [40] Formatiert	Nele	16.08.21 18:50:00
--------------------------	------	-------------------

Schriftart: (Standard) Times New Roman

Seite 1: [40] Formatiert	Nele	16.08.21 18:50:00
--------------------------	------	-------------------

Schriftart: (Standard) Times New Roman

Seite 1: [41] Formatiert	Nele	16.08.21 18:50:00
--------------------------	------	-------------------

Schriftart: (Standard) Times New Roman

Seite 1: [42] Formatiert	Nele	16.08.21 18:50:00
--------------------------	------	-------------------

Schriftart: (Standard) Times New Roman

Seite 1: [43] Formatiert	Nele	16.08.21 18:50:00
Schriftart: (Standard) Times New Roman		
Seite 32: [44] Formatiert	Nele	16.08.21 18:50:00
Nach: 0.63 cm		
Seite 1: [45] Formatiert	Nele	16.08.21 18:50:00
Standard, Block, Einzug: Vor: 0.74 cm, Hängend: 0.74 cm, Zeilenabstand: Doppelt, Keine Aufzählungen oder Nummerierungen		
Seite 1: [46] Formatiert	Nele	16.08.21 18:50:00
Schriftart: (Standard) Times New Roman		
Seite 1: [47] Formatiert	Nele	16.08.21 18:50:00
Block, Zeilenabstand: Doppelt		
Seite 1: [48] Formatiert	Nele	16.08.21 18:50:00
Schriftart: (Standard) Times New Roman, Schriftfarbe: Automatisch		
Seite 1: [49] Formatiert	Nele	16.08.21 18:50:00
Schriftart: (Standard) Times New Roman, Schriftfarbe: Automatisch		
Seite 1: [49] Formatiert	Nele	16.08.21 18:50:00
Schriftart: (Standard) Times New Roman, Schriftfarbe: Automatisch		
Seite 1: [50] Formatiert	Nele	16.08.21 18:50:00
Schriftart: (Standard) Times New Roman		
Seite 1: [51] Formatiert	Nele	16.08.21 18:50:00
Schriftart: (Standard) Times New Roman, Hervorheben		
Seite 1: [52] Gelöscht	Nele	16.08.21 18:50:00
▼		
Seite 1: [53] Formatiert	Nele	16.08.21 18:50:00
Schriftart: (Standard) Times New Roman		
Seite 1: [53] Formatiert	Nele	16.08.21 18:50:00
Schriftart: (Standard) Times New Roman		
Seite 1: [54] Formatiert	Nele	16.08.21 18:50:00
Schriftart: (Standard) Times New Roman		
Seite 1: [55] Formatiert	Nele	16.08.21 18:50:00
Schriftart: (Standard) Times New Roman		
Seite 1: [56] Gelöscht	Nele	16.08.21 18:50:00
▼		
Seite 1: [57] Formatiert	Nele	16.08.21 18:50:00
Schriftart: (Standard) Times New Roman		
Seite 1: [58] Formatiert	Nele	16.08.21 18:50:00
Schriftart: (Standard) Times New Roman		
Seite 1: [59] Gelöscht	Nele	16.08.21 18:50:00

▼

Seite 1: [60] Formatiert	Nele	16.08.21 18:50:00
--------------------------	------	-------------------

Schriftart: (Standard) Times New Roman, Schriftfarbe: Automatisch

Seite 1: [61] Formatiert	Nele	16.08.21 18:50:00
--------------------------	------	-------------------

Schriftart: (Standard) Times New Roman

Seite 1: [62] Formatiert	Nele	16.08.21 18:50:00
--------------------------	------	-------------------

Schriftart: (Standard) Times New Roman

Seite 1: [62] Formatiert	Nele	16.08.21 18:50:00
--------------------------	------	-------------------

Schriftart: (Standard) Times New Roman

Seite 1: [63] Formatiert	Nele	16.08.21 18:50:00
--------------------------	------	-------------------

Schriftart: (Standard) Times New Roman

Seite 1: [64] Gelöscht	Nele	16.08.21 18:50:00
------------------------	------	-------------------

▼

Seite 1: [65] Formatiert	Nele	16.08.21 18:50:00
--------------------------	------	-------------------

Schriftart: (Standard) Times New Roman

Seite 1: [66] Formatiert	Nele	16.08.21 18:50:00
--------------------------	------	-------------------

Schriftart: (Standard) Times New Roman

Seite 1: [67] Formatiert	Nele	16.08.21 18:50:00
--------------------------	------	-------------------

Schriftart: (Standard) Times New Roman

Seite 1: [68] Formatiert	Nele	16.08.21 18:50:00
--------------------------	------	-------------------

Schriftart: (Standard) Times New Roman

Seite 1: [69] Formatiert	Nele	16.08.21 18:50:00
--------------------------	------	-------------------

Schriftart: (Standard) Times New Roman

Seite 1: [70] Formatiert	Nele	16.08.21 18:50:00
--------------------------	------	-------------------

Schriftart: (Standard) Times New Roman

Seite 1: [71] Formatiert	Nele	16.08.21 18:50:00
--------------------------	------	-------------------

Schriftart: (Standard) Times New Roman

Seite 1: [71] Formatiert	Nele	16.08.21 18:50:00
--------------------------	------	-------------------

Schriftart: (Standard) Times New Roman

Seite 1: [72] Formatiert	Nele	16.08.21 18:50:00
--------------------------	------	-------------------

Schriftart: (Standard) Times New Roman

Seite 1: [73] Formatiert	Nele	16.08.21 18:50:00
--------------------------	------	-------------------

Schriftart: (Standard) Times New Roman

Seite 1: [74] Formatiert	Nele	16.08.21 18:50:00
--------------------------	------	-------------------

Schriftart: (Standard) Times New Roman

Seite 1: [74] Formatiert	Nele	16.08.21 18:50:00
--------------------------	------	-------------------

Schriftart: (Standard) Times New Roman

Seite 1: [74] Formatiert	Nele	16.08.21 18:50:00
--------------------------	------	-------------------

Schriftart: (Standard) Times New Roman

Seite 1: [75] Formatiert	Nele	16.08.21 18:50:00
--------------------------	------	-------------------

Schriftart: (Standard) Times New Roman

Seite 1: [76] Formatiert	Nele	16.08.21 18:50:00
--------------------------	------	-------------------

Schriftart: (Standard) Times New Roman

Seite 1: [77] Formatiert	Nele	16.08.21 18:50:00
--------------------------	------	-------------------

Schriftart: (Standard) Times New Roman

Seite 1: [77] Formatiert	Nele	16.08.21 18:50:00
--------------------------	------	-------------------

Schriftart: (Standard) Times New Roman

Seite 2: [78] Formatiert	Nele	16.08.21 18:50:00
--------------------------	------	-------------------

Schriftart: (Standard) Times New Roman, Schriftfarbe: Automatisch

Seite 2: [79] Formatiert	Nele	16.08.21 18:50:00
--------------------------	------	-------------------

Schriftart: (Standard) Times New Roman, Schriftfarbe: Automatisch

Seite 2: [80] Formatiert	Nele	16.08.21 18:50:00
--------------------------	------	-------------------

Schriftart: (Standard) Times New Roman, Schriftfarbe: Automatisch

Seite 2: [81] Formatiert	Nele	16.08.21 18:50:00
--------------------------	------	-------------------

Schriftart: (Standard) Times New Roman, Schriftfarbe: Automatisch

Seite 2: [82] Formatiert	Nele	16.08.21 18:50:00
--------------------------	------	-------------------

Schriftart: (Standard) Times New Roman, Schriftfarbe: Automatisch

Seite 2: [83] Formatiert	Nele	16.08.21 18:50:00
--------------------------	------	-------------------

Schriftart: (Standard) Times New Roman, Schriftfarbe: Automatisch

Seite 2: [84] Formatiert	Nele	16.08.21 18:50:00
--------------------------	------	-------------------

Schriftart: (Standard) Times New Roman, Kursiv, Schriftfarbe: Automatisch

Seite 2: [85] Formatiert	Nele	16.08.21 18:50:00
--------------------------	------	-------------------

Schriftart: (Standard) Times New Roman, Schriftfarbe: Automatisch

Seite 2: [86] Formatiert	Nele	16.08.21 18:50:00
--------------------------	------	-------------------

Schriftart: (Standard) Times New Roman, Schriftfarbe: Automatisch

Seite 2: [87] Gelöscht	Nele	16.08.21 18:50:00
------------------------	------	-------------------

▼

Seite 2: [88] Formatiert	Nele	16.08.21 18:50:00
--------------------------	------	-------------------

Schriftart: (Standard) Times New Roman, Schriftfarbe: Automatisch

Seite 2: [89] Formatiert	Nele	16.08.21 18:50:00
--------------------------	------	-------------------

Schriftart: (Standard) Times New Roman, Schriftfarbe: Automatisch

Seite 2: [90] Formatiert	Nele	16.08.21 18:50:00
--------------------------	------	-------------------

Schriftart: (Standard) Times New Roman, Schriftfarbe: Automatisch

Seite 2: [91] Formatiert	Nele	16.08.21 18:50:00
--------------------------	------	-------------------

Schriftart: (Standard) Times New Roman, Schriftfarbe: Automatisch

Seite 32: [92] Formatiert	Nele	16.08.21 18:50:00
---------------------------	------	-------------------

Nach: 0.63 cm

Seite 3: [93] Formatiert	Nele	16.08.21 18:50:00
--------------------------	------	-------------------

Schriftart: (Standard) Times New Roman, Schriftfarbe: Automatisch

Seite 3: [94] Gelöscht	Nele	16.08.21 18:50:00
------------------------	------	-------------------

Seite 3: [95] Formatiert	Nele	16.08.21 18:50:00
--------------------------	------	-------------------

Schriftart: (Standard) Times New Roman, Schriftfarbe: Automatisch

Seite 3: [96] Formatiert	Nele	16.08.21 18:50:00
--------------------------	------	-------------------

Schriftart: (Standard) Times New Roman, Schriftfarbe: Automatisch

Seite 3: [97] Formatiert	Nele	16.08.21 18:50:00
--------------------------	------	-------------------

Schriftart: (Standard) Times New Roman, Schriftfarbe: Automatisch

Seite 3: [98] Formatiert	Nele	16.08.21 18:50:00
--------------------------	------	-------------------

Schriftart: (Standard) Times New Roman, Schriftfarbe: Automatisch

Seite 3: [99] Formatiert	Nele	16.08.21 18:50:00
--------------------------	------	-------------------

Schriftart: (Standard) Times New Roman, Schriftfarbe: Automatisch

Seite 3: [100] Formatiert	Nele	16.08.21 18:50:00
---------------------------	------	-------------------

Schriftart: (Standard) Times New Roman, Schriftfarbe: Automatisch

Seite 3: [101] Formatiert	Nele	16.08.21 18:50:00
---------------------------	------	-------------------

Schriftart: (Standard) Times New Roman, Schriftfarbe: Automatisch

Seite 3: [102] Formatiert	Nele	16.08.21 18:50:00
---------------------------	------	-------------------

Schriftart: (Standard) Times New Roman, Schriftfarbe: Automatisch

Seite 3: [103] Formatiert	Nele	16.08.21 18:50:00
---------------------------	------	-------------------

Schriftart: (Standard) Times New Roman, Schriftfarbe: Automatisch

Seite 3: [104] Formatiert	Nele	16.08.21 18:50:00
---------------------------	------	-------------------

Schriftart: (Standard) Times New Roman, Schriftfarbe: Automatisch

Seite 3: [104] Formatiert	Nele	16.08.21 18:50:00
---------------------------	------	-------------------

Schriftart: (Standard) Times New Roman, Schriftfarbe: Automatisch

Seite 3: [105] Formatiert	Nele	16.08.21 18:50:00
---------------------------	------	-------------------

Schriftart: (Standard) Times New Roman, Schriftfarbe: Automatisch

Seite 3: [106] Formatiert	Nele	16.08.21 18:50:00
---------------------------	------	-------------------

Schriftart: (Standard) Times New Roman, Schriftfarbe: Automatisch

Seite 3: [107] Formatiert	Nele	16.08.21 18:50:00
---------------------------	------	-------------------

Schriftart: (Standard) Times New Roman, Schriftfarbe: Automatisch

Seite 3: [108] Formatiert	Nele	16.08.21 18:50:00
---------------------------	------	-------------------

Schriftart: (Standard) Times New Roman, Schriftfarbe: Automatisch

Seite 3: [109] Formatiert	Nele	16.08.21 18:50:00
---------------------------	------	-------------------

Schriftart: (Standard) Times New Roman, Schriftfarbe: Automatisch

Seite 3: [110] Formatiert	Nele	16.08.21 18:50:00
---------------------------	------	-------------------

Schriftart: (Standard) Times New Roman, Schriftfarbe: Automatisch

Seite 3: [110] Formatiert	Nele	16.08.21 18:50:00
Schriftart: (Standard) Times New Roman, Schriftfarbe: Automatisch		
Seite 3: [111] Formatiert	Nele	16.08.21 18:50:00
Schriftart: (Standard) Times New Roman, Schriftfarbe: Automatisch		
Seite 3: [112] Formatiert	Nele	16.08.21 18:50:00
Schriftart: (Standard) Times New Roman, Schriftfarbe: Automatisch		
Seite 3: [113] Formatiert	Nele	16.08.21 18:50:00
Schriftart: (Standard) Times New Roman, Schriftfarbe: Automatisch		
Seite 3: [113] Formatiert	Nele	16.08.21 18:50:00
Schriftart: (Standard) Times New Roman, Schriftfarbe: Automatisch		
Seite 3: [114] Formatiert	Nele	16.08.21 18:50:00
Schriftart: (Standard) Times New Roman, Schriftfarbe: Automatisch		
Seite 3: [115] Formatiert	Nele	16.08.21 18:50:00
Schriftart: (Standard) Times New Roman, Schriftfarbe: Automatisch		
Seite 3: [115] Formatiert	Nele	16.08.21 18:50:00
Schriftart: (Standard) Times New Roman, Schriftfarbe: Automatisch		
Seite 3: [115] Formatiert	Nele	16.08.21 18:50:00
Schriftart: (Standard) Times New Roman, Schriftfarbe: Automatisch		
Seite 3: [116] Gelöscht	Nele	16.08.21 18:50:00
▼		
Seite 32: [117] Formatiert	Nele	16.08.21 18:50:00
Nach: 0.63 cm		
Seite 7: [118] Formatiert	Nele	16.08.21 18:50:00
Schriftart: (Standard) Times New Roman, Englisch (Vereinigtes Königreich)		
Seite 7: [119] Formatiert	Nele	16.08.21 18:50:00
Block, Einzug: Vor: 0.74 cm, Hängend: 0.74 cm, Zeilenabstand: Doppelt		
Seite 7: [120] Formatiert	Nele	16.08.21 18:50:00
Schriftart: (Standard) Times New Roman, Nicht Fett, Englisch (Vereinigtes Königreich)		
Seite 7: [121] Formatiert	Nele	16.08.21 18:50:00
Schriftart: (Standard) Times New Roman		
Seite 7: [122] Formatiert	Nele	16.08.21 18:50:00
Schriftart: (Standard) Times New Roman		
Seite 7: [123] Formatiert	Nele	16.08.21 18:50:00
Block, Zeilenabstand: Doppelt		
Seite 7: [124] Formatiert	Nele	16.08.21 18:50:00
Schriftart: (Standard) Times New Roman		
Seite 7: [124] Formatiert	Nele	16.08.21 18:50:00
Schriftart: (Standard) Times New Roman		
Seite 7: [125] Formatiert	Nele	16.08.21 18:50:00

Schriftart: (Standard) Times New Roman

Seite 7: [125] Formatiert	Nele	16.08.21 18:50:00
---------------------------	------	-------------------

Schriftart: (Standard) Times New Roman

Seite 7: [126] Formatiert	Nele	16.08.21 18:50:00
---------------------------	------	-------------------

Schriftart: (Standard) Times New Roman

Seite 7: [127] Formatiert	Nele	16.08.21 18:50:00
---------------------------	------	-------------------

Schriftart: (Standard) Times New Roman

Seite 7: [128] Formatiert	Nele	16.08.21 18:50:00
---------------------------	------	-------------------

Schriftart: (Standard) Times New Roman

Seite 7: [129] Formatiert	Nele	16.08.21 18:50:00
---------------------------	------	-------------------

Schriftart: (Standard) Times New Roman

Seite 7: [130] Formatiert	Nele	16.08.21 18:50:00
---------------------------	------	-------------------

Schriftart: (Standard) Times New Roman

Seite 7: [131] Formatiert	Nele	16.08.21 18:50:00
---------------------------	------	-------------------

Schriftart: (Standard) Times New Roman

Seite 7: [132] Formatiert	Nele	16.08.21 18:50:00
---------------------------	------	-------------------

Standard, Block, Einzug: Vor: 1 cm, Hängend: 1 cm, Zeilenabstand: Doppelt, Keine Aufzählungen oder Nummerierungen

Seite 7: [133] Formatiert	Nele	16.08.21 18:50:00
---------------------------	------	-------------------

Schriftart: (Standard) Times New Roman

Seite 7: [134] Formatiert	Nele	16.08.21 18:50:00
---------------------------	------	-------------------

Block, Zeilenabstand: Doppelt

Seite 7: [135] Formatiert	Nele	16.08.21 18:50:00
---------------------------	------	-------------------

Schriftart: (Standard) Times New Roman

Seite 7: [136] Formatiert	Nele	16.08.21 18:50:00
---------------------------	------	-------------------

Schriftart: (Standard) Times New Roman

Seite 7: [137] Formatiert	Nele	16.08.21 18:50:00
---------------------------	------	-------------------

Schriftart: (Standard) Times New Roman

Seite 7: [138] Formatiert	Nele	16.08.21 18:50:00
---------------------------	------	-------------------

Schriftart: (Standard) Times New Roman

Seite 7: [139] Formatiert	Nele	16.08.21 18:50:00
---------------------------	------	-------------------

Schriftart: (Standard) Times New Roman

Seite 7: [139] Formatiert	Nele	16.08.21 18:50:00
---------------------------	------	-------------------

Schriftart: (Standard) Times New Roman

Seite 7: [140] Formatiert	Nele	16.08.21 18:50:00
---------------------------	------	-------------------

Schriftart: (Standard) +Überschriften CS (Times New Roman)

Seite 7: [141] Formatiert	Nele	16.08.21 18:50:00
---------------------------	------	-------------------

Schriftart: (Standard) +Überschriften CS (Times New Roman)

Seite 7: [141] Formatiert	Nele	16.08.21 18:50:00
---------------------------	------	-------------------

Schriftart: (Standard) +Überschriften CS (Times New Roman)

Seite 7: [142] Formatiert	Nele	16.08.21 18:50:00
Schriftart: (Standard) +Überschriften CS (Times New Roman)		
Seite 7: [143] Formatiert	Nele	16.08.21 18:50:00
Schriftart: (Standard) +Überschriften CS (Times New Roman)		
Seite 7: [143] Formatiert	Nele	16.08.21 18:50:00
Schriftart: (Standard) +Überschriften CS (Times New Roman)		
Seite 32: [144] Formatiert	Nele	16.08.21 18:50:00
Nach: 0.63 cm		
Seite 12: [145] Formatiert	Nele	16.08.21 18:50:00
Schriftart: (Standard) Times New Roman, Englisch (Vereinigtes Königreich)		
Seite 12: [146] Formatiert	Nele	16.08.21 18:50:00
Schriftart: (Standard) +Überschriften CS (Times New Roman), 10 Pt., Fett, Schriftfarbe: Text 1, Englisch (Vereinigtes Königreich)		
Seite 12: [147] Formatiert	Nele	16.08.21 18:50:00
Schriftart: (Standard) Times New Roman, Englisch (Vereinigtes Königreich)		
Seite 12: [148] Formatiert	Nele	16.08.21 18:50:00
Standard, Block, Einzug: Vor: 0.74 cm, Hängend: 0.74 cm, Zeilenabstand: Doppelt, Keine Aufzählungen oder Nummerierungen		
Seite 12: [149] Formatiert	Nele	16.08.21 18:50:00
Schriftart: (Standard) Times New Roman		
Seite 12: [150] Gelöscht	Nele	16.08.21 18:50:00
Seite 12: [151] Formatiert	Nele	16.08.21 18:50:00
Block, Zeilenabstand: Doppelt		
Seite 12: [152] Formatiert	Nele	16.08.21 18:50:00
Schriftart: (Standard) Times New Roman, Schriftfarbe: Automatisch		
Seite 12: [153] Formatiert	Nele	16.08.21 18:50:00
Schriftart: (Standard) Times New Roman, Schriftfarbe: Automatisch		
Seite 12: [154] Formatiert	Nele	16.08.21 18:50:00
Schriftart: (Standard) Times New Roman, Schriftfarbe: Automatisch		
Seite 12: [154] Formatiert	Nele	16.08.21 18:50:00
Schriftart: (Standard) Times New Roman, Schriftfarbe: Automatisch		
Seite 12: [154] Formatiert	Nele	16.08.21 18:50:00
Schriftart: (Standard) Times New Roman, Schriftfarbe: Automatisch		
Seite 12: [154] Formatiert	Nele	16.08.21 18:50:00
Schriftart: (Standard) Times New Roman, Schriftfarbe: Automatisch		
Seite 12: [155] Formatiert	Nele	16.08.21 18:50:00
Standard, Block, Einzug: Vor: 1 cm, Hängend: 1 cm, Zeilenabstand: Doppelt, Keine Aufzählungen oder Nummerierungen		

Seite 12: [156] Formatiert	Nele	16.08.21 18:50:00
Schriftart: (Standard) Times New Roman		
Seite 12: [157] Formatiert	Nele	16.08.21 18:50:00
Schriftart: (Standard) Times New Roman, 9 Pt.		
Seite 12: [158] Formatiert	Nele	16.08.21 18:50:00
Block, Zeilenabstand: Doppelt		
Seite 12: [159] Formatiert	Nele	16.08.21 18:50:00
Schriftart: (Standard) Times New Roman		
Seite 12: [160] Formatiert	Nele	16.08.21 18:50:00
Schriftart: (Standard) Times New Roman		
Seite 12: [161] Formatiert	Nele	16.08.21 18:50:00
Schriftart: (Standard) Times New Roman		
Seite 12: [162] Formatiert	Nele	16.08.21 18:50:00
Schriftart: (Standard) Times New Roman		
Seite 12: [163] Formatiert	Nele	16.08.21 18:50:00
Schriftart: (Standard) Times New Roman		
Seite 12: [164] Formatiert	Nele	16.08.21 18:50:00
Schriftart: (Standard) Times New Roman		
Seite 12: [165] Formatiert	Nele	16.08.21 18:50:00
Schriftart: (Standard) Times New Roman		
Seite 12: [166] Formatiert	Nele	16.08.21 18:50:00
Schriftart: (Standard) Times New Roman		
Seite 12: [167] Formatiert	Nele	16.08.21 18:50:00
Schriftart: (Standard) Times New Roman		
Seite 12: [168] Gelöscht	Nele	16.08.21 18:50:00
▼.....		
Seite 12: [169] Formatiert	Nele	16.08.21 18:50:00
Schriftart: (Standard) Times New Roman		
Seite 12: [170] Formatiert	Nele	16.08.21 18:50:00
Schriftart: (Standard) Times New Roman		
Seite 12: [171] Formatiert	Nele	16.08.21 18:50:00
Schriftart: (Standard) Times New Roman		
Seite 14: [172] Formatiert	Nele	16.08.21 18:50:00
Schriftart: (Standard) Times New Roman, Schriftfarbe: Automatisch		
Seite 14: [173] Formatiert	Nele	16.08.21 18:50:00
Schriftart: (Standard) Times New Roman, Schriftfarbe: Automatisch		
Seite 14: [174] Formatiert	Nele	16.08.21 18:50:00
Schriftart: (Standard) Times New Roman, Schriftfarbe: Automatisch		

Seite 32: [175] Formatiert	Nele	16.08.21 18:50:00
----------------------------	------	-------------------

Nach: 0.63 cm

Seite 15: [176] Formatiert	Nele	16.08.21 18:50:00
----------------------------	------	-------------------

Schriftart: (Standard) Times New Roman

Seite 15: [177] Formatiert	Nele	16.08.21 18:50:00
----------------------------	------	-------------------

Schriftart: (Standard) Times New Roman

Seite 15: [178] Gelöscht	Nele	16.08.21 18:50:00
--------------------------	------	-------------------

▼

Seite 15: [179] Formatiert	Nele	16.08.21 18:50:00
----------------------------	------	-------------------

Schriftart: (Standard) Times New Roman

Seite 15: [180] Formatiert	Nele	16.08.21 18:50:00
----------------------------	------	-------------------

Schriftart: (Standard) Times New Roman

Seite 15: [181] Formatiert	Nele	16.08.21 18:50:00
----------------------------	------	-------------------

Schriftart: (Standard) Times New Roman

Seite 15: [182] Formatiert	Nele	16.08.21 18:50:00
----------------------------	------	-------------------

Schriftart: (Standard) Times New Roman

Seite 15: [182] Formatiert	Nele	16.08.21 18:50:00
----------------------------	------	-------------------

Schriftart: (Standard) Times New Roman

Seite 15: [183] Formatiert	Nele	16.08.21 18:50:00
----------------------------	------	-------------------

Schriftart: (Standard) Times New Roman

Seite 15: [184] Gelöscht	Nele	16.08.21 18:50:00
--------------------------	------	-------------------

▼

Seite 15: [185] Formatiert	Nele	16.08.21 18:50:00
----------------------------	------	-------------------

Schriftart: (Standard) +Überschriften CS (Times New Roman), 10 Pt., Fett, Schriftfarbe: Text
1

Seite 15: [186] Gelöscht	Nele	16.08.21 18:50:00
--------------------------	------	-------------------

▼

Seite 15: [187] Formatiert	Nele	16.08.21 18:50:00
----------------------------	------	-------------------

Schriftart: (Standard) Times New Roman

Seite 15: [188] Formatiert	Nele	16.08.21 18:50:00
----------------------------	------	-------------------

Schriftart: (Standard) Times New Roman, Schriftfarbe: Automatisch

Seite 15: [188] Formatiert	Nele	16.08.21 18:50:00
----------------------------	------	-------------------

Schriftart: (Standard) Times New Roman, Schriftfarbe: Automatisch

Seite 15: [189] Formatiert	Nele	16.08.21 18:50:00
----------------------------	------	-------------------

Schriftart: (Standard) Times New Roman

Seite 15: [190] Formatiert	Nele	16.08.21 18:50:00
----------------------------	------	-------------------

Schriftart: (Standard) Times New Roman

Seite 15: [191] Formatiert	Nele	16.08.21 18:50:00
Schriftart: (Standard) Times New Roman		
Seite 15: [192] Formatiert	Nele	16.08.21 18:50:00
Schriftart: (Standard) Times New Roman		
Seite 15: [193] Formatiert	Nele	16.08.21 18:50:00
Schriftart: (Standard) Times New Roman		
Seite 15: [194] Formatiert	Nele	16.08.21 18:50:00
Schriftart: (Standard) Times New Roman		
Seite 15: [195] Formatiert	Nele	16.08.21 18:50:00
Schriftart: (Standard) Times New Roman		
Seite 15: [195] Formatiert	Nele	16.08.21 18:50:00
Schriftart: (Standard) Times New Roman		
Seite 15: [196] Formatiert	Nele	16.08.21 18:50:00
Schriftart: (Standard) Times New Roman		
Seite 15: [197] Formatiert	Nele	16.08.21 18:50:00
Schriftart: (Standard) Times New Roman		
Seite 15: [198] Formatiert	Nele	16.08.21 18:50:00
Standard, Block, Einzug: Vor: 1 cm, Hängend: 1 cm, Zeilenabstand: Doppelt, Keine Aufzählungen oder Nummerierungen		
Seite 15: [199] Formatiert	Nele	16.08.21 18:50:00
Schriftart: (Standard) Times New Roman		
Seite 15: [200] Gelöscht	Nele	16.08.21 18:50:00
▼.....		
Seite 15: [201] Formatiert	Nele	16.08.21 18:50:00
Schriftart: (Standard) Times New Roman		
Seite 15: [202] Formatiert	Nele	16.08.21 18:50:00
Schriftart: (Standard) Times New Roman		
Seite 15: [203] Formatiert	Nele	16.08.21 18:50:00
Schriftart: (Standard) Times New Roman		
Seite 15: [204] Formatiert	Nele	16.08.21 18:50:00
Schriftart: (Standard) Times New Roman		
Seite 15: [204] Formatiert	Nele	16.08.21 18:50:00
Schriftart: (Standard) Times New Roman		
Seite 15: [204] Formatiert	Nele	16.08.21 18:50:00
Schriftart: (Standard) Times New Roman		
Seite 15: [205] Formatiert	Nele	16.08.21 18:50:00
Schriftart: (Standard) Times New Roman		
Seite 15: [206] Formatiert	Nele	16.08.21 18:50:00
Schriftart: (Standard) Times New Roman		

Seite 15: [207] Formatiert	Nele	16.08.21 18:50:00
Schriftart: (Standard) Times New Roman		
Seite 15: [208] Formatiert	Nele	16.08.21 18:50:00
Schriftart: (Standard) Times New Roman		
Seite 15: [209] Formatiert	Nele	16.08.21 18:50:00
Schriftart: (Standard) Times New Roman		
Seite 17: [210] Formatiert	Nele	16.08.21 18:50:00
Schriftart: (Standard) Times New Roman, Schriftfarbe: Automatisch		
Seite 17: [211] Formatiert	Nele	16.08.21 18:50:00
Schriftart: (Standard) Times New Roman, Schriftfarbe: Automatisch		
Seite 17: [212] Formatiert	Nele	16.08.21 18:50:00
Schriftart: (Standard) Times New Roman		
Seite 17: [212] Formatiert	Nele	16.08.21 18:50:00
Schriftart: (Standard) Times New Roman		
Seite 17: [213] Formatiert	Nele	16.08.21 18:50:00
Schriftart: (Standard) Times New Roman, Schriftfarbe: Automatisch, Englisch (Vereinigtes Königreich)		
Seite 17: [214] Formatiert	Nele	16.08.21 18:50:00
Schriftart: (Standard) Times New Roman		
Seite 17: [214] Formatiert	Nele	16.08.21 18:50:00
Schriftart: (Standard) Times New Roman		
Seite 17: [215] Formatiert	Nele	16.08.21 18:50:00
Schriftart: (Standard) Times New Roman		
Seite 17: [215] Formatiert	Nele	16.08.21 18:50:00
Schriftart: (Standard) Times New Roman		
Seite 17: [216] Gelöscht	Nele	16.08.21 18:50:00
▼.....		
Seite 17: [217] Formatiert	Nele	16.08.21 18:50:00
Schriftart: (Standard) Times New Roman, Schriftfarbe: Automatisch		
Seite 17: [218] Formatiert	Nele	16.08.21 18:50:00
Schriftart: (Standard) Times New Roman, Fett, Schriftfarbe: Rot		
Seite 32: [219] Formatiert	Nele	16.08.21 18:50:00
Nach: 0.63 cm		
Seite 20: [220] Formatiert	Nele	16.08.21 18:50:00
Schriftart: (Standard) Times New Roman		
Seite 20: [220] Formatiert	Nele	16.08.21 18:50:00
Schriftart: (Standard) Times New Roman		
Seite 20: [221] Formatiert	Nele	16.08.21 18:50:00
Block, Einzug: Vor: 1 cm, Hängend: 1 cm, Zeilenabstand: Doppelt		

Seite 20: [222] Formatiert	Nele	16.08.21 18:50:00
----------------------------	------	-------------------

Schriftart: (Standard) Times New Roman

Seite 20: [223] Formatiert	Nele	16.08.21 18:50:00
----------------------------	------	-------------------

Schriftart: (Standard) Times New Roman, Tiefgestellt

Seite 20: [223] Formatiert	Nele	16.08.21 18:50:00
----------------------------	------	-------------------

Schriftart: (Standard) Times New Roman, Tiefgestellt

Seite 20: [224] Formatiert	Nele	16.08.21 18:50:00
----------------------------	------	-------------------

Schriftart: (Standard) Times New Roman

Seite 20: [225] Gelöscht	Nele	16.08.21 18:50:00
--------------------------	------	-------------------

▼

Seite 20: [226] Formatiert	Nele	16.08.21 18:50:00
----------------------------	------	-------------------

Schriftart: (Standard) Times New Roman

Seite 20: [227] Gelöscht	Nele	16.08.21 18:50:00
--------------------------	------	-------------------

▼

Seite 20: [228] Formatiert	Nele	16.08.21 18:50:00
----------------------------	------	-------------------

Schriftart: (Standard) Times New Roman

Seite 20: [229] Formatiert	Nele	16.08.21 18:50:00
----------------------------	------	-------------------

Block, Zeilenabstand: Doppelt, Nicht vom nächsten Absatz trennen

Seite 20: [230] Formatiert	Nele	16.08.21 18:50:00
----------------------------	------	-------------------

Schriftart: (Standard) Times New Roman

Seite 20: [230] Formatiert	Nele	16.08.21 18:50:00
----------------------------	------	-------------------

Schriftart: (Standard) Times New Roman

Seite 20: [230] Formatiert	Nele	16.08.21 18:50:00
----------------------------	------	-------------------

Schriftart: (Standard) Times New Roman

Seite 20: [231] Formatiert	Nele	16.08.21 18:50:00
----------------------------	------	-------------------

Schriftart: (Standard) Times New Roman, Schriftfarbe: Automatisch, Englisch (Vereinigtes Königreich)

Seite 20: [231] Formatiert	Nele	16.08.21 18:50:00
----------------------------	------	-------------------

Schriftart: (Standard) Times New Roman, Schriftfarbe: Automatisch, Englisch (Vereinigtes Königreich)

Seite 20: [231] Formatiert	Nele	16.08.21 18:50:00
----------------------------	------	-------------------

Schriftart: (Standard) Times New Roman, Schriftfarbe: Automatisch, Englisch (Vereinigtes Königreich)

Seite 20: [232] Gelöscht	Nele	16.08.21 18:50:00
--------------------------	------	-------------------

▼

Seite 20: [233] Formatiert	Nele	16.08.21 18:50:00
----------------------------	------	-------------------

Schriftart: (Standard) Times New Roman

Seite 20: [234] Formatiert	Nele	16.08.21 18:50:00
----------------------------	------	-------------------

Schriftart: (Standard) Times New Roman

Seite 20: [235] Formatiert Nele 16.08.21 18:50:00

Schriftart: (Standard) Times New Roman

Seite 20: [235] Formatiert Nele 16.08.21 18:50:00

Schriftart: (Standard) Times New Roman

Seite 20: [236] Gelöscht Nele 16.08.21 18:50:00

Seite 20: [237] Formatiert Nele 16.08.21 18:50:00

Schriftart: (Standard) Times New Roman

Seite 20: [237] Formatiert Nele 16.08.21 18:50:00

Schriftart: (Standard) Times New Roman

Seite 20: [238] Formatiert Nele 16.08.21 18:50:00

Schriftart: (Standard) Times New Roman

Seite 20: [239] Formatiert Nele 16.08.21 18:50:00

Schriftart: (Standard) Times New Roman

Seite 20: [239] Formatiert Nele 16.08.21 18:50:00

Schriftart: (Standard) Times New Roman

Seite 20: [240] Formatiert Nele 16.08.21 18:50:00

Schriftart: (Standard) Times New Roman

Seite 20: [241] Formatiert Nele 16.08.21 18:50:00

Schriftart: (Standard) Times New Roman

Seite 20: [242] Formatiert Nele 16.08.21 18:50:00

Schriftart: (Standard) Times New Roman

Seite 20: [242] Formatiert Nele 16.08.21 18:50:00

Schriftart: (Standard) Times New Roman

Seite 20: [243] Formatiert Nele 16.08.21 18:50:00

Schriftart: (Standard) Times New Roman

Seite 20: [244] Formatiert Nele 16.08.21 18:50:00

Schriftart: (Standard) Times New Roman

Seite 20: [245] Formatiert Nele 16.08.21 18:50:00

Schriftart: (Standard) Times New Roman

Seite 20: [245] Formatiert Nele 16.08.21 18:50:00

Schriftart: (Standard) Times New Roman

Seite 20: [245] Formatiert Nele 16.08.21 18:50:00

Schriftart: (Standard) Times New Roman

Seite 20: [246] Formatiert Nele 16.08.21 18:50:00

Schriftart: (Standard) Times New Roman

Seite 20: [247] Formatiert Nele 16.08.21 18:50:00

Schriftart: (Standard) Times New Roman

Seite 20: [248] Formatiert Nele 16.08.21 18:50:00

Schriftart: (Standard) Times New Roman

Seite 20: [249] Formatiert	Nele	16.08.21 18:50:00
----------------------------	------	-------------------

Schriftart: (Standard) Times New Roman

Seite 20: [250] Formatiert	Nele	16.08.21 18:50:00
----------------------------	------	-------------------

Schriftart: (Standard) Times New Roman

Seite 24: [251] Gelöscht	Nele	16.08.21 18:50:00
--------------------------	------	-------------------

▼

Seite 24: [252] Formatiert	Nele	16.08.21 18:50:00
----------------------------	------	-------------------

Schriftart: (Standard) Times New Roman, Schriftfarbe: Automatisch

Seite 24: [253] Gelöscht	Nele	16.08.21 18:50:00
--------------------------	------	-------------------

▼

Seite 24: [254] Formatiert	Nele	16.08.21 18:50:00
----------------------------	------	-------------------

Schriftart: (Standard) Times New Roman, Schriftfarbe: Automatisch

Seite 24: [255] Formatiert	Nele	16.08.21 18:50:00
----------------------------	------	-------------------

Schriftart: (Standard) Times New Roman, Schriftfarbe: Automatisch

Seite 24: [256] Formatiert	Nele	16.08.21 18:50:00
----------------------------	------	-------------------

Schriftart: (Standard) Times New Roman, Schriftfarbe: Automatisch

Seite 24: [257] Formatiert	Nele	16.08.21 18:50:00
----------------------------	------	-------------------

Schriftart: (Standard) Times New Roman, Schriftfarbe: Automatisch

Seite 24: [258] Formatiert	Nele	16.08.21 18:50:00
----------------------------	------	-------------------

Schriftart: (Standard) Times New Roman, Schriftfarbe: Automatisch

Seite 24: [259] Formatiert	Nele	16.08.21 18:50:00
----------------------------	------	-------------------

Schriftart: (Standard) Times New Roman, Schriftfarbe: Automatisch

Seite 24: [260] Formatiert	Nele	16.08.21 18:50:00
----------------------------	------	-------------------

Schriftart: (Standard) Times New Roman, Schriftfarbe: Automatisch

Seite 26: [261] Gelöscht	Nele	16.08.21 18:50:00
--------------------------	------	-------------------

▼

Seite 26: [262] Gelöscht	Nele	16.08.21 18:50:00
--------------------------	------	-------------------

▼

Seite 28: [263] Gelöscht	Nele	16.08.21 18:50:00
--------------------------	------	-------------------

▼

Seite 28: [264] Gelöscht	Nele	16.08.21 18:50:00
--------------------------	------	-------------------

▼

Seite 28: [265] Formatiert	Nele	16.08.21 18:50:00
----------------------------	------	-------------------

Schriftart: (Standard) Times New Roman, Schriftfarbe: Automatisch

Seite 28: [266] Gelöscht	Nele	16.08.21 18:50:00
--------------------------	------	-------------------

▼

Seite 28: [267] Formatiert	Nele	16.08.21 18:50:00
----------------------------	------	-------------------

Schriftart: (Standard) Times New Roman, Nicht Fett

Seite 28: [268] Gelöscht	Nele	16.08.21 18:50:00
--------------------------	------	-------------------

▼

Seite 28: [269] Formatiert	Nele	16.08.21 18:50:00
----------------------------	------	-------------------

Schriftart: (Standard) Times New Roman, Schriftfarbe: Automatisch

Seite 29: [270] Gelöscht	Nele	16.08.21 18:50:00
--------------------------	------	-------------------

Seite 29: [271] Gelöscht	Nele	16.08.21 18:50:00
--------------------------	------	-------------------

▼

Seite 29: [272] Formatiert	Nele	16.08.21 18:50:00
----------------------------	------	-------------------

Block, Einzug: Erste Zeile: 0 cm, Zeilenabstand: Doppelt

Seite 29: [273] Formatiert	Nele	16.08.21 18:50:00
----------------------------	------	-------------------

Schriftart: (Standard) Times New Roman, Schriftfarbe: Automatisch

Seite 29: [274] Formatiert	Nele	16.08.21 18:50:00
----------------------------	------	-------------------

Schriftart: (Standard) Times New Roman, Schriftfarbe: Automatisch

Seite 29: [275] Formatiert	Nele	16.08.21 18:50:00
----------------------------	------	-------------------

Schriftart: (Standard) Times New Roman, Schriftfarbe: Automatisch

Seite 30: [276] Formatiert	Nele	16.08.21 18:50:00
----------------------------	------	-------------------

Schriftart: (Standard) Times New Roman, Schriftfarbe: Automatisch

Seite 30: [276] Formatiert	Nele	16.08.21 18:50:00
----------------------------	------	-------------------

Schriftart: (Standard) Times New Roman, Schriftfarbe: Automatisch

Seite 30: [276] Formatiert	Nele	16.08.21 18:50:00
----------------------------	------	-------------------

Schriftart: (Standard) Times New Roman, Schriftfarbe: Automatisch

Seite 30: [277] Formatiert	Nele	16.08.21 18:50:00
----------------------------	------	-------------------

Schriftart: (Standard) Times New Roman, Schriftfarbe: Automatisch

Seite 30: [277] Formatiert	Nele	16.08.21 18:50:00
----------------------------	------	-------------------

Schriftart: (Standard) Times New Roman, Schriftfarbe: Automatisch

Seite 30: [278] Formatiert	Nele	16.08.21 18:50:00
----------------------------	------	-------------------

Schriftart: (Standard) Times New Roman

Seite 30: [278] Formatiert	Nele	16.08.21 18:50:00
----------------------------	------	-------------------

Schriftart: (Standard) Times New Roman

Seite 30: [279] Formatiert	Nele	16.08.21 18:50:00
----------------------------	------	-------------------

Schriftart: (Standard) Times New Roman

Seite 30: [279] Formatiert	Nele	16.08.21 18:50:00
----------------------------	------	-------------------

Schriftart: (Standard) Times New Roman

Seite 30: [279] Formatiert	Nele	16.08.21 18:50:00
----------------------------	------	-------------------

Schriftart: (Standard) Times New Roman

Seite 30: [279] Formatiert	Nele	16.08.21 18:50:00
----------------------------	------	-------------------

Schriftart: (Standard) Times New Roman

Seite 30: [279] Formatiert	Nele	16.08.21 18:50:00
----------------------------	------	-------------------

Schriftart: (Standard) Times New Roman

Seite 30: [280] Formatiert	Nele	16.08.21 18:50:00
----------------------------	------	-------------------

Schriftart: (Standard) Times New Roman, Englisch (Vereinigtes Königreich)

Seite 30: [280] Formatiert	Nele	16.08.21 18:50:00
----------------------------	------	-------------------

Schriftart: (Standard) Times New Roman, Englisch (Vereinigtes Königreich)

Seite 30: [281] Gelöscht	Nele	16.08.21 18:50:00
--------------------------	------	-------------------

▼

Seite 30: [281] Gelöscht	Nele	16.08.21 18:50:00
--------------------------	------	-------------------

▼

Seite 30: [281] Gelöscht	Nele	16.08.21 18:50:00
--------------------------	------	-------------------

▼

Seite 31: [282] Gelöscht	Nele	16.08.21 18:50:00
--------------------------	------	-------------------

▼